Genome-wide screenings in attention-deficit/hyperactivity disorder (ADHD): investigation of novel candidate genes *SLC2A3* and *LPHN3*

Genomweite Untersuchungen des Aufmerksamkeitsdefizit/ Hyperaktivitätssyndroms (ADHS): Analyse der neuen Kandidatengene *SLC2A3* und *LPHN3*

Doctoral thesis for a doctoral degree

at the Graduate School of Life Sciences,

Julius-Maximilians-Universität Würzburg

submitted by

Sören Jan Hendrik Merker

from

Soltau, Germany

Würzburg, 2013

The present work was accomplished in the Division of Molecular Psychiatry (Department of Psychiatry, Psychosomatics and Psychotherapy, University of Würzburg) and within the Research Training Group 1253 *'Processing of affective stimuli: from the molecular basis to the emotional experience'* (Speaker: Prof. Dr. Paul Pauli).

Submitted on: .....

Members of the promotion committee:

Chairperson:	Prof. Dr. Manfred Gessler
Primary Supervisor:	Prof. Dr. Klaus-Peter Lesch
Supervisor (second):	Prof. Dr. Erhard Wischmeyer
Supervisor (third):	Prof. Dr. Esther Asan
Supervisor (fourth):	PD Dr. Angelika Schmitt

Date of public defence: .....

Date of receipt of certificates: .....

Table of contents

Summary

Attention-deficit/hyperactivity disorder (ADHD) is a highly prevalent childhood-onset neurodevelopmental disorder that involves a substantial risk of persisting into adolescence and adulthood. A number of genome-wide screening studies in ADHD have been conducted in recent years, giving rise to the discovery of several variants at distinct chromosomal loci, thus emphasising the genetically complex and polygenic nature of this disorder. Accordingly, promising novel candidate genes have emerged, such as the gene encoding the glucose transporter isoform 3 (*SLC2A3*) and the gene encoding the latrophilin isoform 3 (*LPHN3*).

In this thesis, both genes were investigated in form of two separated projects. The first focused on *SLC2A3* polymorphisms associated with ADHD and their potential physiological impact. For this purpose, gene expression analyses in peripheral cell models were performed as well as functional EEG measurements in humans. The second project concerned the murine gene *Lphn3* including the goal of developing a mouse line containing a genetically modified *Lphn3* with conditional knockout potential. In this respect, a specific DNA vector was applied to target the *Lphn3* gene locus in murine embryonic stem (ES) cells as a prerequisite for the generation of appropriate chimeric mice.

The results of the first project showed that *SLC2A3* duplication carriers displayed increased *SLC2A3* mRNA expression in peripheral blood cells and significantly altered event-related potentials (ERPs) during tests of cognitive response control and working memory, possibly involving changes in prefrontal brain activity and memory processing. Interestingly, ADHD patients with the rs12842 T-allele, located within and tagging the *SLC2A3* gene, also exhibited remarkable effects during these EEG measurements. However, such effects reflected a reversed pattern to the aforementioned *SLC2A3* duplication carriers with ADHD, thus indicative of an opposed molecular mechanism. Besides, it emerged that the impact of the aforementioned *SLC2A3* variants on different EEG parameters was generally much more pronounced in the group of ADHD patients than the healthy control group, implying a considerable interaction effect. Concerning the second project, preliminary results were gathered including the successful targeting of *Lphn3* in murine ES cells as well as the production of highly chimeric, phenotypically unremarkable and

mostly fertile mouse chimeras. While germline transmission of the modified *Lphn3* allele has not yet occurred, there are still several newborn chimeric mice that will be tested in the near future.

In conclusion, the findings suggest that *SLC2A3* variants associated with ADHD are accompanied by transcriptional and functional changes in humans. Future research will help to elucidate the molecular network and neurobiological basis involved in these effects and apparently contributing to the complex clinical picture of ADHD. Moreover, given the increasing number of publications concerning latrophilins in recent years and the multitude of research opportunities provided by a conditional knockout of *Lphn3* in mice, the establishment of a respective mouse line, which currently is in progress, constitutes a promising approach for the investigation of this gene and its role in ADHD.

Zusammenfassung

Das Aufmerksamkeitsdefizit/Hyperaktivitätssyndrom (ADHS) ist eine hoch prävalente und bereits in der Kindheit beginnende Neuroentwicklungsstörung, die eine erhebliche Persistenz ins Jugend- und Erwachsenenalter aufweist. In den vergangenen Jahren wurde eine Vielzahl von genomweiten Studien zu ADHS durchgeführt, welche zur Identifizierung zahlreicher genetischer Varianten an unterschiedlichen chromosomalen Loci geführt und somit die genetisch komplexe polygene Natur dieser Störung zur Geltung gebracht haben. Auf diese Weise traten auch neue Kandidatengene zutage, wie zum Beispiel das Gen für die Glukosetransporter-Isoform-3 (*SLC2A3*) und das Gen, welches Latrophilin-3 kodiert (*LPHN3*).

Innerhalb dieser Thesis wurden beide Gene in Form von zwei voneinander getrennten Projekten untersucht. Das erste Projekt beschäftigte sich mit humanen ADHS-assoziierten *SLC2A3*-Polymorphismen und ihrer potentiellen physiologischen Bedeutung. Für diesen Zweck wurden Genexpressionsanalysen in peripheren Zellmodellen sowie funktionelle EEG-Messungen im Menschen durchgeführt. Im zweiten Projekt ging es um das murine Gen *Lphn3* mit dem Ziel, eine Mauslinie zu entwickeln, die ein genetisch verändertes *Lphn3* mit konditionalem Knockout-Potenzial aufweist. In diesem Zusammenhang wurde ein spezifischer DNA-Vektor

verwendet, der auf den *Lphn3*-Genlocus in murinen embryonalen Stammzellen (ES-Zellen) abzielte, was eine Voraussetzung für die Erzeugung von geeigneten chimären Mäusen darstellt.

Die Ergebnisse des ersten Projektes legten nahe, dass *SLC2A3*-Duplikationsträger erhöhte *SLC2A3*-mRNA-Expression in peripheren Blutzellen aufweisen sowie signifikant veränderte ereigniskorrelierte Potentiale während eines Tests kognitiver Reaktionskontrolle sowie eines Arbeitsgedächtnis-Tests, was möglicherweise von veränderter präfrontaler Hirnaktiviät bzw. Gedächtnis-Prozessierung begleitet wird. Interessanterweise zeigten ADHS-Patienten mit T-Allel des im *SLC2A3*-Gen liegenden SNPs rs12842 ebenfalls deutliche Effekte während dieser EEG-Messungen, allerdings in entgegengesetzter Form zu den zuvor genannten *SLC2A3*-Duplikationsträgern mit ADHS, was auf einen gegensätzlichen molekularen Mechanismus hindeutet. Zudem stellte sich heraus, dass der Einfluss der zuvor genannten *SLC2A3*-Varianten auf verschiedene EEG-Parameter innerhalb der ADHS-Gruppe generell deutlich stärker ausgeprägt war als in der gesunden Kontrollgruppe, also einen beachtlichen Interaktionseffekt impliziert. Bezüglich des zweiten Projektes konnten bisher Zwischenergebnisse erzielt werden: das erfolgreiche Targeting des *Lphn3*-Gens in murinen ES-Zellen sowie die Produktion hochchimärer, phänotypisch unauffälliger und größtenteils fertiler Maus-Chimären. Obgleich die Keimbahntransmission des modifizierten *Lphn3*-Allels bislang noch nicht eingetreten ist, gibt es noch eine Reihe an neugeborenen chimären Mäusen, die in nächster Zeit erst noch getestet werden müssen.

Zusammenfassend deuten die Ergebnisse darauf hin, dass Variationen des *SLC2A3*-Gens, die mit ADHS assoziiert sind, mit transkriptionellen und funktionellen Veränderungen im Menschen einhergehen. Zukünftige Forschungsarbeiten werden dabei helfen, die molekularen Netzwerke und neurobiologischen Grundlagen zu verdeutlichen, die an diesen Effekten beteiligt sind und offenbar zu dem komplexen klinischen Bild von ADHS beitragen. Angesichts der steigenden Zahl an Publikationen über Latrophiline in den letzten Jahren und der unzähligen Forschungsmöglichkeiten, die ein konditionaler Knockout von *Lphn3* in Mäusen bietet, stellt die derzeit laufende Etablierung einer entsprechenden Mauslinie einen vielversprechenden Ansatz dar, dieses Gen und seine Rolle für ADHS zu untersuchen.

1 Introduction

1.1 Attention-deficit/hyperactivity disorder (ADHD)

1.1.1 Characteristics and clinical diagnosis

Attention-deficit/hyperactivity disorder (ADHD) is a complex and clinically heterogeneous neurobehavioural disorder which is characterised by developmentally inappropriate deficits in attention, increased activity and impulsivity as well as emotional dysregulation. With a worldwide prevalence estimated at around 5-10% in children and 2-4% in adults (Fayyad *et al.*, 2007) ADHD constitutes one of the most common neuropsychiatric disorders.

Published in 1994 by the American Psychiatric Association, the fourth edition of the Diagnostic and Statistical Manual of Mental Disorders (DSM-IV) describes distinct diagnostic criteria for ADHD, essentially listing two main dimensions as inattention and hyperactivity/impulsivity. For diagnosis of ADHD, a sufficient number of symptoms of at least one dimension must have appeared within the past six months and to an extent that is maladaptive and not appropriate to the child's developmental stage. If at least six of nine symptomatic criteria of both dimensions are met, the combined subtype of ADHD is diagnosed. By contrast, if only one dimension applies, it will be referred to as a predominantly inattentive or hyperactive subtype, respectively. In any case, some maladaptive symptoms have to emerge before the age of seven and in more than one area of the child's life (e.g. at home and in school).

Despite ADHD being rather known as a childhood disorder, it has been found to exhibit a high degree of persistence into adolescence and adulthood, amounting to approximately 40-60% (Faraone *et al.*, 2006). Whereas symptoms of hyperactivity tend to decline with increased age or change into the feeling of inner restlessness, attention deficits frequently remain and are for example manifest in daydreaming or poor concentration. ADHD often involves severe impairments affecting the academic, economic and social life of patients. Among others, ADHD status tends to be a predictor for antisocial behaviour, substance abuse and unemployment (Barkley *et al.*, 2004; Halmøy *et al.*, 2009).

1.1.2 Comorbidities

ADHD patients are known to show significantly higher prevalence of comorbid psychiatric disorders throughout their lifespan. During childhood, ADHD is often accompanied by oppositional defiant disorder, followed by anxiety and learning disorders, mood disorders as well as conduct disorder, whereas the most frequent comorbidities in ADHD adults are anxiety and mood disorders as well as antisocial and substance use disorders (Biederman, 2005).

1.1.3 Therapy

ADHD therapy involves a range of pharmacological and non-pharmacological interventions that mainly aim to reduce symptoms and help patients to cope with their situation. Pharmacotherapy is primarily based on psychostimulants such as methylphenidate or d-amphetamine. However, non-stimulants including clonidine or atomoxetine have also been shown to treat ADHD with some efficacy (for a review, see Antshel *et al.*, 2011). Most ADHD drugs target the central monoaminergic systems, and particularly the neurotransmitters dopamine and norepinephrine. For example, MPH is referred to as a dopamine and norepinephrine transporter blocker (Hannestad *et al.*, 2010) while clonidine is considered an α_2-adrenoceptor agonist (Fu *et al.*, 2001). Such pharmacological interventions are generally thought to increase the synaptic availability of particular monoaminergic neurotransmitters.

On the other hand, several non-pharmacological treatments are available for ADHD, such as cognitive behavioural therapy, school interventions or parent training in behaviour management. In many cases an individualised multimodal therapy is recommended, namely a combination of both pharmacological and non-pharmacological interventions, especially if treatment is not restricted to the amelioration of mere symptoms but also includes practices in social or self-structuring skills which are often poorly developed in ADHD patients.

1.1.4 Heritability and molecular genetics

It has been known for many decades that ADHD symptoms tend to aggregate in families both within and across generations. Numerous family, twin and adoption studies emphasise the comparably strong genetic component of ADHD, with a heritability ranging at approximately 0.76 (Faraone *et al.*, 2005). However, similar to many other neuropsychiatric disorders, the genetic background of ADHD is considered complex and heterogeneous, implicating a multitude of potential risk genes with a likely modest to very small individual contribution to the pathogenesis.

Concerning the molecular genetics of ADHD, important progress has been made by means of genome-wide linkage scans that help to find chromosomal regions shared unusually often within ADHD-affected families. Typically, this method relies on a vast panel of genetic markers spread out across the genome and whose segregation pattern is compared among family members. In a meta-analysis estimating the results of seven genome-wide linkage studies of ADHD, Zhou and colleagues found 10 different genomic regions with at least nominally significant linkage signals, albeit with only 16q23.1 reaching genome-wide significance (Zhou *et al.*, 2008). Given that linkage studies largely serve to identify loci with moderate or large effects, other strategies, and particularly via the genome-wide association study (GWAS) methodology, have to be pursued in discovering common genetic variants with minor effects. A GWAS is typically based upon a large array of genome-wide distributed genetic markers such as single-nucleotide polymorphisms (SNPs), yet unlike linkage scans the focus does not lie on extended pedigrees but rather on huge cohorts of patients that are compared with unaffected subjects (case-control design). Remarkably, most GWASs to date have not been successful in discovering variants that reached genome-wide significance in terms of an association with ADHD (Hinney *et al.*, 2011), underlining the polygenic and multifactorial character of this disorder. Nonetheless, such studies have contributed to finding new potential risk genes, for example *CDH13,* which reached high rankings in a reproducible manner (Banaschewski *et al.*, 2010).

Another genome-wide approach to investigate ADHD-linked genes has recently emerged, namely copy number variation (CNV) studies. These analyses help to detect micro-duplications and micro-deletions in the genome possibly implicated in the pathogenesis of ADHD. Thus far, several CNVs of potential relevance have been suggested, including a duplication comprising the gene for the neuropeptide Y (*NPY*; Lesch *et al.*, 2011), a deletion affecting the gene for the metabotropic glutamate receptor 5 (*GRM5*; Elia *et al.*, 2012), and a duplication involving the gene *CHRNA7* which encodes the alpha-7 subunit of the neuronal nicotinic acetylcholine receptor (Williams *et al.*, 2012).

Besides these hypothesis-free approaches, there have also been numerous ADHD candidate gene association studies in recent years, concentrating on selected genes which were supposed to play a role in the disorder, based upon theoretical or empirical hints. Among all investigated genetic loci, those closely related to monoaminergic neurotransmission were the most frequent. For instance, significant association with ADHD was reported for genes of the D4 dopamine receptor (*DRD4*), the D5 dopamine receptor (*DRD5*), the dopamine transporter (*DAT*, *SLC6A3*), the dopamine beta-hydroxylase (*DBH*), the serotonin transporter (*5-HTT*, *SLC6A4*), the serotonin 1B receptor (*HTR1B*) and the synaptosomal associated protein of 25kDa (*SNAP25*; Faraone and Mick, 2010).

1.1.5 Environmental risk factors

Besides the important influence of heritability on the pathophysiology of ADHD, various environmental risk factors are also considered playing a role, including certain substances, such as polychlorinated biphenyls (PCBs) and also foetal exposure to alcohol or maternal smoking. Moreover, pregnancy and delivery complications, a low birth weight as well as psychosocial adversity, e.g. maltreatment and emotional trauma, have also been shown to correlate with the disorder (for a review see Banerjee *et al.*, 2007).

Besides, it has been suggested that an interplay between genes and environment (G × E interaction) may reflect an important cause of phenotypic complexity of ADHD. For example, Kahn and colleagues reported an association between a 480-

bp *SLC6A3* risk allele and impulsivity/hyperactivity in children, albeit only when these children had been previously exposed to maternal prenatal smoking (Kahn *et al.*, 2003).
Therefore, despite the origins of ADHD apparently lying in genes, the course of the disorder may be considerably affected by the manner in which these inherited factors modulate the response to environmental conditions.

1.1.6 Neurobiology

Concerning the neurobiology of ADHD, dysregulations of different central neurotransmitter systems belong to the major aspects being discussed. These concepts initially arose from the observation that many substances known as being efficacious in treating ADHD seem to share a common mechanism of action, namely an impact on monoaminergic neurotransmission. For instance, this includes the aforementioned compounds methylphenidate and atomoxetine, which block the dopamine and/or norepinephrine transporter, and the selective serotonin-norepinephrine reuptake inhibitor venlafaxine (Muth *et al.*, 1986).

A multitude of insights has been gained via structural neuroimaging studies in search of neuroanatomical correlates of ADHD. Among other things, it could be shown that overall brain volumes of children with ADHD were consistently reduced in comparison to healthy controls throughout childhood and adolescence (Castellanos *et al.*, 2002). More precisely, decreased volumes were reported for brain regions such as cerebellum, frontal cortex and basal ganglia, with the latter two regions also found to exhibit alterations in structural symmetry (for a review, see Krain and Castellanos, 2006). In a meta-analysis conducted by Frodl and Skokauskas, further regions were described as being volumetrically different in ADHD patients, including the anterior cingulated cortex and the amygdala (Frodl and Skokauskas, 2012).

In parallel to these structural findings, ADHD patients were also found to display functional anomalies in particular parts of their brain. A consistent pattern of dysfunction could be discovered by means of neuropsychological approaches and functional imaging techniques such as single photon emission computed tomography (SPECT), functional magnetic resonance imaging (fMRI), positron emission

tomography (PET) or electroencephalography (EEG), not only in prefrontal and dorsal anterior cingulate cortex but also in striatal parts like the caudate and putamen as well as in other regions such as the parietal cortex, thalamus and cerebellum (for a review, see Bush *et al.*, 2005).

Based on these and other findings, it has been suggested that ADHD is accompanied by dysfunctions of frontal–striatal–cerebellar circuits, resulting in distinctive intermediary traits. Rather known as 'endophenotypes' and located at the level between gene function and behaviour, these heritable traits are thought to constitute objective quantitative parameters, possibly helping to predict an individual's risk of developing the characteristic behavioural symptoms of a disorder. In terms of ADHD, deficits in response inhibition, temporal processing and working memory, as well as shortened delay gradients are discussed as promising endophenotypes (for a review, see e.g. Rommelse, 2008).

1.1.7 Animal models

Animal models can be valuable when investigating human phenomena as they provide certain advantages. For instance, they allow a large variety of interventions, often display a high degree of genetic homogeneity and can be assessed in a controlled environment. However, an animal model should be reasonably similar to human cases with regard to behaviour, physiology, symptomatology and treatment. To estimate their validity, animal models of human mental disorders typically are evaluated based on three criteria, namely construct validity, face validity and predictive validity (Willner, 1986). While construct validity refers to the model's theoretical rationale, face validity describes the ability to mirror the basic behavioural characteristics of the disorder and predictive validity assesses the model's efficiency in predicting certain aspects of the disorder, for example with regards to pharmacological treatment.

Various potential animal models of ADHD have been developed and described in the literature in recent decades. Despite several of these models not meeting all three validation criteria, at least face validity is a very common feature, and especially in terms of hyperactivity. Beyond that, many models show predictive validity in terms of

treatment with ADHD drugs. However, construct validity is only insufficiently fulfilled by many animal models of ADHD, not least due to the complex pathology of ADHD (Kostrzewa *et al.*, 2008).

Irrespective of validity, animals proposed as ADHD models can be divided into subcategories, depending on the method used to generate them. For instance, there are some animal models of ADHD – in this case rat models – that were produced by physical trauma, such as x-radiation (Gazzara and Altman, 1981) or hypoxia (Gramatte and Schmidt, 1986), while other ADHD models were obtained via pharmacological interventions, for example exposure to lead, cadmium or 6-hydroxydopamine during early stages of development (Kostrzewa *et al.*, 2008). However, many of these models only partially mimic ADHD symptoms, or are so remote from ADHD etiology that they did not attract significant publicity.

Another subcategory of potential ADHD models - and maybe the most popular - comprises animals with genetic peculiarities. One of the most widely studied animal models for ADHD is the Spontaneously Hypertensive Rat (SHR) which was obtained by inbreeding the Wistar-Kyoto (WKY) strain. Besides high blood pressure, these rats also display ADHD-like symptoms, in terms of increased impulsivity, lack of attention and hyperactivity with this latter symptom shown to be ameliorated by treatment with ADHD drugs (Sagvolden, 2000). Furthermore, frequently used genetic ADHD models include the *Dat/Slc6a3* knockout Mouse which was developed by targeted genetic engineering, as well as the Coloboma Mutant Mouse, produced as a product of neutron irradiation and exhibiting mutations which include the gene *Snap25*. Both of these murine ADHD models were shown to fulfill face validity as well as predictive validity criteria (for a review, see Arime *et al.*, 2011).

1.2 Glucose transporters

The monosaccharide glucose constitutes one of the most important molecules in the energy metabolism of nearly every organism, acting as a substrate for both catabolic and anabolic processes. Given that plasma membranes are impermeable for hydrophilic molecules, the transport of glucose from extracellular fluid into the cell requires the presence of particular transporter proteins.

Two glucose transporter families can essentially be distinguished: on the one hand, the group of sodium glucose-linked transporters (SGLTs), which belong to the

SLC5A gene family and mediate the secondary active co-transport of glucose; and on the other hand, the group of facilitative glucose transporters (GLUTs), encoded by the *SLC2A* gene family and enabling the passive diffusion of glucose into a cell.

1.2.1 The *SLC2A* family of glucose transporters (GLUTs)

In the majority of mammalian tissues, glucose uptake is mediated via glucose transporters of the GLUT protein family, which belongs to the Major Facilitator Superfamily (MFS) of membrane transporters (Pao *et al.*, 1998). At present, the GLUT protein family is known to comprise 14 isoforms, each displaying particular properties in terms of kinetics, substrate specificity and tissue expression. However, members of this family also share several common features given that they all facilitate the bidirectional energy-independent transport of glucose and/or other hexoses, and all are characterised by twelve transmembrane spanning helices and an oligosaccharide side chain located either on the first or fifth extracellular loop (see Figure 1).

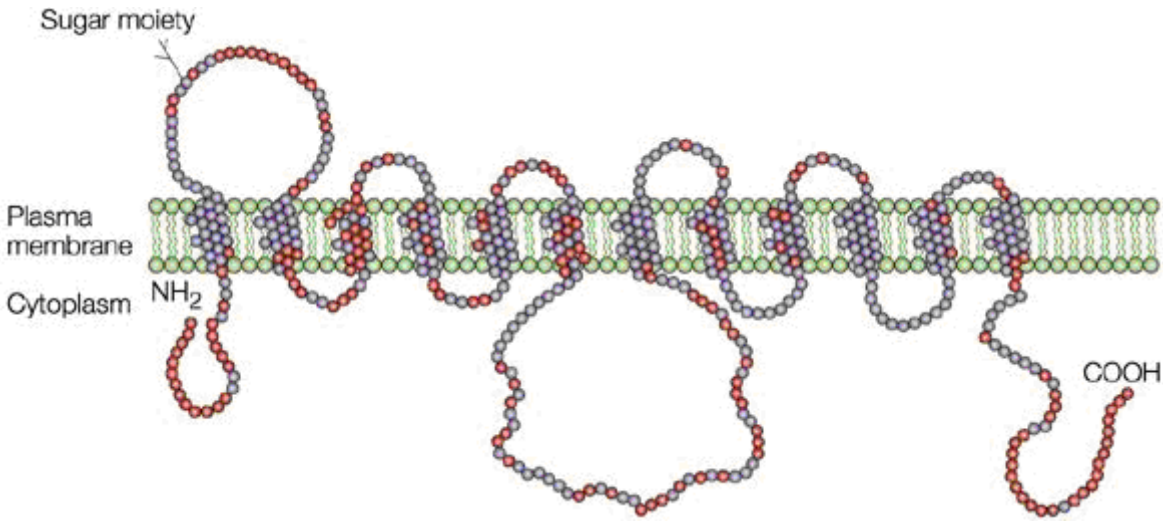

Fig. 1: Schematic illustration of a facilitative glucose transporter

Displayed are the characteristic 12 transmembrane segments, connected by intra- and extracellular loops that can exhibit oligosaccharide side chains (sugar moieties). The amino- (NH2) and the carboxy-terminus (COOH) are both located intracellularly. The image includes a homology plot between GLUT1 and GLUT4, with amino acid residues being unique to GLUT4 highlighted in red [adapted from Bryant *et al.*, 2002].

Based on similarities of primary sequence, three subclasses of glucose transporters can be distinguished. Class I includes the ‘classical’ isoforms GLUT1-4 and GLUT14, which is a highly similar paralog of GLUT3. Class II comprises the ‘odd’ transporters GLUT5, 7, 9 and 11, while class III involves the even number isoforms (GLUT6, 8, 10 and 12) as well as the proton-dependent myoinositol transporter HMIT (GLUT13) (see Figure 2).

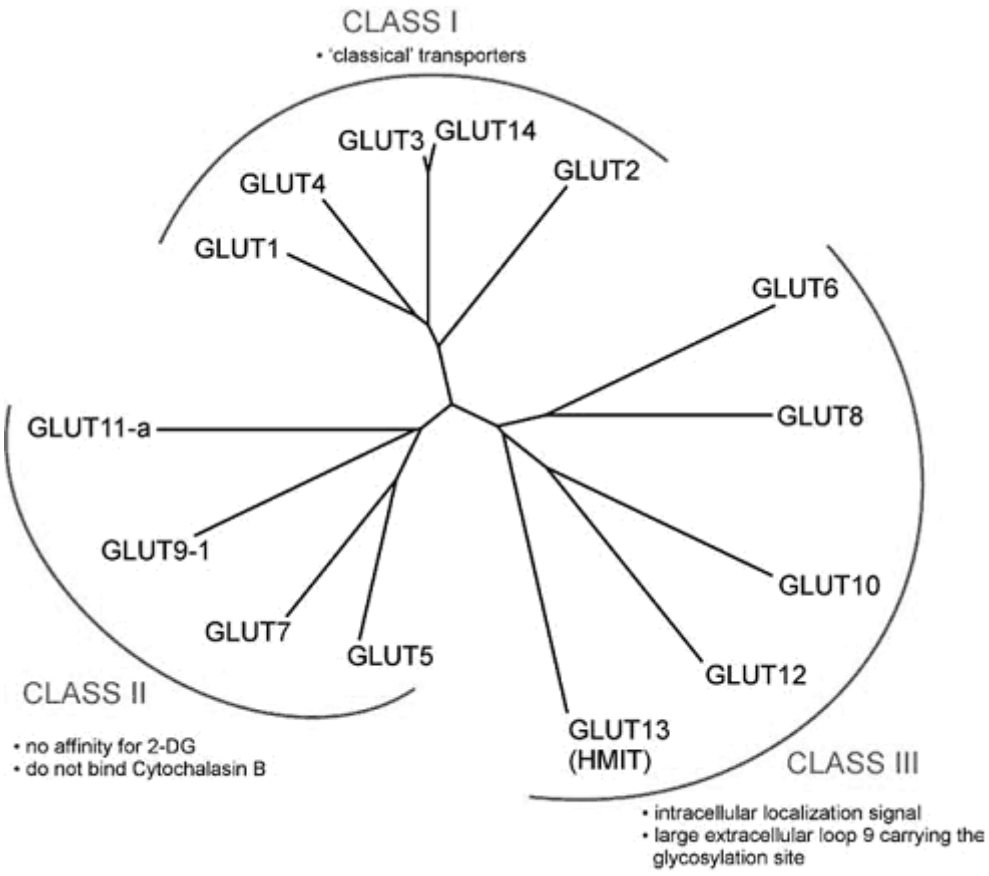

Fig. 2: Overview of the family of facilitative glucose transporters

Based on sequence similarities, the 14 members of this family can be subdivided into 3 different classes [adapted from Augustin, 2010].

1.2.2 The glucose transporter GLUT3

As implied by its name, the protein GLUT3, which is encoded by the gene *SLC2A3,* was the third glucose transporter isoform to be cloned (Kayano *et al.*, 1988). The human gene is located at the short arm of chromosome 12, with a size of approximately 17 kb. Currently, the database Ensembl (www.ensembl.org) lists eleven human *SLC2A3* mRNA transcripts, although only two are described as protein-coding. The first of these two transcripts contains all ten exons of the gene and leads to a protein of 496 amino acids (53.9 kDa), whereas the other only includes parts of the coding sequence (4 exons), thus producing a 142 amino acid protein (15.0 kDa).

SLC2A3 was shown to be expressed in various peripheral tissues such as placenta and kidney (Kayano *et al.*, 1988), and also in skeletal muscle (Stuart *et al.*, 1999), white blood cells (Mantych *et al.*, 1992) and testis (Haber *et al.*, 1993). However, the gene is predominantly known for its high expression in the brain, where GLUT3 is suggested to constitute the main neuronal glucose transporter, thus assuring the extensive energy supply of these cells (Kayano *et al.*, 1988; Nagamatsu *et al.*, 1992; Vannucci *et al.*, 1997).

At the subcellular level, GLUT3 is primarily located in the plasma membrane, i.e. the cell surface. However, in certain cell types considerable amounts of this protein were found enclosed by intracellular vesicles. In 1997, for example, Heijnen and colleagues reported on the appearance of GLUT3 in α-granule membranes of platelets (Heijnen *et al.*, 1997). Within neurons and PC12 cells, the transporter was described as located within a distinct homogenous population of synaptic-like vesicles (Thoidis *et al.*, 1999). In both cases, it was suggested that GLUT3 is stored within these intracellular membranes until eventually being translocated to the cellular surface.

From a structural perspective, GLUT3 essentially displays the characteristic features of a class I glucose transporter, among others 12 transmembrane domains (TM) and a long extracellular loop between TM1 and 2, including a glycosylation site. However, compared to other class I facilitative glucose transporters, GLUT3 was shown to

exhibit a quite low K_m value for glucose, implicating a strong affinity for this particular carbohydrate (for a review, see Simpson *et al.*, 2008). Nevertheless, glucose is not the only molecule conveyed by GLUT3 as some other hexoses and closely related compounds, such as galactose, mannose or dehydroascorbic acid also serve as adequate substrates (Gould *et al.*, 1991; Rumsey *et al.*, 1997).

1.2.3 Clinical background of *SLC2A3*

Recent animal and human studies have suggested that *SLC2A3* plays a role in several psychiatric disorders. In 2008, Liu and colleagues reported on a correlation between decreased central levels of GLUT3 and histopathological indications of Alzheimer disease, such as hyperphosphorylation of tau protein in the human brain (Liu *et al.*, 2008). Furthermore, a genome-wide expression analysis in schizophrenia, published in 2009, revealed several genes - amongst others *SLC2A3* - whose expression was significantly altered in the patient group (Kuzman *et al.*, 2009). The authors of another genome-wide scan, in this case concerning dyslexia, concluded that a two-marker haplotype which could be associated with a particular neurophysiological endophenotype of dyslexia had a transregulatory impact on *SLC2A3* expression (Roeske *et al.*, 2011).

A rodent study focusing on mice heterozygously deficient for *Slc2a3*, listed some behavioural peculiarities including that these genetically modified mice were found to exhibit perturbed cognitive flexibility, impaired social behaviour and reduced vocalization at low-frequency, as well as stereotypic behaviours in certain environmental conditions. Based on these observations, the authors suggested that *Slc2a3* haploinsufficiency in mice leads to characteristic features, resembling symptoms typically found in patients with autism spectrum disorders (Zhao *et al.*, 2010).

In addition, *SLC2A3* was identified by two unrelated genome-wide copy number variation (CNV) scans, both initiated in order to discover micro-duplications and micro-deletions potentially implicated in certain psychiatric disorders. While the first study analysed a three-generation Old Order Amish pedigree with the focus on affective disorders (Yang *et al.*, 2009), the latter was conducted in a cohort of European ADHD patients (Lesch *et al.*, 2011). Interestingly, both studies detected a

duplication on chromosome 12p13.31, which is known as a common CNV in the general population. The duplicated chromosomal region has a size of approximately 130kb, and encompasses the entire gene locus of *SLC2A3* and the pseudogene *NANOGP1* as well as the anterior exons of *SLC2A14*.

A significant excess of *SLC2A3* duplication carriers was found in a subsequent analysis of a German population sample (251 childhood and 675 adult ADHD cases vs. 767 controls): while 4.9% of cases displayed this CNV, it was only 2.6% of subjects in the control group (Merker *et al*., manuscript in preparation). Moreover, the same study showed that the T-allele of the SNP rs12842, which is located within the 3'UTR of the *SLC2A3* gene, is significantly associated with ADHD in an analysis of four European population samples.

1.3 Latrophilins

1.3.1 Discovery

Latrophilins were originally discovered as receptors for α-latrotoxin (α-LTX), a potent neurotoxin and component of the black widow spider (*Latrodectus mactans*) venom (Davletov *et al.*, 1996; Krasnoperov *et al.*, 1997), which exerts its toxic effects by inducing a massive release of neurotransmitters and hormones from various secretory cells in vertebrates (Grishin, 1998).

Besides latrophilins, two other proteins were found to bind this toxin specifically: neurexins and protein tyrosine phosphatase σ (Ushkaryov *et al.*, 1992; Krasnoperov *et al.*, 2002). Despite the mechanism of action being complex and thus still subject of research, it has been known for many years that α-LTX-triggered neuronal exocytosis can occur both in the presence and in absence of extracellular Ca^{2+}-ions, although not in absence of toxin-specific receptors (for a review, see Ushkaryov *et al.*, 2008).

Given that Ca^{2+}-influx is not required for latrophilin-mediated toxic effects, latrophilins are also referred to as **C**a^{2+}-**i**ndependent **r**eceptors of α-**L**TX (CIRLs) or as Lectomedins – a term derived from the names of certain protein domains in these receptors (see description below).

1.3.2 Latrophilin family

Three latrophilin homologs can be distinguished in human (latrophilin-1, -2 and -3), encoded by the genes *LPHN1, 2* and *3* at chromosome 19, 1 and 4, respectively.

The three members of this family exhibit a notable rate of sequence homology that gives rise to a very similar protein structure. However, it has been suggested that latrophilin proteins of the same type from different animal species show higher rates of identity than different latrophilin homologs within the same species which is indicative of a considerable level of specialisation (Matsushita *et al.*, 1999). According to the database Ensembl (www.ensembl.org), latrophilin orthologs can be found in more than 40 different animal species including not only mammals such as chimpanzees, mice or dogs but also members of other biological classes, such as amphibians, reptiles, birds, fishes and nematodes. A very common characteristic of the family of latrophilins is the presence of multiple splicing sites which result in different protein variants, exhibiting modifications in several intra- and extracellular domains (Matsushita *et al.*, 1999).

However, the members of the latrophilin family show considerable differences concerning their interaction with α-LTX: while latrophilin-1 binds the toxin with comparatively high affinity, latrophilin-2 and latrophilin-3 display only weak intermolecular interaction, if at all (Sugita *et al.*, 1998; Ichtchenko *et al.*, 1999).

1.3.3 Expression

The majority of published data about latrophilin expression arises from experiments with human and rat tissue, namely species that exhibit three different latrophilin homologs. *Lphn1* was shown to be expressed highly in the brain, and to a lesser extent, in other tissues, for example lung, kidney and spleen (Sugita *et al.*, 1998; Matsushita *et al.*, 1999). By contrast, *Lphn2* tissue expression appears to be much more universal and widespread. Furthermore, it was found preferentially outside of the brain, and particularly in lung, liver and placenta (Ichtchenko *et al.*, 1999). While most tissue-specific expression was displayed by *Lphn3*, which could be detected particularly in the brain, the absolute amounts of *Lphn3* transcript in rat brain were apparently lower than those of *Lphn1* (Matsushita *et al.*, 1999). In humans, *LPHN3* mRNA showed a non-uniform distribution within the brain, preferentially occurring in regions such as the amygdala, cerebellum and cerebral cortex, indicative of a high

level of functional specialisation (Arcos-Burgos *et al.*, 2010). A comparable expression pattern can be found in mouse brain with high *Lphn3* mRNA levels in regions such as the cerebral cortex, hippocampus and cerebellum (see Figure 3).

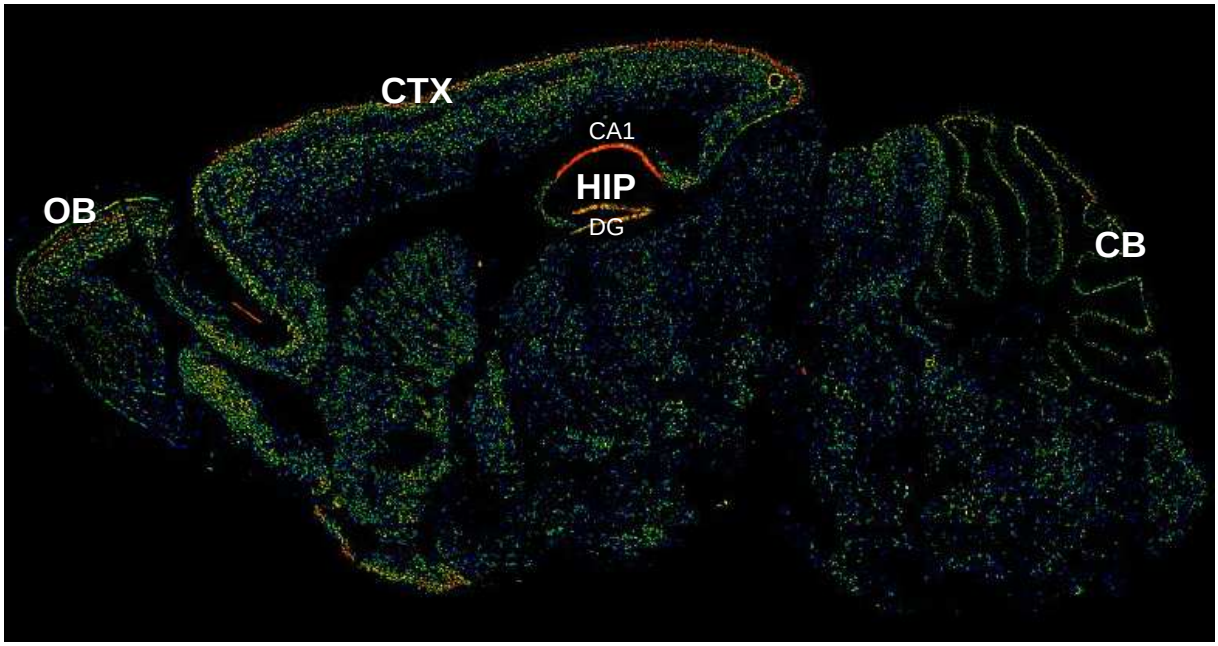

Fig. 3: *Lphn3* in situ hybridisation of a sagittal mouse brain slice (expression mask image)

Lphn3 gene expression is highlighted based upon the following heat map colour scale:

The brain regions with prominent *Lphn3* gene expression include the cerebral cortex (CTX), the olfactory bulb (OB) and the cerebellum (CB), as well as some divisions of the hippocampus (HIP), especially the CA1 layer and the dentate gyrus (DG) [adapted and modified from Allen Brain Atlas, www.brain-map.org].

1.3.4 Protein structure

Latrophilins are integral membrane proteins that belong to the prominent group of G protein-coupled receptors (GPCRs): a superfamily which comprises more than 800 members (Katritch *et al.*, 2012). Despite latrophilins exhibiting the common GPCR-topology of 7 transmembrane spanning α-helices, they still substantially differ from most other members of this protein family in terms of their peculiar domains (see Figure 4).

The intracellular (i.e. carboxy terminal) region of latrophilins contains multiple potential sites for phosphorylation and palmitoylation which are presumably involved in the modulation of receptor activity. Moreover, various PEST sequences (rich in proline, glutamic acid, serine and threonine) can be found (Matsushita *et al.*, 1999).

Latrophilins are confined to the plasma membrane via seven hydrophobic trans-membrane segments (TMs), resembling those found in secretin/calcitonin GPCRs: a family of receptors whose members often bind peptide hormones and are implicated in secretory processes (Lelianova *et al.*, 1997).

The extracellular (i.e. amino-terminal) division of a latrophilin receptor includes motifs with remarkable sequence similarity to rather uncommon molecules, for instance a rhamnose binding lectin-like domain and an olfactomedin-like domain.

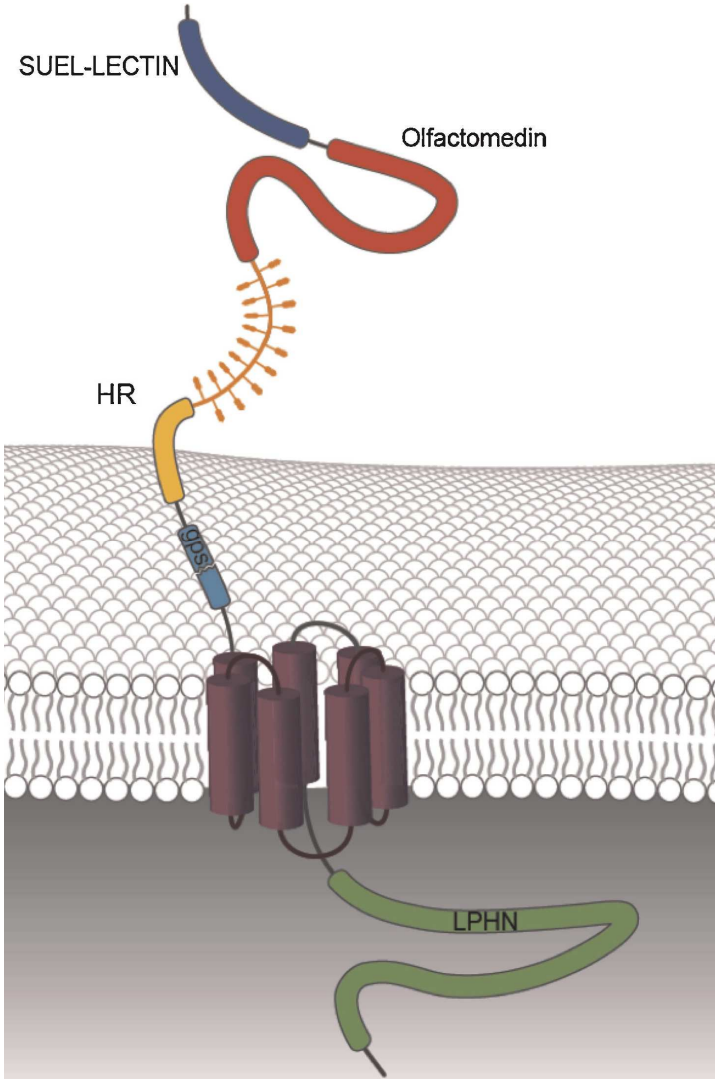

Fig. 4: Schematic illustration of the general latrophilin protein structure

The protein essentially consists of a long extracellular part connected to the intracellular latrophilin tail (LPHN) via seven transmembrane helices. Among others, the extracellular part comprises a sea urchin egg lectin-like (SUEL) domain, an olfactomedin-like domain and a GPCR proteolysis site (GPS), as well as a homology region (HR) shared with brain-specific angiogenesis inhibitors [adapted from Domene *et al.*, 2011].

While the first was originally described as a protein domain in eggs of sea urchins, playing a role for monosaccharide recognition (Ozeki *et al.*, 1991), the latter is known from olfactomedins, a multifaceted family of secreted glycoproteins likely implicated in mechanisms such as chemoreception (Snyder *et al.*, 1991). Moreover, the extracellular division of latrophilins exhibits a homology region shared with brain-specific angiogenesis inhibitors, with these molecules constituting another family of GPCRs, comprising three members (BAI1, 2 and 3) and possibly playing a role in the suppression of glioblastoma (Shiratsuchi *et al.*, 1997). On the other hand, the extracellular latrophilin division exhibits both a hormone receptor domain and a short cysteine-rich sequence, thus two motifs also shared by other GPCRs (Perrin *et al.*, 1998; Sugita *et al.*, 1998). Importantly, the cysteine-rich domain comprises a GPCR proteolysis site (GPS) located approximately 20 amino acids upstream of the first transmembrane segment. Cleavage at this site gives rise to two fragments: an extracellular amino-terminal subunit and a (smaller) carboxy-terminal subunit confined to the membrane. According to their approximate molecular weight [kDa] observed during electrophoresis, the first fragment was termed p120 and the latter p85 (Krasnoperov *et al.*, 1997).

Like other GPCRs containing such a proteolysis site, latrophilins were suggested to undergo proteolytic processing in the endoplasmic reticulum. After cleavage, the two resulting subunits were demonstrated as remaining non-covalently bound to each other at the cell surface although, they can also dissociate again under certain conditions (Krasnoperov *et al.*, 2009). Remarkably, upon binding of α-LTX to the p120 fragment, both subunits reassemble and induce intracellular signalling cascades (Silva *et al.*, 2009).

1.3.5 Functions

Given that the p120 subunit of latrophilins contains several motifs that were demonstrated as participating in cell adhesion processes (for instance the lectin-like domain and the olfactomedin-like domain), latrophilins are considered part of a subgroup of GPCRs: the so-called adhesion GPCR family (Fredriksson *et al.*, 2003). Members of this family are regarded as naturally occurring chimeras of cell adhesion molecules and signaling receptors, which are possibly able to convert cell–cell interactions into intracellular signals (Martinez *et al.*, 2011).

Like other GPCRs, latrophilins were shown to interact with intracellular G proteins – a prominent family of molecules implicated in transmitting signals from the outside to the inside of a cell. In 1997, Lelianova and colleagues reported that latrophilin-1 could be co-purified with the heterotrimeric G protein subunit $G\alpha_o$ in brain extracts of rat and cow and also described that α-LTX-induced synthesis of the secondary messenger molecules inositol trisphosphate (IP_3) and cAMP is notably increased in COS cells transfected with latrophilin-1 (Lelianova *et al.*, 1997). Furthermore, these results were confirmed and supplemented by another group, who found that latrophilin signaling was not only linked to $G\alpha_o$ but also to $G\alpha_{q/11}$, namely a subunit known to induce phospholipase C-mediated intracellular signal transduction pathways (Rahman *et al.*, 1999). Important insights were also achieved concerning the potential physiological role of latrophilins by a study focusing on the arrangement of cell division planes during early embryogenesis of C. elegans. By interacting with a mitotic spindle orientation pathway, latrophilin-1 was shown to exert a remarkable influence on the anterior–posterior tissue polarity of the embryo, with the Lectin-like latrophilin domain found to be particularly important for this function (Langenhan *et al.*, 2009).

On the other hand, much effort has been applied towards discovering endogenous ligands of latrophilins during the past decade. Via affinity chromatography of the extracellular division of latrophilin-1, Silva and colleagues were successful in isolating a protein from rat brain extracts which they termed Lasso. This protein was found to constitute a splice variant of teneurin-2 known as a brain-specific orphan cell surface receptor implicated in processes such as synaptogenesis and neuronal pathfinding. In addition, this workgroup was able to prove that latrophilin-1 and Lasso form transsynaptic complexes capable of inducing presynaptic signal pathways (Silva *et al.*, 2011).

Shortly after, Boucard and colleagues surprisingly reported on a binding interaction between latrophilin-1 and neurexins, which (as previously mentioned) also belong to the group of α-LTX binding proteins. In this study, it was found that the olfactomedin-like domain of latrophilin-1 forms transsynaptic adhesion complexes with neurexins, thus suggesting that both receptors are part of the same molecular pathway (Boucard *et al.*, 2012).

While nothing is yet known about potential ligands for latrophilin-2, new insights have been gained regarding the third homolog. In 2012, a study was published demonstrating that FLRT3, a molecule belonging to the family of **f**ibronectin **l**eucine-rich **r**epeat **t**ransmembrane proteins with supposed functions in cell migration and axon guidance, is a specific endogenous ligand for latrophilin-3 (O'Sullivan *et al.*, 2012). Indeed, the authors provided evidence for a strong transsynaptic binding interaction between the ectodomains of both proteins, also finding that manipulations targeting these complexes gave rise to significantly reduced glutamatergic synapse densities in cultivated neurons.

1.3.6 Clinical background

Latrophilin genes, and especially *LPHN3*, have received increasing attention within clinical research in recent years. The gene coding for latrophilin-3 has been suggested as being involved in a wide range of pathological conditions such as brain ischemia (Bin Sun *et al.*, 2002), addiction (Liu *et al.*, 2006), cancer (Kan *et al.*, 2010), dyslexia (Field *et al.*, 2013) and autism (Gau *et al.*, 2012).

Moreover, *LPHN3* has also been investigated in the context of the psychiatric disorder ADHD. In 2010, Arcos-Burgos and colleagues published the results of a genetic linkage analysis conducted for a South American population isolate on the basis of microsatellite markers, with subsequent fine-mapping of targeted regions and the examination of several American and European population samples. The study revealed a risk haplotype in the *LPHN3* gene (chromosomal location: 4q13.2) that was significantly associated with ADHD (Arcos-Burgos *et al.*, 2010). Moreover, it could be demonstrated that this *LPHN3* susceptibility haplotype was accompanied by histological and functional changes including an inverse correlation between the dosage of the haplotype and the neuronal number in brain regions of the frontal–striatal–cerebellar circuit, as assessed by the ratio of N-acetylaspartate to creatine (Arcos-Burgos *et al.*, 2010). When undergoing neurophysiological tasks of cognitive response control, homozygous haplotype carriers were also found to make more omission errors and show less NoGo-Anteriorisation which represents a marker of prefrontal functioning (Fallgatter *et al.*, 2012).

Beyond these human studies, some ADHD-related publications have also analysed the role of latrophilin-3 orthologs in other animals. For instance, the corresponding gene *lphn3.1* was found to exert a considerable influence on the distribution and number of dopaminergic neurons in the ventral diencephalon of zebrafish (Lange *et al.*, 2012). Additionally, the authors showed that a loss of *lphn3.1* function led to a hyperactive/impulsive phenotype in zebrafish, which interestingly could be rescued by methylphenidate and atomoxetine, namely two drugs efficacious in treating ADHD.

On the other hand, a recent study with *Lphn3* mutant mice generated on the basis of gene-trap mutagenesis reported that a lack of *Lphn3* gene function gave rise to a number of phenotypical peculiarities (Wallis *et al.*, 2012). Among other things, these mutant mice displayed altered expression levels for several genes well-known from monoaminergic systems, as well as neurochemical changes in terms of increased serotonin and dopamine amounts in the dorsal striatum. Significantly, *Lphn3* mutant mice exhibited higher locomotor activity in the open field test than wildtype mice, both under normal conditions and following the application of a stimulant drug (cocaine).

1.4 Goals of this thesis

There is a notable social, scientific and economic interest in broadening the understanding and refining the treatment of mental disorders, given that they can have severe impacts on the lives of affected patients and their families. One of the most frequent psychiatric disorders, and particularly during childhood and adolescence, is the neurodevelopmental syndrome ADHD. Despite the complex and insufficiently understood mechanisms involved in its etiology, ADHD has long been known as a highly heritable disorder, which has prompted an intensive search of risk genes. Several genome-wide screenings focusing on ADHD were conducted in recent years, leading to the identification of numerous polymorphisms at different genetic loci, thus underlining the polygenic nature of this disorder. The list of detected polymorphisms included some located within the gene *SLC2A3,* coding for the glucose transporter isoform 3, and the gene *LPHN3*, encoding the latrophilin isoform 3.

Accordingly, the present thesis will focus on these two genes, albeit with different approaches:

In the first case, the role of *SLC2A3* polymorphisms (SNP and CNV) will be investigated in human. For this purpose, methods such as functional EEG measurements, gene expression analyses and cellular glucose uptake assays will be applied. The latter two methods will involve two easily available peripheral cell models: lymphoblastoid cell lines (LCLs) and native peripheral blood mononuclear cells (PBMCs).
The overall aim of all such methods is to elucidate the molecular and functional consequences arising from *SLC2A3* variants, with particular attention paid to the aforementioned duplication of this gene. Carriers of this duplication are expected to show gene dose-dependent elevated *SLC2A3* expression (~50%) on RNA and protein level, implicating higher cellular transport of glucose and consequently functional anomalies in the brain such as altered prefrontal activity.

With regards to *LPHN3,* the corresponding ortholog in mouse (*Lphn3*) will be investigated via the generation of a new genetically modified mouse model with conditional knockout potential.
In contrast to the aforementioned *Lphn3* gene-trap mice (Wallis *et al.*, 2012) which lack the gene in a constitutive-like manner, a conditional *Lphn3* knockout involves the advantage of latrophilin-3 deficiency being restricted to a particular cell type or a particular developmental stage, which might allow a more precise and compelling interpretation of the resulting phenotype. Based on the reported findings for different animal models of latrophilin-3 deficiency, it is expected that conditional *Lphn3* knockout mice show alterations in monoaminergic - especially dopaminergic - systems, and behavioural peculiarities resembling those traits typically observed in human ADHD patients.

Despite merely constituting small pieces within the huge puzzle of ADHD genetics, the expected results of theses analyses should contribute to the knowledge concerning the physiological and pathophysiological role of *SLC2A3* and *LPHN3*.

2 Material and Methods

2.1 Material

2.1.1 *SLC2A3*

Human samples

CNV gene expression analysis and cellular glucose uptake assay: For these cell culture-based experiments, participants with two gene copies (= control subjects) and with three copies (= duplication carriers) were recruited.

EBV-infected lymphoblast cell samples were part of a randomised population kindly provided by the workgroup of Prof. Dr. Clemens Müller-Reible (Department of Human Genetics, University of Würzburg). Among these were 15 control and 6 duplication samples, all deriving from subjects without any known psychiatric history. The remaining lymphoblast samples with *SLC2A3* duplication were obtained by means of blood samples from patients of the Department of Psychiatry in Würzburg (among these 8 ADHD patients and 2 patients with bipolar disorder). Since diagnostic status of duplication carriers did not turn out to have a notable influence on *SLC2A3* gene expression results, respective data were pooled.

On the other hand, native peripheral blood mononuclear cell (PBMC) samples were collected at the Department of Psychiatry in Würzburg. All respective duplication carriers were ADHD patients of the KFO125 Clinical Research Unit, whereas the control group with two gene copies consisted of healthy participants as well as ADHD patients. Again, diagnostic status did not exert a notable effect on *SLC2A3* gene expression so that data of control samples were pooled.

Functional EEG measurements: 144 adult ADHD in- and outpatients at the Department of Psychiatry in Würzburg (among these 38 rs12842 T-allele carriers) as well as 71 healthy controls (among these 14 rs12842 T-allele carriers) were recruited. On the other hand, 9 ADHD patients with *SLC2A3* duplication were compared to 9 ADHD patients with normal copy number. These groups were carefully matched with regard to age, gender, smoking status, handedness, medication and ADHD subtype-diagnosis. Additionally, two healthy control groups were analyzed, each exhibiting a size of 5 persons. One of these groups comprised duplication carriers and the other

one subjects with a copy number of 2. Again, groups were thoroughly matched in terms of the above-mentioned criteria (excluding medication and ADHD diagnosis).

SLC2A3 genotyping

Product / Device	Manufacturer
TaqMan Copy Number Assay for SLC2A3 (Hs04406005_cn)	Applied Biosystems
TaqMan RNase P Control Reagents Kit	Applied Biosystems
C1000 Thermal Cycler incl CFX384 Real-Time System	Bio-Rad
CopyCaller, version 1.0	Applied Biosystems
BAC clone RP11-277E18	BACPAC Resources
A1 epifluorescence microscope	Zeiss
FISHView EXPO, version 2.0	Applied Spectral Imaging
QIAquick PCR Purification Kit	Qiagen
BioPrime Array CGH Genomic Labeling System	Invitrogen
4000B scanner	Axon Instruments
Genepix, version 5.0	Axon Instruments
iPlex SNP assay	Sequenom
Autoflex mass spectrometer	Bruker Daltonics

Lymphoblast cell culture

Medium	Content	Manufacturer
Lymphoblast culture medium	RPMI 1640 Medium	Invitrogen
	17.5% HI FBS	Invitrogen
	1% L-Glutamine 200mM	Invitrogen
	1% Gentamicin 50mg/ml	Invitrogen

Product / Device	Manufacturer
Ficoll-Paque Plus	GE Healthcare
RNAprotect Cell Reagent	Qiagen
Leucosep 12 ml Tube	Greiner
Cellometer SD100 Counting Chambers	Nexcelom Bioscience
Cellometer Auto T4 cell counter	Nexcelom Bioscience

RNA extraction and quantitative reverse transcription (qRT) PCR

Product / Device	Manufacturer
RNeasy Plus Mini Kit	Qiagen
Experion automated electrophoresis station	Bio-Rad
iScript cDNA Synthesis Kit	Bio-Rad
NanoDrop ND-1000 Spectrophotometer	Peqlab
iQ SYBR Green Supermix	Bio-Rad
C1000 Thermal Cycler incl CFX384 Real-Time System	Bio-Rad
Bio-Rad CFX Manager	Bio-Rad
GeNorm, version 3.5	Ghent University Hospital
LinRegPCR, version 11.1	Academic Medical Center

Primer	Sequence	Manufacturer
SLC2A3 qRT forward	5'-GGGTATGATCGGCTCCTTTT-3'	Metabion
SLC2A3 qRT reverse	5'-GCATTTCAACCGACTTAGCTACT-3'	Metabion
HS_GAPDH_2_SG	Trade secret	Qiagen
HS_PGK_1_SG	Trade secret	Qiagen
HS_B2M_1_SG	Trade secret	Qiagen
HS_ALAS1_1_SG	Trade secret	Qiagen

Protein extraction and Western blotting

Solution	Content	Manufacturer
External chamber buffer	5% NuPAGE MOPS SDS Running buffer	Invitrogen
Internal chamber buffer	External chamber buffer 0.25% NuPAGE Antioxidant	in-house production Invitrogen
Loading buffer	5µl NuPAGE LDS Sample buffer 2µl NuPAGE Sample reducing agent Xµl protein lysate (10µg) 13 – Xµl ddH20	Invitrogen Invitrogen
Transfer buffer	5% Nupage Transfer Buffer 10% Methanol 0.1% NuPAGE Antioxidant	Invitrogen Merck Invitrogen
Stripping buffer	3mM SDS 200mM Glycine 1% Tween 20 0.1% NuPAGE Antioxidant, pH 2.2	AppliChem Fluka Sigma-Aldrich Invitrogen

Product / Device	Manufacturer
Complete Mini EDTA-free Protease Inhibitor Cocktail Tablets	Roche
BCA Protein Assay	Thermo Scientific
Novex Sharp Protein Standard	Invitrogen
Nitrocellulose Paper Sandwich 0.45µm pore size	Invitrogen
NuPAGE 4-12% Bis-Tris Gels, 1.0 mm	Invitrogen
ECL Prime	GE Healthcare
Multiskan Spectrum Microplate Spectrophotometer	Thermo Labsystems
ChemiDoc system	Bio-Rad
Quantity One, version 4.6.8	Bio-Rad
Aida 2D Densitometry, version 2.0	Raytest Isotopenmessgeräte
Multiskan Spectrum, version 1.0	Thermo Labsystems

Antibodies	Final concentration	Manufacturer
Rabbit Anti-GLUT3 [ab15311]	1/400	Abcam
Goat anti-rabbit IgG-HRP [sc-2054]	1/7500	Santa Cruz
Mouse anti-beta-actin (HRP) [ab20272]	1/10000	Abcam

Cellular glucose uptake assay

Product / Device	Manufacturer
2-Deoxy-D-Glucose-1,2-^{3}H(N), Specific Activity: 5-10Ci/mmol	Perkin Elmer
Cytochalasin B	AppliChem
RPMI 1640 Medium, no Glucose	Invitrogen
Rotiszint eco plus	Roth
LS6500 Multipurpose Scintillation Counter	Beckman Coulter

Functional EEG measurements

Device / Software	Manufacturer
32-channel DC BrainAmp amplifier	Brain Products
Brain Vision Recorder, version 1.01	Brain Products
Vision Analyzer	Brain Products

2.1.2 *Lphn3*

Lphn3 targeting vector

Product	Manufacturer
Lphn3 Knockout-First Targeting Vector (47572)	Helmholtz Center Munich
OneShot TOP10F´ Chemically Competent *E. coli*	Invitrogen
Endofree Plasmid Maxi Kit	Qiagen
Restriction endonuclease AsiS I	New England Biolabs

Murine embryonic stem (ES) cell culture

Medium	Content	Manufacturer
ES cell medium	Knockout DMEM Medium	Invitrogen
	1% L-Glutamine 200 mM (GlutaMAX)	Invitrogen
	0.2% Beta-mercaptoethanol 50mM	Invitrogen
	100U/ml Leukemia Inhibitory Factor (LIF)	Millipore
	15% HI FBS	Invitrogen
	1% Penicillin Streptomycin (Pen Strep)	Invitrogen
SNL cell medium	DMEM High Glucose Medium	Invitrogen
	10% HI FBS	Invitrogen
	1% MEM Non-Essential Amino Acids Solution	Invitrogen
	1% Penicillin Streptomycin (Pen Strep)	Invitrogen
Trypsin solution	PBS	Lonza
	0.25% Trypsin Solution	Invitrogen
	1% Chicken Serum	Invitrogen
	0.2g/L EDTA	Sigma
	1g/L D-Glucose → filter-sterilised (0.22µm)	Sigma
Cell lysis buffer	100mM Tris, pH 8.5	Roth
	5mM EDTA, pH 8.0	AppliChem
	0.2% SDS	AppliChem
	200mM NaCl	Sigma-Aldrich
	100µg/ml Proteinase K	AppliChem

Product	Manufacturer
JM8A3.N1 mouse embryonic stem cells	Sanger Institute
SNL 76/7 mouse fibroblast STO cell line	Sanger Institute
Mouse ES Cell Nucleofector Kit	Amaxa
Lookout Mycoplasma PCR Detection Kit	Sigma

PCR

Primer	Vector construct specificity	Sequence	Manufacturer
5' FRT site forward	-	5'-AAACGTAGGCAAGTAATTCACAAAA-3'	Metabion
5' FRT site reverse	Binds only within construct	5'-CCCAACCCCTTCCTCCTACATAGT-3'	Metabion
3' FRT site forward	Binds only within construct	5'-GGGTACCGCGTCGAGAAGTTC-3'	Metabion
3' FRT site reverse	-	5'-AGGACTTTACACACTTTGGCTTTTC-3'	Metabion
3' loxP site forward	-	5'-TCCGGGCACAGACGTCATCAT-3'	Metabion
3' loxP site reverse	Binds only within construct	5'-GGCGAGCTCAGACCATAACTTC-3'	Metabion
5' long-range forward	-	5'-CAGGTCTGGCAAATGGATGTTACAC-3'	Metabion
5' long-range reverse	Binds only within construct	5'-CCCAACCCCTTCCTCCTACATAGT-3'	Metabion
3' southern probe forward	-	5'-ATCCTCCCTCCAAACCCCATGT-3'	Metabion
3' southern probe reverse	-	5'-GGAACAGAAAGGTGGCACAACAGT-3'	Metabion

Product	Manufacturer
dNTPs (2.5mM)	Promega
Taq DNA polymerase	in-house production
iProof DNA polymerase	Bio-Rad
GeneRuler 100bp Plus DNA Ladder	Fermentas
GeneRuler 1kb DNA Ladder	Fermentas

Buffers	Content	Manufacturer
Standard PCR buffer	500mM KCl	Merck
	100mM Tris, pH 8.3	Roth
	15mM MgCl2	Fluka
	0.25% Tween 20	Sigma-Aldrich
	2.5% BSA	Sigma-Aldrich
iProof HF buffer		Bio-Rad

Southern blotting

Product	Manufacturer
MinElute Gel Extraction Kit	Qiagen
Maxtract high density tubes	Qiagen
Restriction endonuclease KpnI	New England Biolabs
Restriction endonuclease Spe I	New England Biolabs
GeneRuler 1kb DNA Ladder	Fermentas
GeneRuler 1kb Plus DNA Ladder	Fermentas
Nylon membrane, positively-charged	Roche
Prime-a-Gene Labeling System	Promega
[α-^{32}P]-dCTP, Specific Activity: 3000Ci/mmol (10mCi/ml)	Perkin Elmer
illustra MicroSpin S-400 HR Columns	GE Healthcare

Buffers	Content	Manufacturer
Depurination buffer	0.2N HCl	AppliChem
Denaturation buffer	0.5N NaOH 1.5M NaCl	AppliChem Sigma-Aldrich
Neutralisation buffer	0.5M Tris, pH 7.5 1.5M NaCl	Roth Sigma-Aldrich
Transfer buffer	20x SSC	Sigma-Aldrich
Hybridisation buffer	0.5M sodium phosphate 1mM EDTA 5% SDS 100µg/ml salmon sperm DNA	Merck Sigma AppliChem Invitrogen
Washing buffer 1	2x SSC 0.05% SDS	Sigma-Aldrich AppliChem
Washing buffer 2	0.1x SSC 0.1% SDS	Sigma-Aldrich AppliChem

2.2 Methods

2.2.1 *SLC2A3*

SLC2A3 genotyping

CNV: A TaqMan Copy Number Assay was performed to genotype the CNV comprising the *SLC2A3* gene locus, based on a quantitative PCR (qPCR) reaction. The TaqMan assay 'Hs 04406005_cn' produces an amplicon of 98 bp length, located within intron 6 of *SLC2A3* (Chr12: 8081061). While the 'Hs 04406005_cn' probe is labelled with a FAM-dye, the reference probe that targets the RNase P gene is VIC-dye-labelled. This gene was selected for normalisation as it is known to always have two copies.

The qPCR reaction mix contained 5µl TaqMan Universal PCR Mix, 3µl H_2O, 0.5µl TaqMan 'Hs 04406005_cn' solution, 0.5µl TaqMan RNase P solution as well as 1µl DNA (10ng/µl). The reaction took place in a CFX 384 PCR cycler using the following programme:

Step	Temperature	Number of cycles	Duration
Preheating	50℃	1	2min
Activation of enzyme	95℃	1	10min
Denaturation Annealing/Extension	95℃ 60℃	40	15sec 1min

During the programme, an automatic threshold in the logarithmic phase of the amplification was assessed and expression was indicated based upon cycle threshold (Ct) values. Data was analysed with the assistance of the CopyCaller software by assuming that the overall copy number of the samples is 2. Samples were measured in triplicates and repeated if different from 2 or showing a range greater than 0.5.

SNP: The SNP rs12842, located within the 3'UTR of the *SLC2A3* gene (see Figure 5), was investigated by the Sequenom iPlex method according to the manufacturer's instructions. PCR was performed using iPlex chemistry as recommended in the MassArray iPlex standard operating procedure and using 40ng genomic DNA. The SNP was then genotyped by primer extension and analysed by matrix-assisted laser-desorption/ionisation time-of-flight mass spectrometry (MALDI-TOF MS).

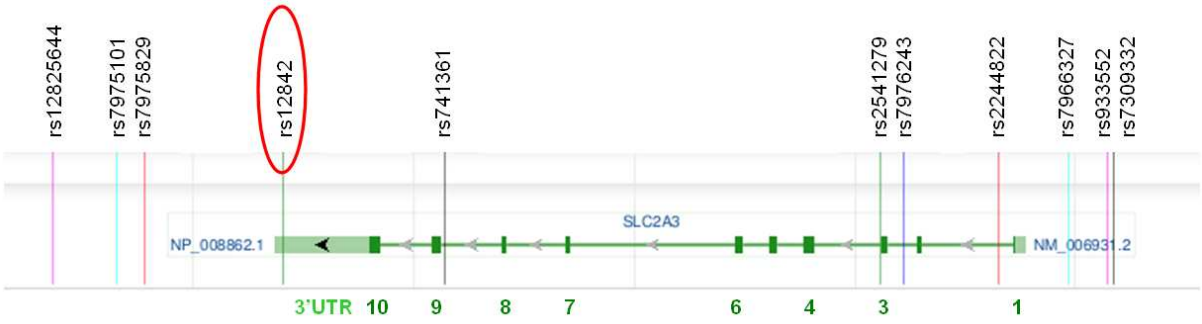

Fig. 5: Position of the SNP rs12842 within the *SLC2A3* gene

The location of eleven SNPs within and around the *SLC2A3* gene locus is illustrated. The exons of *SLC2A3* are represented by dark green rectangles and the SNP rs12842, located within the 3'UTR of *SLC2A3*, is highlighted in red [adapted and modified from www.ncbi.nlm.nih.gov/projects/SNP; hg19].

Confirmation of *SLC2A3* CNV genotyping

To confirm the results of the aforementioned TaqMan genotyping assay, Fluorescence *In Situ* Hybridisation (FISH) and Array Comparative Genomic Hybridisation (array CGH) was used. While the required cell lines and DNA samples were prepared at the Department of Psychiatry in Würzburg, the experiments themselves were conducted by Dr. Indrajit Nanda (Department of Human Genetics, University of Würzburg) and Dr. Reinhard Ullmann (MPI for Molecular Genetics, Berlin).

Fluorescence In Situ Hybridisation (FISH): lymphoblastoid cell lines were obtained from two individuals whose TaqMan results were suggestive of a *SLC2A3* duplication (3 copies), and also from a control subject with 2 copies. Metaphase chromosomes of LCLs were prepared according to standard procedures and the BAC clone RP11-277E18 was used, encompassing the region corresponding to the *SLC2A3* gene. By means of nick translation, BAC DNA was directly labelled with Fluorescein-12-dUTP, followed by overnight hybridisation to denatured chromosomal DNA. After counterstaining with DAPI and mounting in Antifade medium, slides were examined with an epifluorescence microscope.

Array Comparative Genomic Hybridisation (array CGH): Genomic DNA samples from twelve subjects with a TaqMan-assessed *SLC2A3* copy number of 3 were used together with reference DNA samples (two copies). For array CGH, total genomic DNA was sonicated to a length of 0.1-2kb, purified with a PCR Purification Kit and subsequently labelled by means of a Random Prime Labeling System, using Cy3-dUTP for sample DNA and Cy5-dUTP for reference DNA. After denaturation, labeled DNA samples were co-hybridised onto arrays of genomic BAC clones spotted on epoxy-coated slides, before finally high-stringency washed slides were analysed by means of an Axon 4000B scanner and the software Genepix. Fluorescence intensities of all spots were calculated after subtraction of local background and copy number variations were determined by conservative log2 ratio thresholds of 0.3 and -0.3, respectively.

Cell culture

Peripheral blood samples were collected in EDTA tubes and subsequently subjected to Ficoll density gradient centrifugation to isolate mononuclear cells (such as monocytes and lymphocytes). Around one half of this fraction was used directly as native samples (peripheral blood mononuclear cells, PBMCs) with the other half undergoing an immortalisation procedure based on Epstein-Barr virus (EBV) infection. For this purpose, cells were incubated overnight in medium supplemented by sterile-filtered supernatant of B95.8 monkey epithelial cells infected with EBV. The resulting immortalised cells which derive from b-lymphocytes and are known as lymphoblastoid cell lines were propagated in lymphoblast culture medium for several weeks.

RNA extraction and quantitative reverse transcription (qRT) PCR

PBS-washed PBMC or LCL pellets were stored in RNAprotect Cell Reagent at -20℃ until RNA extraction was performed. Total RNA of cells was isolated according to manufacturer's instructions by means of an RNeasy Plus Mini Kit. RNA concentration and purity were determined via a NanoDrop spectrometer, while RNA integrity was assessed based upon agarose gel electrophoresis and an automated electrophoresis system (Experion). For reverse transcription, a cDNA Synthesis Kit was used according to the supplier's protocol, with 500ng of total RNA serving as template. The resulting cDNA containing solution was diluted in TE buffer (1:5) and stored at -20℃.

The qRT-PCR took place in a C1000 Thermal Cycler whose wells contained a volume of 10µl each (5µl iQ Sybr Green Supermix, 3µl H_2O, 1µl primer and 1µl cDNA solution). Samples were run in triplicates and underwent the following programme:

Step	Temperature	Number of cycles	Duration
Initial denaturation	95℃	1	5min
Denaturation	95℃	40	10sec
Annealing/Extension	60℃		30sec
Melt curve	95℃ for 10sec, then gradient from 65 to 95℃ (temperature increment: 0.5℃ per 0.05sec)		

In addition to self-designed primers specific to human *SLC2A3* cDNA, Qiagen quantitect primers for human *PGK1, ALAS1, B2M* and *GAPDH* were used as loading controls. In order to determine mean PCR efficiency values for each primer, raw measuring data were processed by means of LinRegPCR software, and subsequently the relative *SLC2A3* expression was normalised according to the most stable loading controls, with the assistance of the software geNorm.

Protein extraction and Western blotting

PBS-washed PBMC or LCL pellets were sonicated in RIPA buffer supplemented by Protease inhibitors and resulting lysates were subjected to centrifugation at 10000g for 10min at 4℃. Protein concentration of supernat ants was assessed based upon a BCA assay using a microplate spectrophotometer. For LDS-based electrophoresis under reducing conditions, 10µg protein was loaded into each well of a 4-12% Bis-Tris Gel and subsequently transferred onto a nitrocellulose membrane. After blocking in Tris-buffered saline with 0.1% Tween-20 (TBS-T) containing 5% non-fat dry milk, the membrane was incubated overnight with Rabbit Anti-GLUT3 antibody. The following day, membrane was incubated with a secondary antibody (anti-Rabbit labeled with horseradish peroxidase) and then with ECL detection system (ECL Prime). Furthermore, the membrane was placed into a ChemiDoc system in order to take a photo of the chemiluminescence signal. After the removal of antibodies from the membrane via stripping buffer and blocking in TBS-T containing 5% BSA, the membrane was incubated with a loading control antibody directed against beta-actin and detected as described above. Densitometric quantification of GLUT3 protein amounts was performed by means of the software AIDA, and GLUT3 intensities were divided by the respective ones of the loading control (beta-actin) for normalisation.

Cellular glucose uptake assay

To measure glucose uptake in LCLs, every cell sample was cultivated under standardised conditions 48h prior to the experiment. For this purpose, PBS-washed LCLs were transferred from their normal culture flasks into 24-well plates with each well containing $5x10^5$ cells in 2ml lymphoblast culture medium.

On the day of the uptake measurement, cells were counted again with a cellometer, washed with PBS and pelletted. Each sample ($5x10^5$ cells) was subsequently incubated for 20min at 37℃ in 300µl glucose-free R PMI medium supplemented by 1.5µl ^{3}H-labelled deoxy-glucose. After centrifugation, cell pellets were washed with PBS and then lysed with 400µl 0.05N NaOH. Having added 4ml Rotiszint scintillation cocktail to every sample, radioactivity was measured via an LS6500 Multipurpose Scintillation Counter. Samples were run in pentaplicates along with ‘Cyt B control’ samples, incubated in the presence of cytochalasin B (100µM) in order to correct for non-specific glucose uptake.

Functional EEG measurements

Performed by Dr. Ann-Christine Ehlis (Department of Psychiatry, University of Tübingen), participants in this study were subjected to a Continuous Performance Test (CPT) and an n-back test. During both tasks, event-related potentials (ERPs), i.e. the electrophysiological responses of the brain to a specific stimulus, were measured via Electroencephalography (EEG).

CPT: This test is known as a neuropsychological task that helps to assess characteristics, such as selective attention and cognitive response control (Riccio *et al.*, 2002; Fallgatter *et al.*, 2012).
In our case participants sat in front of a computer screen showing a pseudo-randomised sequence set of 12 different letters with a stimulus presentation time of 200ms and an interstimulus interval of 1650ms. Whenever the letter 'O' was directly followed by the letter 'X', participants had to press the space bar of a keyboard (Go-condition) with their right hand, whereas and otherwise had to suppress this reaction in case any letter other than 'X' appeared (NoGo condition). The CPT started following a short training session and took approximately 13min. Both accuracy and response speed were emphasised.
An important CPT parameter is the so-called NoGo-Anteriorisation (NGA) that reflects the anteriorisation of the positive EEG field area (centroid) during the NoGo compared to the Go condition. Generally, NGA is considered a topographical ERP marker of cognitive response control, indicating prefrontal brain activity during motor inhibition (Fallgatter *et al.*, 2002).
For the calculation of the NGA values in the P300 time window (~300ms after the stimulus), the localisation of the NoGo centroid was subtracted from that of the Go centroid. Given that the measuring unit reflects the relative electrode position, an NGA value of 1.0 implies that the centroid is shifted precisely one electrode position in the anterior direction during a CPT NoGo trial.

n-back test: This task resembles the aforementioned CPT, yet is designed as a measure of working memory (Cohen *et al.*, 1997), with 9 different letters sequentially presented for this paradigm (using the same stimulus and interstimulus duration as described above). Participants had to press a response button whenever the current letter matched the one from *n* steps earlier in the sequence. In our case, both a 1-

back and a 2-back condition were carried out, each comprising 216 trails, and only trials with a correct response were included. Key measures of the test were perceptual sensitivity (participant's ability to distinguish between targets and non-targets) and response bias (participant's readiness to respond).

For both the CPT and the n-back, EEG signals were recorded from 21 scalp electrodes placed according to the international 10-20 system, by means of a 32-channel DC BrainAmp amplifier and the software Brain Vision Recorder. For the examination of eye movements (electrooculogram), three additional electrodes were placed around the eyes: two at the outer canthi of both eyes (reference for horizontal eye movements) and one below the right eye (reference for vertical eye movements). Ocular artifacts were corrected by means of an algorithm included in the Vision Analyzer software.

Statistical Analysis

Student’s t-test was used for gene expression analyses and cellular glucose uptake assay. However, if assumption of normal distribution could not be upheld, a Mann-Whitney-U (MWU) test was conducted instead.

For the EEG measurements, ANOVAs and Student’s t-tests for independent samples were applied to examine the potential influence of *SLC2A3* duplication status and rs12842 genotype on EEG data. Student’s t-tests for independent or matched samples were used to conduct post-hoc analyses and check potential effects of *SLC2A3* duplication status on reaction times, NGA values and Go/NoGo centroids. Furthermore, variables to which the assumption of normal distribution did not apply were confirmed using non-parametric testing.
All p-values smaller than 0.05 were considered statistically significant, whereas p-values between 0.1 and 0.05 were considered as a statistical trend.

2.2.2 *Lphn3*

The knockout technique

The principle of generating targeted and inheritable genetic mutations in mammals was developed in the 1980s, and has been primarily established for mice. If the introduced modification gives rise to a completely dysfunctional gene, it is referred to as being ‘knocked-out’ and the resulting mice are termed as ‘knockout mice’.
Several steps are necessary in achieving this goal, commencing with a gene-specific DNA vector that is transfected into cultivated murine embryonic stem (ES) cells. Those ES cells that have correctly integrated the modified allele into their genome by replacing the respective wildtype allele (homologous recombination) are selected and injected into early mouse embryos (morula or blastula stage). If implanted into the uterus of surrogate mothers, these embryos have the potential to develop into so-called chimeric mice, whose body cells derive both from injected and from host ES cells. After germline transmission of the modified allele, heterozygous offspring can be bred with each other in order to yield mice carrying the mutation homozygously.

Design of *Lphn3* targeting vector

With regard to the murine *Lphn3* gene, *in silico* analysis revealed that targeting its 6th exon should result in a reliable knockout allele, given that the excision of this 214bp DNA sequence produces a frameshift mutation and thus a premature stop codon in the 9th exon, giving rise to a truncated and likely non-functional protein.
We decided to use the so-called recombineering technique (recombination-mediated genetic engineering) to generate a DNA vector that targets *Lphn3* exon 6. This comparatively new method is based on insertion of DNA fragments into a plasmid backbone via homologous recombination which occurs *in vivo*, i.e. in certain E. coli strains, capable of expressing recombination genes of the bacteriophage λ (Copeland *et al.*, 2001).
A BAC clone (RP24-74E24) comprising parts of the murine *Lphn*3 genomic region was ordered at the BACPAC Resources Center (Oakland, USA) and electroporated into DY380 E. coli cells (Liu *et al.*, 2003). On the other hand, short homologous sequences, corresponding with parts of the *Lphn3* exon 6 region, were added to the high-copy plasmid PL253 (kindly provided by Dr. Tobias Langenhan, Department of Physiology, University of Würzburg) via an anchor primer-based PCR reaction. This

linear PCR product was subsequently electroporated into the aforementioned BAC-containing DY380 bacteria which were supposed to facilitate the subcloning of the *Lphn3* exon 6 region into the high-copy plasmid ('gap-repair') based upon homologous recombination (see Figure 6). However, for unknown reasons, this recombination process did not work out in our case, despite the experiment being performed several times with all components double-checked (for example via DNA sequencing of the BAC). Fortunately, in the meantime a final *Lphn3* targeting vector was produced and offered by the Helmholtz Center in Munich.

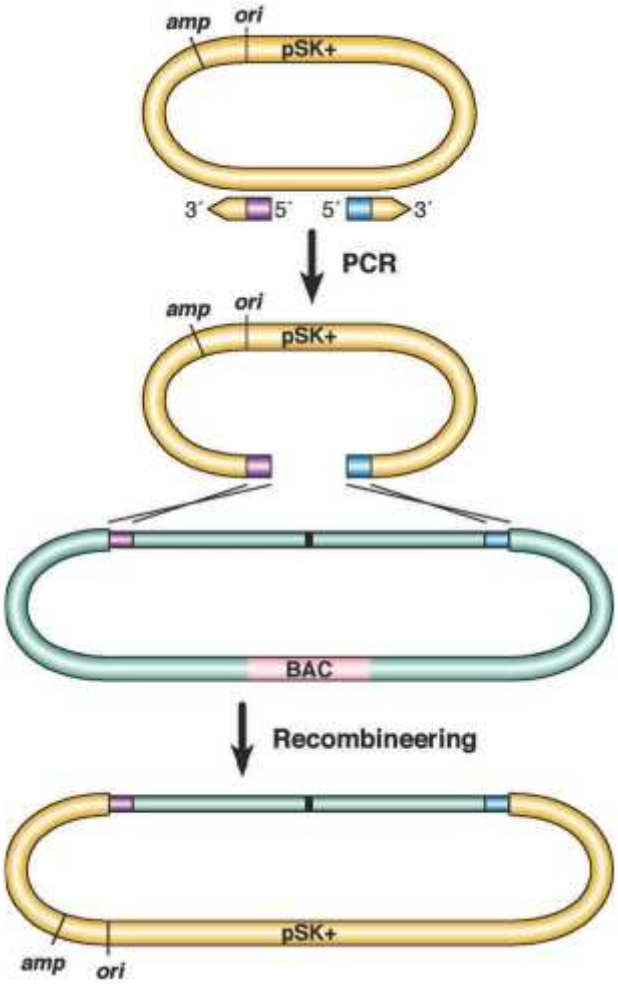

Fig. 6: Subcloning of a DNA sequence from a BAC into a high-copy plasmid via recombineering

Using an anchor primer-based PCR reaction, short homologous sequences (violet and blue rectangles) can be added to a high-copy plasmid backbone (pSK+). Subsequently, this PCR product is transformed into recombination-competent bacteria which already contain a particular BAC (exhibiting the above-mentioned homologous sequences as well). Within these cells, recombineering results in a gap-repaired plasmid that can be selected via its ampicillin (amp) resistance [adapted and modified from Liu *et al.*, 2003].

Like the one we were planning, this vector targets the 6th exon of *Lphn3* and exhibits all features necessary for the generation of knockout mice, thus prompting our decision to use it. As can be seen in Figure 7, the vector contains a high-copy pD223-based backbone, including a diphtheria toxin A (DTA) cassette for negative selection of ES cells. Furthermore, the backbone comprises a spectinomycin resistance cassette (SpecR) for positive selection of bacteria as well as a single AsiSI restriction site that can be used for linearisation.

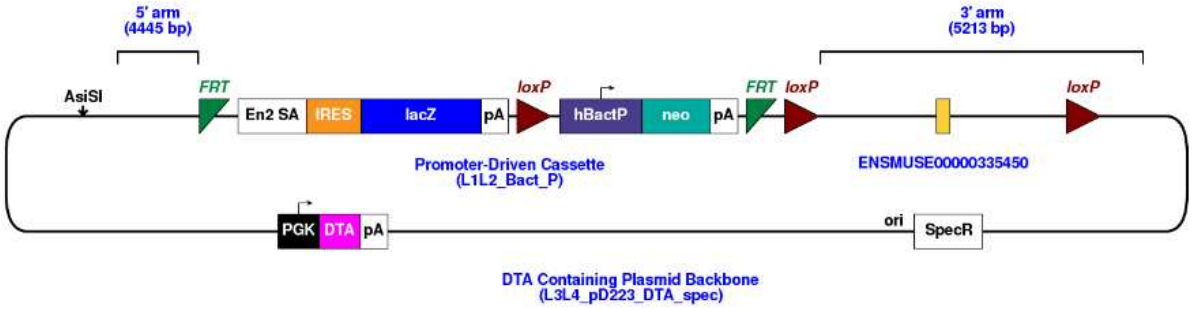

Fig. 7: Illustration of the final *Lphn3* targeting vector (provided by the Helmholtz Center, Munich)

Among others, the vector contains the exon 6 of *Lphn3* (ENSMUSE00000335450; current name: ENSMUSE00001133342) and the anterior parts of its flanking introns (5' arm and 3' arm). Moreover, a lacZ trapping cassette and a neomycin resistance cassette (neo) can be found. Importantly, exon 6 is surrounded by loxP sites, whereas the lacZ and neo cassettes are surrounded by FRT sites [adapted from www.knockoutmouse.org/martsearch/project/40290].

The gene-specific part of the vector consists of *Lphn3* exon 6 (ENSMUSE00000335450; current name: ENSMUSE00001133342) and the anterior parts of its flanking introns (5' arm and 3' arm). These two arms allow the replacement of the respective wildtype allele in ES cells via homologous recombination. Importantly, exon 6 is surrounded by loxP sites in the vector construct. These short DNA sequences are known as recognition sites for the viral enzyme Cre recombinase. If two loxP sites are equally oriented on the same DNA strand, the sequence between these sites is termed as 'floxed' (flx) and can be excised by Cre. If the Cre gene is placed under the control of an appropriate promoter, its expression can be tightly regulated, allowing to delete the floxed sequence in a tissue- or time-specific manner (conditional knockout principle). Between the 5' arm and the floxed exon 6, the vector contains a lacZ trapping cassette and a neomycin resistance cassette (neo). While the first can be used to simultaneously disrupt and report *Lphn3* gene function in mice (knockout-first principle), the latter serves as a positive selectable marker when growing ES cells in

the presence of geneticin (G418). Both cassettes are flanked by so-called FRT sites, which function analogously to the aforementioned Cre-loxP recombination system, albeit depending on the enzyme Flp recombinase.

Amplification and linearisation of *Lphn3* targeting vector

The targeting vector was transformed into TOP10F´ E.coli bacteria, amplified and purified by means of a Maxiprep Kit following the manufacturer's instructions. Using the restriction endonuclease AsiSI, the vector was linearised and subsequently rinsed with ethanol. Finally, the precipitated vector was resuspended in PBS and stored at -70℃.

Murine embryonic stem (ES) cell culture

ES cells were grown on mitomycin C-inactivated SNL feeder cells in gelatinised Petri dishes. ES cell medium was changed every 24h and ES cells were passaged every 48h, i.e. SNL cells were replaced. For electroporation, ES cells were trypsinised and separated from the SNL layer. After dissociation, $6x10^6$ ES cells were washed in PBS, resuspended in Nucleofector solution and electroporated with 3.5µg linearised *Lphn3* targeting vector. Cells were grown under normal conditions during the first 48h after electroporation and subsequently in the presence of 150µg/ml G418. After several days, ES cell colonies that had survived the selection process were selected and propagated in G418-containing medium.

PCR

Short-range PCR: To prove the presence of three critical sequences in the ES cell genome (5' FRT site, 3' FRT site as well as 3' loxP site; see Fig. 7), short-range PCR was performed, resulting in amplicons of 224bp, 544bp and 413bp, respectively. For this purpose, PBS-washed cell pellets were lysed in Cell lysis buffer and DNA was purified by isopropanol precipitation. The short-range PCR reaction mix contained 18.2µl H_2O, 2.5µl Standard PCR buffer, 1µl dNTPs, 1µl forward primer, 1µl reverse primer, 1µl template DNA (genomic DNA: 25ng; vector DNA: 0.1g) and 0.3µl Taq DNA polymerase. All samples underwent the following programme:

Step	Temperature	Number of cycles	Duration
Initial denaturation	95℃	1	120sec
Denaturation	95℃	30	30sec
Annealing	60℃		30sec
Extension	72℃		90sec
Final extension	72℃	1	120sec

Long-range PCR: Samples that showed correct amplicons in all three short-range PCR reactions were further checked by means of a single long-range PCR reaction, with the corresponding amplicon having a size of 4807bp and spanning the whole 5' arm of the vector construct. The target sequence of the forward primer was located in the *Lphn3* intronic region upstream of the 5' homology arm (i.e. not present in the vector construct), while the reverse primer was bound to a construct-specific sequence near the 5' FRT site (see Figure 8). Accordingly, this PCR reaction was able to verify the site-directed integration of the vector construct into the ES cell genome at the 5' homology arm. The long-range PCR reaction mix contained 14.75µl H_2O, 5µl iProof HF buffer, 2µl dNTPs, 1µl forward primer, 1µl reverse primer, 1µl template DNA (25ng) and 0.25µl iProof DNA polymerase. Samples underwent a Touchdown PCR programme, implicating that annealing temperature started at 70℃ and was reduced by 0.5℃ every cycle down to a 'tou chdown' point of 60℃:

Step	Temperature	Number of cycles	Duration
Initial denaturation	98℃	1	120sec
Denaturation	98℃	32	10sec
Annealing	Touchdown		20sec
Extension	72℃		150sec
Final extension	72℃	1	300sec

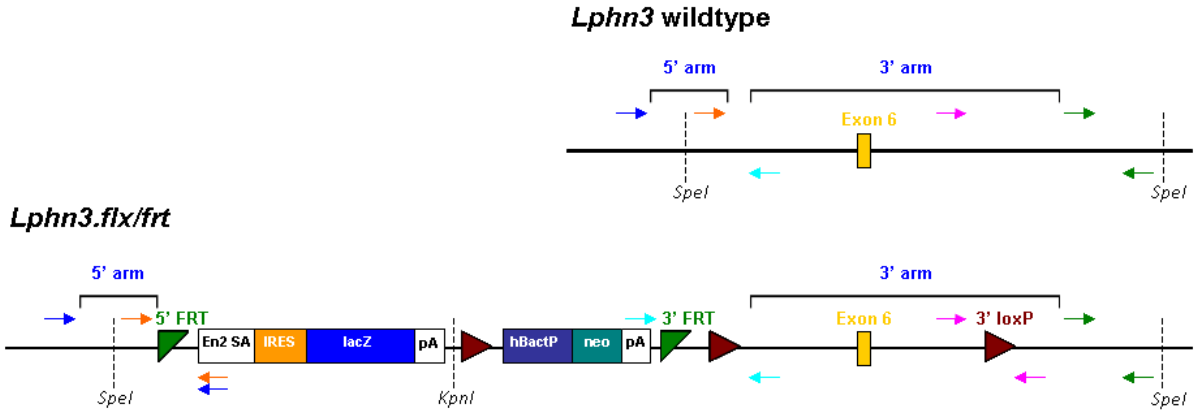

Fig. 8: Comparison of the *Lphn3* exon 6 wildtype allele with the *Lphn3*.flx/frt allele

The expected *Lphn3*.flx/flrt allele originates from homologous recombination between the *Lphn3* targeting vector and the corresponding genomic region of *Lphn3*. PCR primers are illustrated by small arrows (dark blue: 5' long-range PCR, orange: 5' FRT short-range PCR, light blue: 3' FRT short-range PCR, pink: 3' loxP short-range PCR, green: southern probe PCR). Dashed vertical lines represent restriction recognition sites for the endonucleases SpeI or KpnI.

Southern blotting

To prove the site-directed integration of the vector construct into the ES cell genome at the 3' homology arm, Southern blotting experiments were performed.

A 965bp DNA probe that targeted the *Lphn3* genomic region immediately downstream to the 3' homology arm (see Figure 8) was PCR-amplified following a protocol analogous to that described above (short-range PCR protocol), before the probe was subsequently gel-purified by means of a Gel Extraction Kit. The same protocol as for PCR was used for ES cell DNA extraction and purification, albeit with a phenol-chloroform extraction step by means of Maxtract tubes. 10-15µg DNA per sample were double-digested with the restriction endonucleases SpeI as well as KpnI, and subsequently subjected to a 0.8% TAE-buffered agarose gel. The restriction fragment which was later detected by the aforementioned probe, had a size of 9586bp in wildtype DNA, while homologous recombination with the *Lphn3* targeting vector was predicted to lead to an additional restriction site (KpnI) and thus a shorter fragment size (7962bp) in heterozygous *Lphn3.flx/frt* ES cells (see Figure 8). After electrophoresis, the gel was incubated successively in three different buffers (depurination, denaturation and neutralisation) followed by capillary transfer of DNA bands to a nylon membrane. The membrane was subsequently dried at 80℃, and DNA bands were crosslinked using UV light.

According to the supplier's instructions, the probe was labelled with ^{32}P by means of a DNA Labeling Kit, and non-incorporated α-^{32}P-dCTPs were removed via MicroSpin

Columns. Prehybridisation of the membrane was carried out in hybridisation buffer at 65℃ for 1h, with this buffer subsequently replaced by a fresh hybridisation buffer supplemented with denatured radioactive probe (20µl/ml). Following overnight hybridisation at 65℃, the membrane was rinsed several times in washing buffer 1 and 2 with increasing temperature, and then placed onto an autoradiography film developed the next day with the help of conventional photo laboratory equipment.

Additional quality checks

DNA sequencing: To verify the integrity of FRT and loxP sites in the genome of ES cell clones that had passed all preceding quality checks, amplicons of the aforementioned short-range PCRs were gel-purified via a Gel Extraction Kit and subsequently forwarded to the company Eurofins MWG Operon for DNA sequencing.
Mycoplasma test: To check for the potential infection of ES cells with Mycoplasma bacteria, a subset of cells was cultivated separately for several days without the presence of any antibiotics, and the medium was examined for Mycoplasma-specific DNA sequences using a Mycoplasma PCR Detection Kit according to the supplier's descriptions. This kit includes two control samples: a negative control which produces a PCR product of 481bp and a positive control, giving rise to both a 481bp and a 259bp amplicon.

Karyotyping: Moreover, ES cell chromosomes were prepared and stained with DAPI to obtain respective karyograms, with at least 15 different cells in metaphase analyzed for each clone. All karyotyping experiments were kindly performed by Dr. Indrajit Nanda (Department of Human Genetics, University of Würzburg).

Morula injection

For the production of embryos, female mice were superovulated with intraperitoneal injections of pregnant mare serum gonadotrophin (PMSG) and human chorionic gonadotrophin (hCG). Chimeric Lphn3.flx/frt mice were generated by laser-assisted injection of successfully recombined ES cells (JM8A3 cell line; carrying the agouti coat colour gene) into 8-cell stage embryos (morulae) deriving from mice with black coat colour (C57BL/6), while pseudopregnant female mice produced via mating with vasectomised males were used as recipients for injected embryo transfer. All

manipulations were performed by Ronald Naumann and his colleagues (MPI-CBG, Dresden).

Mice breeding and genotyping

Mice were kept under controlled humidity (44-48%) and temperature (22-23℃) conditions with a regular 14/10 hour light-dark cycle. Drinking and feeding were *ad libitum.*

Chimeras were crossed to C57BL/6 mice and screened by PCR for germline transmission. This duplex PCR was capable of producing amplicons of varying sizes, given that every reaction mix contained one forward primer and two reverse primers (one of which was vector construct-specific). While the *Lphn3* wildtype allele corresponded to a PCR product of 446bp, the Lphn3.flx/frt allele produced a 224bp amplicon (and theoretically an additional amplicon of 7540bp). DNA from mouse tail tips was used as PCR template, extracted analogously to the ES cell DNA (see above).

The PCR reaction mix contained 18µl H_2O, 2.5µl Standard PCR buffer, 1µl dNTPs, 1µl forward primer (5' FRT site forward), 0.5µl reverse primer #1 (5' FRT site reverse), 0.5µl reverse primer #2 (3' FRT site reverse), 1µl template DNA (25ng) and 0.5µl Taq DNA polymerase. Samples underwent a Touchdown PCR programme, implying that annealing temperature started at 66℃ and was reduced by 0.5℃ every cycle down to a 'touchdown' point of 56℃:

Step	Temperature	Number of cycles	Duration
Initial denaturation	95℃	1	120sec
Denaturation	95℃	35	30sec
Annealing	Touchdown		30sec
Extension	72℃		90sec
Final extension	72℃	1	120sec

3 Results

3.1 *SLC2A3*

3.1.1 Confirmation of *SLC2A3* CNV genotyping

Two additional methods were performed in order to verify the specificity of the *SLC2A3* TaqMan CNV assay.

Fluorescence *In Situ* Hybridisation (FISH)

Metaphase chromosomes of all three analysed subjects exhibited the fluorescence hybridisation signals at the expected site of chromosome 12 (p13.31). However, the signal intensity on one of the homologous chromosomes was significantly brighter in both *SLC2A3* duplication carriers, and covered a larger region (see Figure 9). The hybridised region emerged as two distinct blocks during some metaphase stages, which implies the presence of additional copies of the BAC probe. Furthermore, when the same BAC was hybridised on metaphase chromosomes of the control subject (who had 2 *SLC2A3* copies according to the TaqMan assay) or when other BACs covering the short arm of chromosome 12 were used, the presence of additional copies of the probe could not be revealed (data not shown).

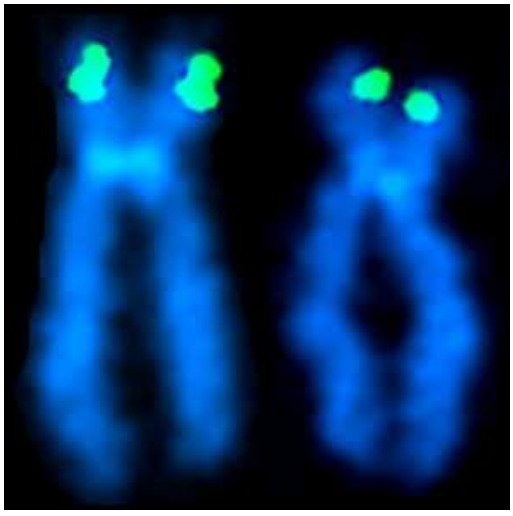

Fig. 9: *SLC2A3* Fluorescence *In Situ* Hybridisation (FISH) on human chromosomes

For hybridisation, the BAC RP11-277E18 comprising the *SLC2A3* gene locus on chromosome 12 (p13.31) was used. The image shows two labelled homologous chromosomes of an individual that was a carrier of three *SLC2A3* copies according to TaqMan-based genotyping. Importantly, one of the homologs (left) displayed a considerably brighter and larger signal implying additional copies of the BAC probe [by courtesy of Dr. Indrajit Nanda, Department of Human Genetics, University of Würzburg].

Array Comparative Genomic Hybridisation (array CGH)

DNA samples of twelve human individuals were examined, with each showing evidence of three *SLC2A3* copies in preceding TaqMan assays. In all cases, a duplication comprising the *SLC2A3* gene locus could be confirmed. Moreover, this duplication was consistently found to have a minimal size of 127482bp (chr12:7996763-8124244, hg19) and a maximal size of 132017bp (chr12:7993703-8125719; see Figure 10). Given that both chromosomal breakpoints were located in segmental duplications showing a high degree of sequence similarity (first duplicon at chr12:7995630-7998390, second duplicon at chr12:8124315-8128199; fraction matching: 0.9214), non-allelic homologous recombination (NAHR) appears to be the duplication's most likely cause.

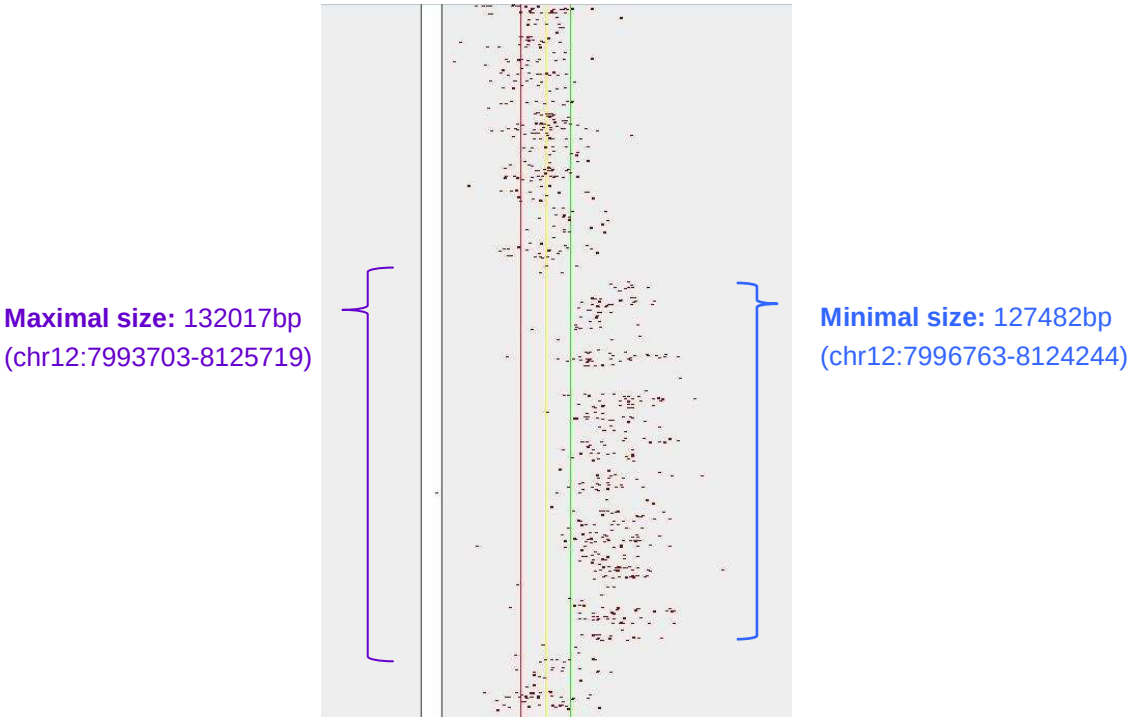

Fig. 10: Illustration of array CGH data for chromosome12: 7166455-8822108 (hg19)

This representative image shows the findings for a human individual whose TaqMan results were indicative of three *SLC2A3* copies. Signal intensity ratios of Cy3 and Cy5 are displayed for each BAC clone. The red line corresponds to a log2 ratio of -0.3 (loss), whereas the green line represents a log2 ratio of 0.3 (gain). The duplication comprising the *SLC2A3* gene locus was found to have a minimal size of 127482bp and a maximal size of 132017bp [Image kindly provided by Dr. Reinhard Ullmann, MPI for Molecular Genetics, Berlin].

3.1.2 Quantitative reverse transcription (qRT) PCR

Real-time qRT-PCR was performed to analyse the expression of *SLC2A3* in two easily available peripheral human cell models. The *SLC2A3* comprising CNV exerted a strong influence on *SLC2A3* mRNA levels in both native (PBMCs) and immortalised cells (LCLs). As shown in Figure 11, mean normalised relative expression values (mean Q_n) were significantly higher in the group of duplication carriers (copy number: 3) than the group of controls (copy number: 2). This difference was 73.1% in terms of LCLs (MWU test, $p<0.01$), while it amounted to 220% in PBMCs (MWU test, $p<0.001$).

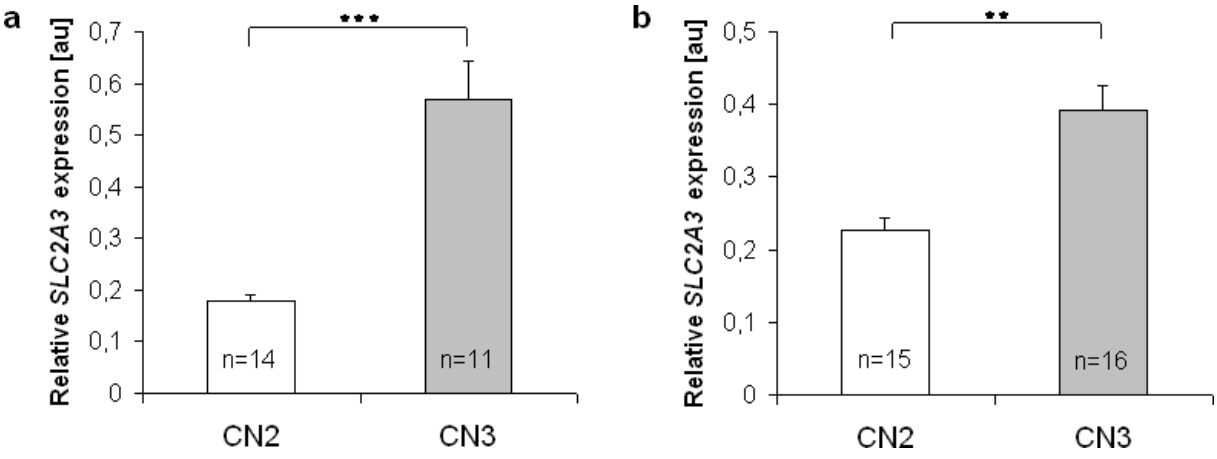

Fig. 11: Real-time qRT-PCR for *SLC2A3*

The histograms display mean normalised relative expression values (mean Qn ± SEM in arbitrary units) for carriers of the *SLC2A3* duplication (CN3) and control individuals (CN2). Figure **a** corresponds to peripheral blood mononuclear cell (PBMC) samples and figure **b** to lymphoblastoid cell line (LCL) samples [Mann-Whitney U test: ** $p<0.01$, *** $p<0.001$, n: sample size].

3.1.3 Western blotting

SLC2A3 expression analysis at the protein level was conducted using the aforementioned peripheral cell models. For this purpose, densitometrically determined relative GLUT3 protein levels were compared between carriers of the *SLC2A3* duplication (3 gene copies) and control subjects (2 gene copies). However, no significant impact of the *SLC2A3* CNV on whole cell GLUT3 protein quantity could be found. As seen in Figure 12, which refers to Western blotting experiments in native cells (PBMCs), duplication carriers exhibited nominally increased (37%) GLUT3 protein amounts in comparison to controls, albeit without reaching the level of significance (t-test, $p=0.265$). In immortalised cells (LCLs), GLUT3 protein levels

proved to be non-significantly diminished by 21% in duplication carriers (t-test, p=0.219; data not shown).

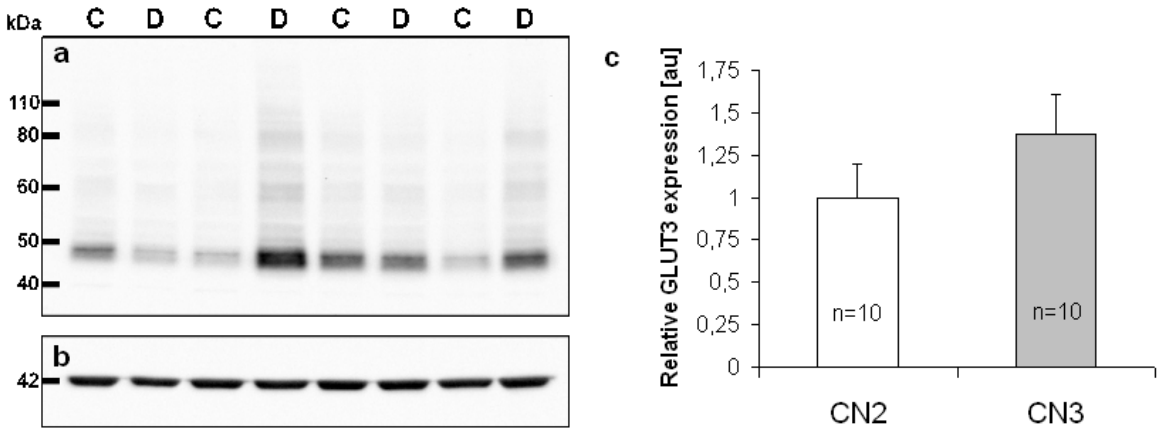

Fig. 12: Western blotting for GLUT3

Figure **a** shows the image of a representative immunoblot, reflecting whole cell GLUT3 protein amounts of *SLC2A3* duplication carriers ('D") and control subjects ('C") in peripheral blood mononuclear cells (PBMCs). GLUT3 levels were normalised by means of the loading control protein beta-actin (Figure **b**). The histogram in Figure **c** displays the relative GLUT3 protein expression in PBMCs (± SEM in arbitrary units) which was non-significantly higher (37%; p=0.219) in *SLC2A3* duplication carriers (CN3) than individuals with two gene copies (CN2) [Mann-Whitney U test, n: sample size].

3.1.4 Cellular glucose uptake assay

LCLs were incubated in the presence of ^{3}H-labelled 2-Deoxy-D-glucose for the analysis of GLUT-mediated glucose uptake. As displayed in Figure 13, no significant differences in cellular glucose uptake were found between duplication carriers (3 *SLC2A3* copies) and control individuals with 2 copies. Mean scintillation recordings amounted to 36375±5440 counts per minute (cpm) in the duplication, and 38494±7629 cpm in the control group (MWU test, p=0.894).

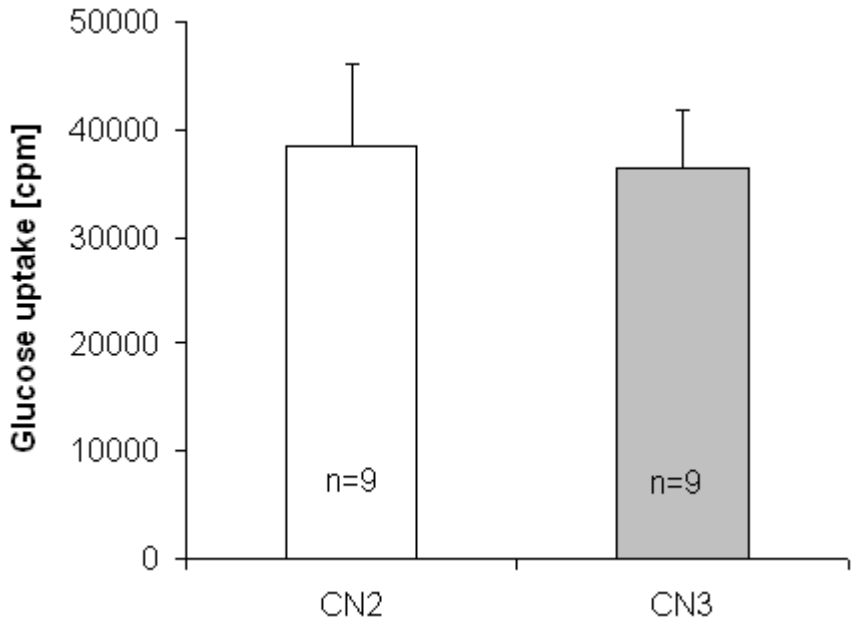

Fig. 13: GLUT-mediated glucose uptake in lymphoblastoid cell lines (LCLs)

^{3}H-labelled 2-Deoxy-D-glucose uptake (counts per minute ± SEM) is displayed for human carriers of the *SLC2A3* duplication (CN3) and control subjects with two copies (CN2). Group differences were not significant [Mann-Whitney U test, p=0.894, n: sample size].

3.1.5 Functional EEG measurements

In order to investigate the functional impact of *SLC2A3* SNP and CNV in humans, functional EEG measurements were conducted while participants underwent a Continuous Performance Test (CPT) and an n-back test.

CPT

It emerged that ADHD patients with a duplication of *SLC2A3* (3 copies) showed a significantly diminished NoGo-Anteriorisation (NGA; 0.31±0.57 electrode positions) compared to ADHD patients with a *SLC2A3* copy number of 2 (0.85±0.37 electrode positions; t_{16}=2.36, p=0.031, see Figure 14). Indeed, this effect was due to the centroid of the Go condition, which appeared significantly more anterior (3.33±0.52 vs. 3.91±0.25 electrode positions; t_{12}=3.008, p=0.011), whereas the NoGo topography did not reveal significant differences between these two groups (t_{16}=0.302, p=0.767). Additionally, *SLC2A3* duplication carriers with ADHD showed a statistical trend towards increased reaction times to Go stimuli (606.6±189.8ms) compared to ADHD patients with 2 *SLC2A3* gene copies (483.70 ± 72.0ms; t_{10}=1.82,

p<0.1). However, no group differences could be found concerning NoGo-related behavioural indices such as commission errors.

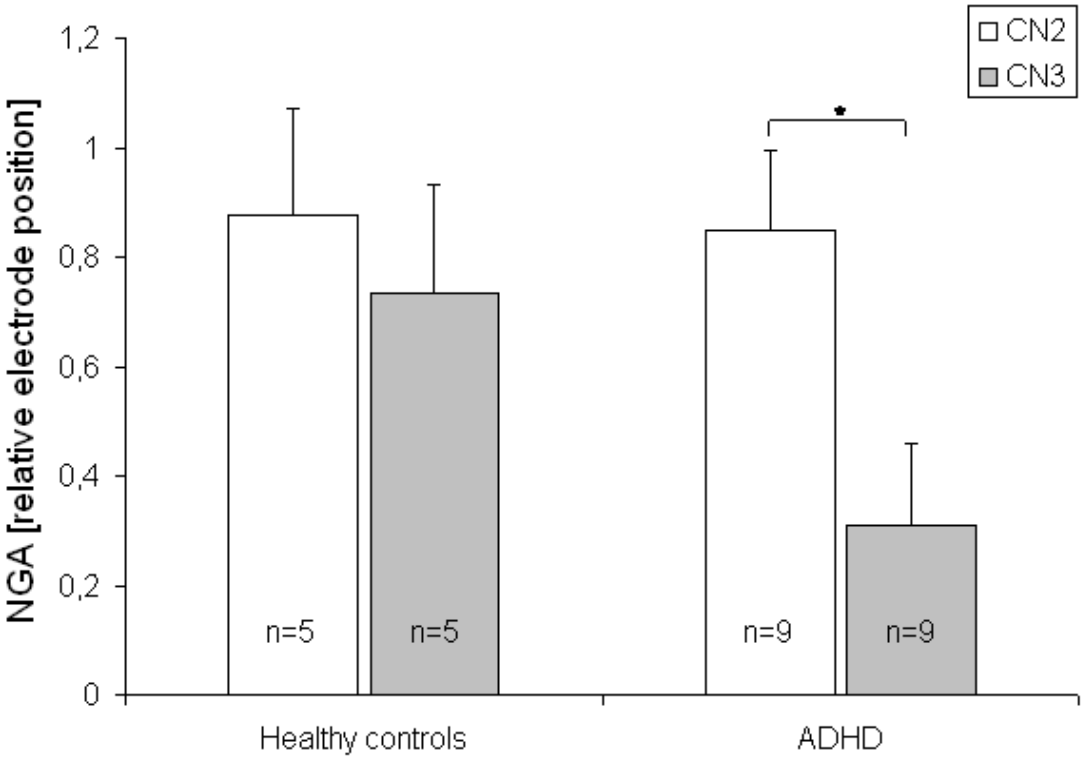

Fig. 14: NoGo-Anteriorisation (NGA) values for participants with different *SLC2A3* copy number

The histogram shows NGA values during Continuous Performance Test (CPT) for ADHD patients and healthy controls, carrying either two or three *SLC2A3* gene copies. NGA was significantly reduced in ADHD patients with three copies (CN3) when compared to ADHD patients with a copy number of 2 (CN2) [n: sample size, error bar: SEM, * p<0.05; by courtesy of Dr. Ann-Christine Ehlis, Department of Psychiatry, University of Tübingen].

Overall, ADHD patients in this study did not significantly differ from healthy controls, despite the ADHD subgroup with 3 *SLC2A3* copies displaying a tendency towards diminished NGA values compared to the healthy subgroup with 3 copies (t_{12}=2.03, p=0.07). Furthermore, no significant genotype effect appeared when considering the whole control group (t_8=0.67, p=0.52).

Concerning the SNP rs12842 within the *SLC2A3* gene (see Figure 5), a significant interaction between both factors ($F_{1,211}$=4.16, p<0.05) emerged when performing an ANOVA including the between-subject variables ‘genotype’ (T-allele vs. C-allele carriers) and ‘diagnosis’ (ADHD vs. healthy controls; see Figure 15). Using a post-hoc t-test, it was possible to pinpoint that T-allele carriers within the ADHD group

showed slightly increased NGA values compared to ADHD patients with rs12842 C-allele (t_{142}=1.91, p=0.058). By contrast, this genotype effect was reversed in healthy controls, albeit without reaching the level of significance. Additionally, the ADHD group displayed a significant reduction of NGA values compared to the controls, yet only in terms of the subgroup with C-allele (t_{161}=2.99, p=0.003)

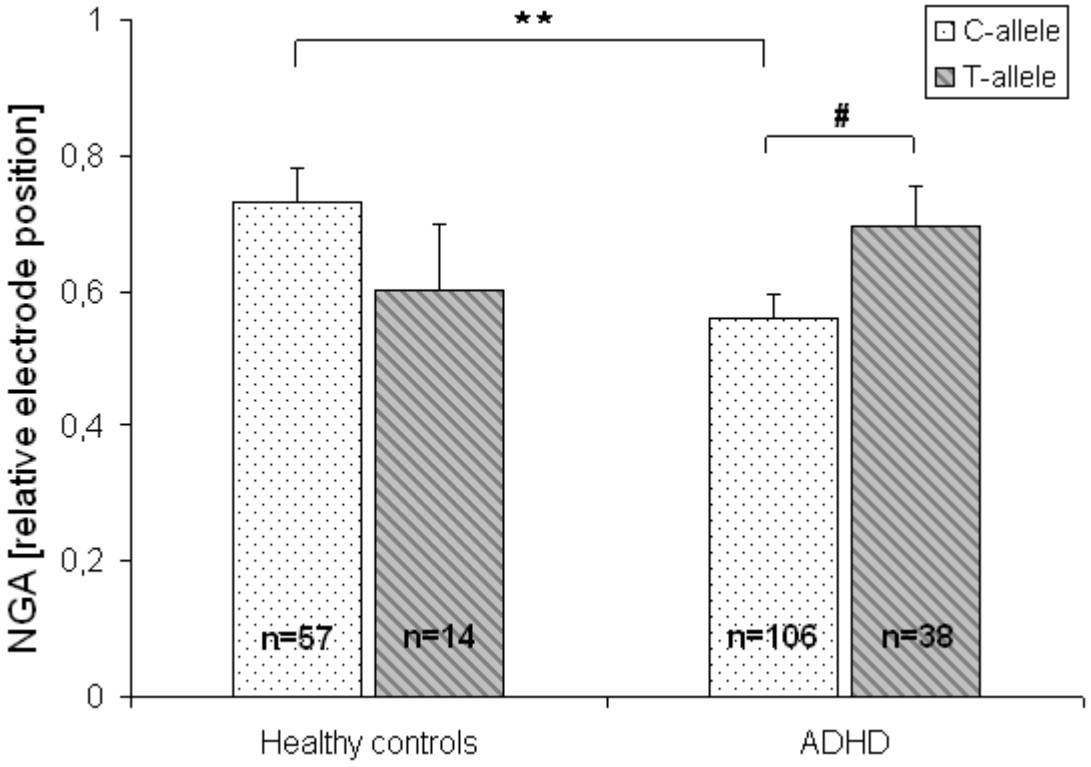

Fig. 15: NoGo-Anteriorisation (NGA) values for participants with different rs12842 allele

NGA values during Continuous Performance Test (CPT) are displayed for ADHD patients and healthy controls, carrying either rs12842 C- or T-allele. A significantly reduced NGA was found in ADHD patients with the C-allele when compared to ADHD patients with the same gene variant. Moreover, a tendency towards increased NGA values in T-allele carriers emerged within the ADHD group [n: sample size, error bar: SEM, ** p<0.01, # p<0.1; data kindly provided by Dr. Ann-Christine Ehlis, Department of Psychiatry, University of Tübingen].

n-back test

Using ANOVA for repeated measurements of the amplitude of the P300 time window, a significant main effect of genotype (2 vs. 3 *SLC2A3* copies) was found within the group of ADHD patients ($F_{1,16}$=11.91, p=0.003), implying lower overall values in subjects with three gene copies. Moreover, significant interactions between '*SLC2A3* copy number' and 'condition' (1-back vs. 2-back; $F_{1,16}$=5.74, p=0.029), as well as 'trial type' (target vs. non-target; $F_{1, 16}$=4.70, p=0.046), indicated that this effect was

particularly pronounced in 1-back trials (t_{16}=3.94, p=0.001) and target trials (t_{14}=3.44, p=0.004; see Figure 16). Additionally, a decrease in P300 amplitudes from 1-back to 2-back blocks as well as target to non-target trials only emerged within ADHD non-duplication group (t_8=5.38, p=0.01 and t_8=3.08, p=0.015).

On the other hand, *SLC2A3* copy number neither exerted a significant influence on P300 amplitudes in the group of healthy controls (p≥0.1), nor did it affect P300 latencies in either of the two diagnosis groups (all F-values < 1.5, p>0.25).

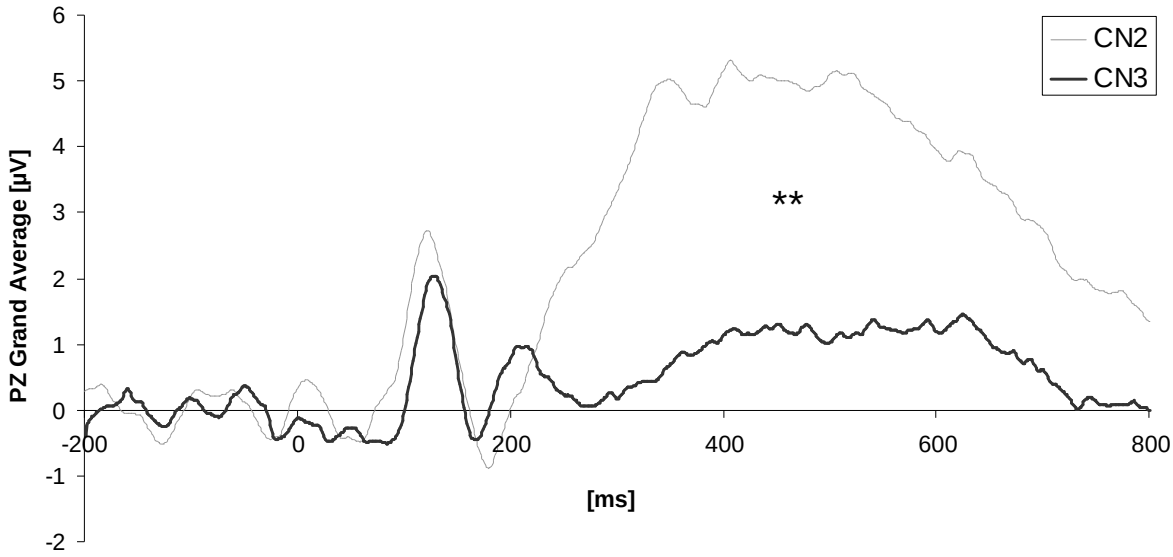

Fig. 16: Electroencephalogram (EEG) during n-back test (1-back condition, target trials)

For a time window of 1000ms, mean amplitudes [µV] of ADHD patients with different *SLC2A3* copy number are depicted at electrode position PZ (midline parietal). Across a notable time span and particularly involving the P300 component, the *SLC2A3* duplication group (CN3) showed significantly diminished amplitudes compared to control subjects with two copies (CN2) [** p<0.01; by courtesy of Dr. Ann-Christine Ehlis, Department of Psychiatry, University of Tübingen].

Regarding the SNP rs12842, genotype status had no significant impact on the P300 component. However, ANOVA showed a statistical trend ($F_{1,173}$=2.87, p<0.1) towards a main effect 'genotype' for another ERP component, namely N200. Interestingly, this effect was highly dependent on the n-back trial type (target vs. non-target), given that both factors significantly interacted with each other ($F_{1,173}$=8.37, p=0.004). Furthermore, by means of post-hoc analysis, C-allele carriers in both diagnostic groups exhibited a significant increase in N200 latencies in non-target trials (214.2±19.3ms) compared to target trials (199.7±24.2ms; t_{134}=8.13, p<0.001; Wilcoxon-Z=8.0, p<0.001), whereas such an effect was not evident in T-allele carriers (t_{41}=1.15, Z=1.90, n.s.; see Figure 17).

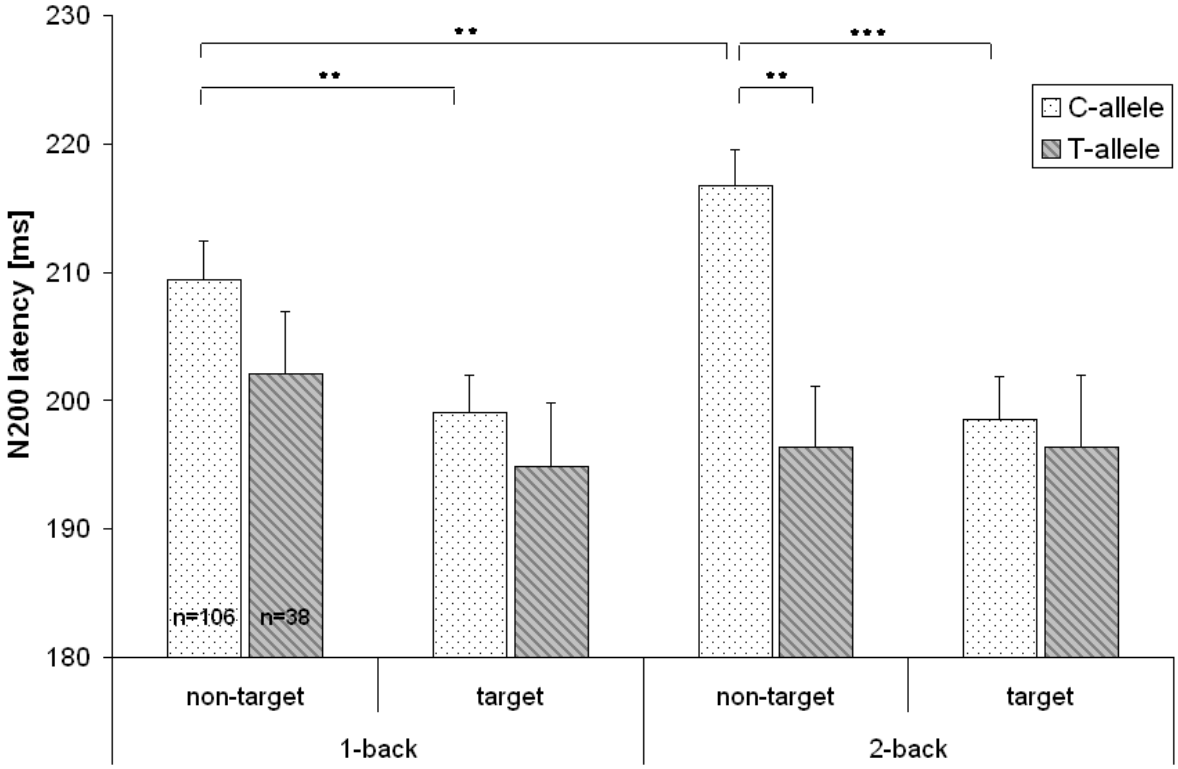

Fig. 17: N200 latencies during n-back-test

N200 latencies are shown for ADHD patients with rs12842 C- or T-allele during different n-back test conditions (1-back vs. 2-back) and trial types (target vs. non-target stimuli). Highly significant effects were found in C-allele carriers concerning trial type, test condition and genotype [n: sample size, error bar: SEM, *** p<0.001, ** p<0.01; data kindly provided by Dr. Ann-Christine Ehlis, Department of Psychiatry, University of Tübingen].

3.2 *Lphn3*

3.2.1 Confirmation of homologous recombination in murine ES cells

Following several repeated electroporation experiments using the *Lphn3* targeting vector, a total of 133 ES cell clones were chosen; 46 of which survived the subsequent selection with the antibiotic G418 and appeared morphologically normal (undifferentiated) throughout the propagation. The DNA of these clones was checked for vector-specific sequences and targeted homologous recombination by means of PCR and Southern blotting.

PCR

Short-range PCR: As illustrated by Figure 18, the expected short-range PCR amplicons only appeared in around half of the tested ES cell clones. Overall, 25 ES

cell clones were positive for all three short-range PCR experiments (5' FRT, 3' FRT and 3' loxP PCR).

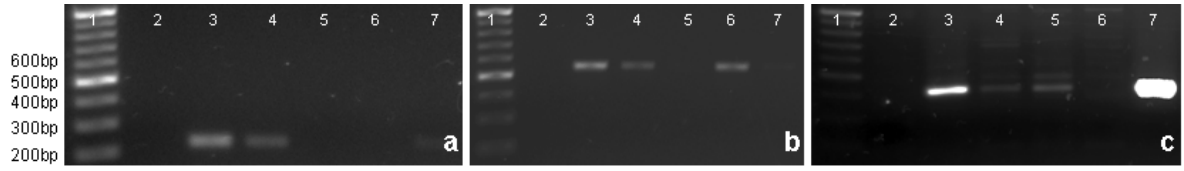

Fig. 18: Short-range PCRs for the detection of *Lphn3* vector-specific sequences

Figure **a** refers to the 5' FRT PCR (expected amplicon: 224bp), Figure **b** to the 3' FRT PCR (expected amplicon: 544bp) and Figure **c** to the 3' loxP PCR (expected amplicon: 413bp). About half of the ES cell samples were positive for all three PCR reactions [Lane 1: DNA size marker ('GeneRuler 100bp Plus'), Lane 2: negative control (wildtype ES cell clone), Lane 3: positive control (*Lphn3* targeting vector), Lanes 4-7: transfected ES cell clones].

Long-range PCR: These 25 clones were further tested for correct homologous recombination at the 5' arm with long-range PCR (see Figure 19), with a total of 10 different ES cell clones exhibiting the expected PCR amplicon of 4807bp.

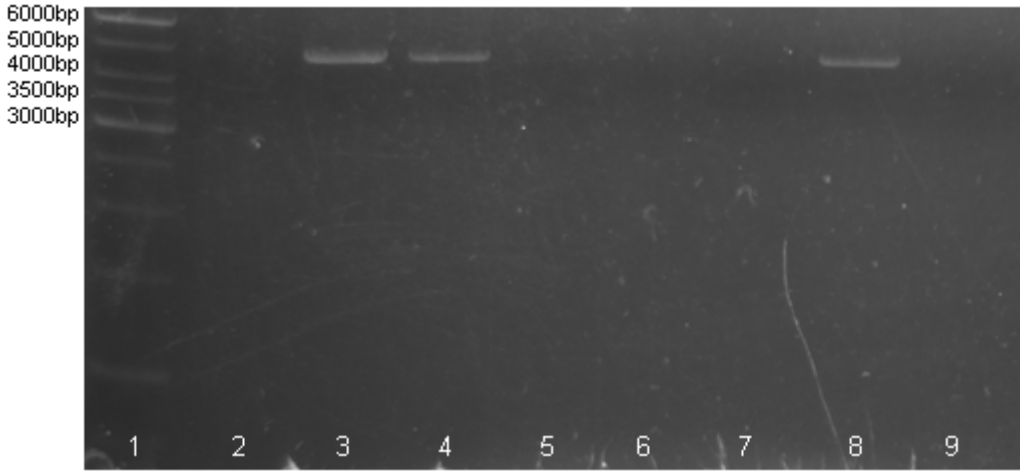

Fig. 19: Long-range PCR for 5' homology arm (*Lphn3*)

The image shows an exemplary photo of electrophoretically separated 5' long-range PCR products. Some ES cell clones exhibited the predicted amplicon of 4807bp [Lane 1: DNA size marker ('GeneRuler 1kb'), Lane 2: negative control (wildtype ES cell clone), Lanes 3-9: transfected ES cell clones].

Southern blotting

As an additional confirmation of homologous recombination, albeit with regard to the 3' homology arm, the DNA of the ten ES cell clones that passed all PCR experiments was checked by means of Southern blotting (see Figure 20). In addition to the 9586bp *Lphn3* wildtype fragment, all but two clones showed the expected 7962bp

fragment, indicating correct homologous recombination between the *Lphn3* targeting vector and the corresponding sequences within the *Lphn3* genomic region.

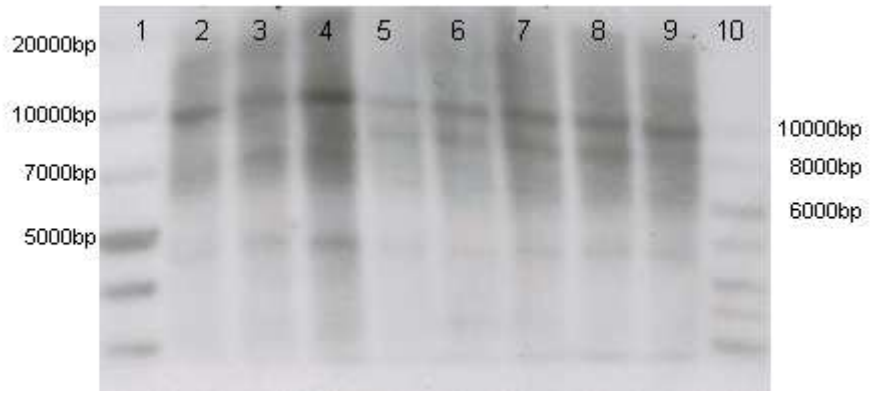

Fig. 20: Southern blotting for 3' homology arm (*Lphn3*)

The autoradiography image shows DNA fragments detected by the 3' southern probe. Besides the omnipresent 9586bp *Lphn3* wildtype fragment, several ES cell clones also exhibited the 7962bp fragment that indicated targeted integration of the *Lphn3* vector at the 3' arm. Samples with ambiguous results (Lanes 3 & 4) were repeated [Lane 1: DNA size marker ('GeneRuler 1kb Plus'), Lane 2: wildtype ES cell clone, Lanes 3-8: transfected ES cell clones, Lane 9: wildtype ES cell clone. Lane 10: DNA size marker ('GeneRuler 1kb')].

3.2.2 Additional quality checks for recombined ES cells

The eight ES cell clones that emerged positive from all previous tests were further checked by means of the following three approaches:

<u>DNA sequencing</u>

To ensure the correctness of some particularly important sequences within the *Lphn3*.flx/frt allele, the aforementioned short-range PCR amplicons (5' FRT, 3' FRT and 3' loxP PCR) were purified and subjected to DNA sequencing. In all cases, all three PCR products fully complied with the predicted sequence (data not shown).

<u>Mycoplasma test</u>

ES cells checked for potential infection by means of a PCR-based Mycoplasma test only gave rise to the 481bp negative control amplicon, yet not the 259bp positive control amplicon (see Figure 21).

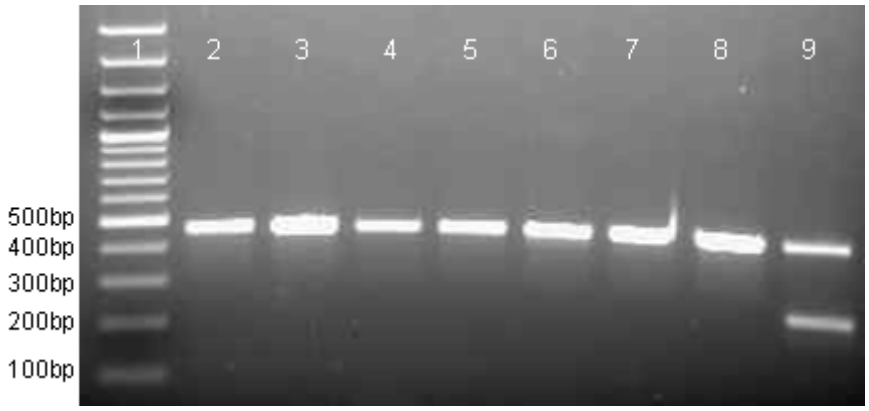

Fig. 21: Mycoplasma test PCR for murine ES cell clones

Mycoplasma PCR products are shown for 6 of the 8 tested ES cell clones. All clones exhibited only the negative control amplicon of 481bp, yet not an additional 259bp positive control band which indicates Mycoplasma infection of cells [Lane 1: DNA size marker, Lane 2-7: transfected ES cell clones, Lane 8: negative control, Lane 9: positive control].

Karyotyping

Murine ES cells were karyotyped to check for gross structural and numerical rearrangements of chromosomes. Overall, seven ES cell clones showed the expected number of 40 acrocentric chromosomes, which appeared macrostructurally normal in all analysed metaphases. One ES cell clone was rejected, given that it repeatedly gave rise to karyograms with a diploid chromosomal number of 41 (see Figure 22).

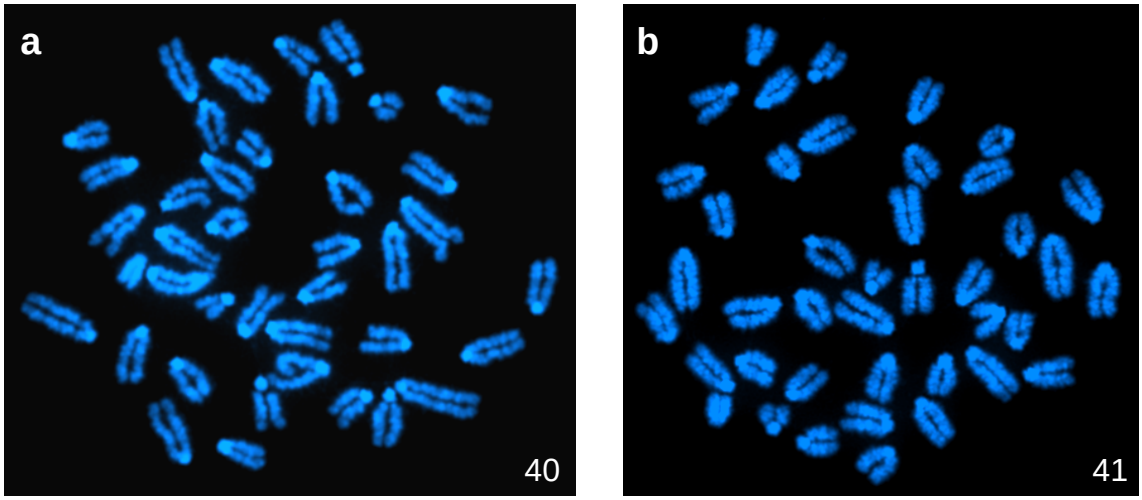

Fig. 22: Karyotyping of murine ES cell clones

Two exemplary karyograms are shown, both comprising DAPI-stained chromosomes in random order. Whereas the ES cell clone in Figure **a** exhibited the expected number of 40 metaphase chromosomes per cell, the clone in Figure **b** repeatedly produced karyograms with 41 chromosomes [Image kindly provided by Dr. Indrajit Nanda, Department of Human Genetics, University of Würzburg].

3.2.3 Generation of chimeric mice

Among the seven ES cell clones that passed all preceding quality checks, four were chosen for morula injection; one of them led to offspring with a poor rate of chimerism (estimated on the basis of ES cell contribution to coat colour), whereas the others gave rise to highly chimeric mice whose body fur appeared almost entirely in agouti colour and that did not exhibit any pathological findings. These promising chimeras were raised and crossed with C57BL/6 mice. Animals of the next generation were carefully screened for germline transmission of the *Lphn3*.flx/frt allele on the basis of their coat colour and PCR genotyping (see Figure 23). However up to now, all mice of this generation (>100 animals) were found to be black-coated and homozygously wildtype in terms of the *Lphn3* gene. Thus, the project is still in progress.

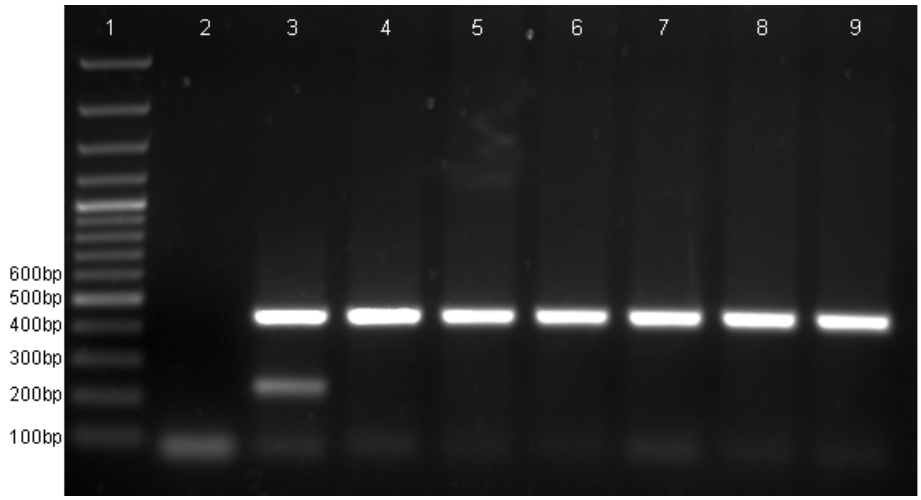

Fig. 23: *Lphn3* genotyping PCR for mice

Depending on *Lphn3* genotype, this duplex PCR was able to yield products of varying sizes: an amplicon of 446bp corresponded to the *Lphn3* wildtype allele, whereas the *Lphn3*.flx/frt allele produced a 224bp amplicon. All mice tested thus far only displayed the wildtype band [Lane 1: DNA size marker, Lane 2: negative control (H_2O), Lane 3: positive control (recombined ES cell clone), Lanes 4-9: offspring of chimeric mice].

4 Discussion

Several genome-wide screenings for ADHD have recently been conducted in a multitude of populations worldwide, suggesting a number of genes that may play a role in this highly prevalent neurodevelopmental disorder. In this context, two relatively new ADHD candidate genes have emerged: *SLC2A3* which is known as the gene of the facilitative glucose transporter type 3, as well as *LPHN3,* encoding the protein latrophilin-3.

Within this thesis, both genes were examined based upon two independent projects. In the first case, the focus was adopted on polymorphisms of *SLC2A3* and their physiological consequences in humans, whereas the latter project involved developing a mouse model of latrophilin-3 deficiency.

4.1 *SLC2A3*

4.1.1 Confirmation of *SLC2A3* CNV genotyping

The reliability of the TaqMan Gene Expression Assay, routinely applied for *SLC2A3* CNV genotyping, could be confirmed in all cases by using two additional methods, namely Array Comparative Genomic Hybridisation (array CGH) and Fluorescence *In Situ* Hybridisation (FISH). Moreover, the extent of the duplication at the chromosomal location 12p13.31 was narrowed down to a maximal size of 132.017kb (chr12:7993703-8125719; hg19), which complies relatively well with the findings described in previous publications. For example, Yang and colleagues referred to a 132.4kb duplication at chr12:7884583-8017012 (hg18; Yang *et al.*, 2009), whereas Izumi and colleagues described a 128.8kb duplication at chr12:7888157–8017012 (hg18; Izumi *et al.*, 2012).

When analysing the genomic region flanking the duplication, we found segmental duplications around the chromosomal breakpoints that exhibited a substantial level of sequence similarity (>92%), thus indicating a likely cause of non-allelic homologous recombination (NAHR) which is known to occur when low-copy repeats in the genome misalign during meiosis, leading to a gain or loss of genetic material. Interestingly, a Doctoral Thesis at the University of Leicester, United Kingdom,

focusing on the same CNV at 12p13.31 also considered NAHR the best explanation model (Reekie, 2011). However, the author surprisingly provided evidence of two distinct historical recombination events apparently having taken place at 12p13.31, resulting in two considerably different duplication alleles. The first, termed ‘B9/B10’, involves a duplication of the whole *SLC2A3* gene locus and the anterior exons of *SLC2A14,* whereas the other duplication allele, termed ‘B5/B6’, implicates a *SLC2A3-SLC2A14* fusion gene that may give rise to the synthesis of hybrid mRNA. However, according to Reekie and her colleagues, to date the B5/B6 recombination event has merely been verified in two related individuals of a West African population sample, and thus may possibly be restricted to this geographical region. Moreover, this allele is unlikely to be detected as a copy number change by the *SLC2A3* TaqMan Copy Number Assay used in the present thesis, given that the respective primers bind within intron 6/7 of *SLC2A3* (nearby Chr12:8081061), i.e. a DNA sequence that should only appear once in the B5/B6 duplication allele.

On the other hand, Reekie thoroughly described a deletion allele at 12p13.31 that she suggested to be associated with a lower risk of developing the autoimmune disorder rheumatoid arthritis (based on an association study of a Swedish and British population sample). Such a deletion corresponds to a *SLC2A3* copy number of 1, which was also found in a number of samples of the Department of Psychiatry in Würzburg via TaqMan- and SNP array-based CNV analysis. Until present, this deletion cohort has not been included in studies, owing to its comparably low sample size and absence of a consistent clinical phenotype. In contrast to mice demonstrating autism-like behavioural features when heterozygously deficient for *Slc2a3* (Zhao *et al.*, 2010), a clear-cut clinical picture of psychiatric disorders has not yet been observed in terms of human *SLC2A3* deletion carriers. Future work will possibly shed light on whether the potential physiological consequences of diminished *SLC2A3* copy number may constitute a quasi-reversed effect of those accompanying an increased copy number, or whether a heterozygous deficiency of *SLC2A3* can be compensated comparatively easily.

4.1.2 Quantitative reverse transcription (qRT) PCR

As expected, duplication of the *SLC2A3* gene was accompanied by substantially elevated *SLC2A3* mRNA levels both in lymphoblastoid cell cultures (LCLs) and native peripheral blood mononuclear cells (PBMCs). Considering that a copy number gain from 2 to 3 should theoretically involve 50% higher amounts of corresponding gene product, measured increases were even more pronounced than anticipated. The qRT-PCR results revealed highly significant differences between carriers of 2 and 3 *SLC2A3* gene copies, namely an upregulation of *SLC2A3* gene expression in the latter group by more than 200% in terms of PBMCs, and more than 70% in terms of immortalised cells (LCLs). At least the latter result complies with the findings reported by Yang and colleagues in 2009, who found significantly elevated *SLC2A3* mRNA levels (approximately 75%) in *SLC2A3* duplication carriers when analysing 48 fibroblast samples via qRT-PCR (Yang *et al.*, 2009).

4.1.3 Western blotting

Despite striking genotype effects at mRNA level, corresponding protein amounts were found to be unremarkable. Semi-quantitative analysis of whole-cell GLUT3 protein did not result in any significant differences between carriers of 2 and carriers of 3 *SLC2A3* gene copies, neither in LCLs nor in PBMCs.

When considering the Western blotting data, comparatively high standard errors of the mean (SEM) are notable in both genotype groups, amounting to approximately 20% of the respective mean values and hence around twice as much as for the qRT-PCR data. Accordingly, this indicates a higher method- and/or biology-based variance for GLUT3 protein, hindering the identification of potential genotype effects.

However, on the other hand, inconsistencies between mRNA and protein levels of glucose transporters have been previously reported in comparable studies. In a gene expression analysis of PBMCs, Estrada and colleagues did not detect any correlation between *SLC2A3* mRNA and GLUT3 protein amounts (Estrada *et al.*, 1994), neither did the authors of a study focusing on *SLC2A4* expression in muscle cells (Bourey *et al.*, 1990).

One possible explanation for this peculiar finding is that pre-translational mechanisms may delimit the quantity of glucose transporter protein being produced in these peripheral cells under basal conditions, thus masking increased *SLC2A3* mRNA levels detected in *SLC2A3* duplication carriers. Such regulatory mechanisms of GLUT3 have been suggested for example in a study focusing on the expression of glucose transporters in early rat brain (Nehlig *et al.*, 2006), with the authors discovering that seizure-induced upregulation of *Slc2a1* and *Slc2a3* mRNA was not accompanied by an increase of respective protein levels, implying a storage of untranslated mRNA within the cytoplasm.

Moreover, the inconsistencies may also be attributed to post-translational mechanisms. Many cells are able to adapt to situations of altered energy demand by changing the ratio of active to inactive glucose transporter molecules. This is known to happen via trafficking of different GLUT isoforms from intracellular vesicular pools to the cellular surface (Wilson *et al.*, 1995; Malide *et al.*, 1998). Despite unremarkable whole-cell GLUT3 protein levels, it is thus conceivable that the subcellular distribution of GLUT3 protein may still differ between carriers of 2 and 3 *SLC2A3* gene copies. Additional methods such as fluorescence microscopy or cell fractionation, will probably help to investigate the proportion of GLUT3 protein in the plasma membrane. Another post-translational regulatory principle for glucose transporters was introduced by Khayat and colleagues in 1998. The authors referred to the regulatory effect of the chemical compound 2,4-dinitrophenol (DNP), which is well-known as an uncoupler of mitochondrial oxidative phosphorylation, giving rise to a rapid decline of cellular ATP. When chronically exposed to DNP, rat muscle cells were found to exhibit a variety of adaptive responses, leading to elevated cellular uptake of glucose, among others. Interestingly, this is not only achieved by *de novo* biosynthesis of GLUT1 and GLUT3 but also by prolonging the half-lives of both proteins. In this respect, the turnover rates of GLUT3 particularly emerged as being regulable over a wide range (Khayat *et al.*, 1998). Therefore, metabolic labeling of cells with [^{35}S]methionine, as was performed in that study, may also constitute a useful tool for comparing the biosynthesis and degradation of GLUT3 *in vivo* between carriers of different *SLC2A3* copy number.

4.1.4 Cellular glucose uptake assay

An additional gene copy of *SLC2A3* did not emerge to be accompanied by a significantly altered cellular glucose uptake in our immortalised peripheral cell model (LCLs). Despite being consistent with the aforementioned Western blotting results for LCLs that indicated similar whole cell GLUT3 protein amounts in *SLC2A3* duplication carriers and controls, this data does not correspond with our initial hypothesis, predicting a positive correlation between *SLC2A3* copy number and glucose uptake. Supposing that all cell culture results are valid, a very likely explanation for this unexpected outcome is that regulatory mechanisms in these peripheral cells (see chapter 4.1.3) restrict the total GLUT3 amounts and hence the glucose transport, despite enhanced *SLC2A3* mRNA levels. In this regard, it is certainly interesting to question whether such regulatory mechanisms constitute an individual feature of peripheral (blood) cells or if they also occur in the brain. Investigating central glucose metabolism via Positron emission tomography (PET) or using a neuronal cell model with *SLC2A3* overexpression may help to approach this problem.

Furthermore, the question arises of whether an additional *SLC2A3* gene copy could be redundant in situations of sufficient energy supply (as is possibly the case in our peripheral cell model under basal conditions) yet might constitute a metabolic advantage when cellular energy sources run short. Accordingly, it may be very useful to investigate the effects of glucose deprivation or treatment with substances that target cellular respiration (e.g. the aforementioned DNP) on our cell cultures.

Similar to the Western blotting data, SEM values of glucose uptake were rather high (~15% of the respective mean values in the duplication group and ~20% in controls), indicating a pronounced statistical variance and consequently constraining the evaluation of the glucose uptake. SEM values were initially even higher, but could be substantially improved by modifications of the experimental protocol; for example, in terms of pre-incubation of cells in 24-well plates, or the centrifugal speed. To disentangle whether this high variance is rather due to physiological or technical factors, future uptake experiments should involve alternative methods such as flow cytometry or other cell models such as fibroblasts. In principle, uptake experiments can also be performed with native cells as reported for instance by Piątkiewicz and

colleagues, working with PBMCs (Piatkiewicz *et al.*, 2007). Using native cells reduces potential artefacts caused by the immortalisation and cultivation of cells, yet involves other problems, such as the delimited viability and availability of cells. Moreover, in contrast to LCLs, which are considered a homogenous population of EBV-transformed B lymphocytes (Sie *et al.*, 2009), PBMCs constitute a heterogeneous mixture of various mononuclear cell types (~60% T lymphocytes, ~15% monocytes/ macrophages, ~15% natural killer cells and ~10% B lymphocytes; Rowland-Jones and McMichael, 1999), thus hindering clear-cut interpretations.

4.1.5 Functional EEG measurements

For this experiment, participants underwent a Continuous Performance Test (CPT) and n-back test while an ongoing electroencephalogram (EEG) was recorded in parallel. Both CPT and n-back are neuropsychological tests that have been proved reliable and valuable in assessing a variety of cognitive traits, particularly cognitive response control (in terms of the CPT) and working memory (in terms of the n-back test), namely two traits discussed as endophenotypes for ADHD (for a review, see Fallgatter *et al.*, 2005; Kasper *et al.*, 2012)

CPT

Concerning our CPT-linked measurements, significantly diminished NoGo-Anteriorisation (NGA) values emerged in ADHD patients with 3 *SLC2A3* gene copies compared to those in the ADHD group carrying two copies. Given that NGA is regarded as an endophenotypic marker of prefrontal brain activity during processes of cognitive response control (Fallgatter *et al.*, 2012), this result is indicative of altered prefrontal functioning.

Surprisingly, the effect was due to the centroid of the Go-condition being located considerably more anterior in duplication carriers with ADHD while NoGo-related centroids did not show a group difference. However, this quite exceptional pattern has been previously observed, namely within a study focusing on ADHD risk alleles of the *TPH2* gene (Baehne *et al.*, 2009). The authors reported that participants carrying the rs11178997 T/T-allele had a significantly smaller NGA than those with T/A-allele, which could be attributed to more anterior Go-centroids in the first group.

Although this result did not allow clear-cut assumptions about altered EEG topography during response inhibition (as opposed to response execution), it was still suggestive of an exceptional (prefrontal) brain functioning in rs11178997 T/T-allele carriers during the whole task. Accordingly, the aforementioned aberrant topographical EEG pattern of *SLC2A3* duplication carriers within the ADHD group can be interpreted as an indicator of altered brain activity during a cognitive response control task, albeit not as clear-cut proof of impaired response inhibition itself.

On the other hand, our CPT-linked EEG measurements for the *SLC2A3* CNV did not confirm a general effect of ADHD status: irrespective of *SLC2A3* copy number, the ADHD group did not show lower NGA values than healthy controls, as was expected based upon previous reports (Fallgatter *et al.*, 2005). However, taking the rather small sample size into account, this observation may simply be due to a lack of statistical power and the stratification of ADHD samples on the basis of differing genotype. Indeed, the tendency towards diminished NGA amounts in *SLC2A3* duplication carriers of the ADHD group compared to healthy *SLC2A3* duplication carriers speaks in favour of this notion.

Beyond that, we found an interaction between genotype and ADHD diagnosis in another CPT analysis, focusing on the SNP rs12842 within the *SLC2A3* gene. It emerged that ADHD patients with a C-allele at this genomic position exhibited significantly reduced NGA values when compared to healthy controls with the same allele. Additionally, within the ADHD patient group, NGA values emerged to be marginally higher in T-allele than in C-allele carriers, albeit without reaching the level of significance. According to the NCBI reference assembly hg19, rs12842 is a biallelic SNP, with ‘C’ being the ancestral and ‘T’ the minor allele (global minor allele frequency: 0.093). The polymorphism is located within the 3' untranslated region (3’UTR) of *SLC2A3* mRNA (see Figure 5), implying that the substitution of cytosine by thymine does not affect the amino acid sequence of the translated protein. However, it is conceivable that this SNP within the 3’UTR may exert influence on the secondary structure and stability of *SLC2A3* mRNA, thereby altering its translational efficiency (for a review, see Mazumder *et al.*, 2003). While the rs12842 T-allele was found to be significantly over-transmitted to offspring affected by ADHD (Merker *et al.,* manuscript in preparation), at present there is no clinical relevance known for the

C-allele. The first finding, i.e. significantly lower NGA values in ADHD patients than in healthy controls (yet only in terms of C-allele carriers), is consistent with earlier reports suggesting reduced NGA as a useful marker for ADHD-related endophenotypes (Fallgatter *et al.*, 2005). Although a clear-cut genotype effect could not be determined for rs12842, the significant interaction effect between the variables 'genotype' and 'diagnosis' still speaks in favour of an implication of this SNP in ADHD. Moreover, the trend towards higher NGA values in T-allele carriers was very close to the level of significance (p=0.058) and thus should not be completely omitted. Based on the present data, it appears that the rs12842 T-allele differentially influences EEG topography in response control tasks, which is apparently accompanied by an amelioration of reduced NGA in ADHD patients. According to this view, the T-allele possibly seems to have a rather beneficial influence on altered prefrontal brain functioning in ADHD patients during processes of cognitive response control. Naturally, replicating the experiment with other cohorts and larger sample sizes is essential to draw a more reliable conclusion.

n-back test

Subgroups of adult ADHD patients and healthy participants carrying either two or three *SLC2A3* gene copies were investigated with ERP recordings during an n-back task. Essentially, EEG data revealed drastically diminished P300 amplitudes in ADHD patients carrying three *SLC2A3* copies compared to subjects with the same diagnosis yet without the duplication. Given that the P300 component is commonly regarded as a measure of attentional and working memory processes (Polich, 2007), the results indicate a considerable impact of *SLC2A3* copy number on these mental processes.

Working memory is well-known as an attention-requiring limited capacity to hold and manipulate information in the mind for several seconds, and is considered to play an important role in reasoning, comprehension, planning and learning (Baddeley, 1992). In accordance with this definition, which underlines the importance of attention, significant working memory deficits have been described for ADHD patients both during child- (Kasper *et al.*, 2012) and adulthood (Hervey *et al.*, 2004).

When analysing working memory or other processes based upon tasks that involve an active decision, a pronounced positive voltage deflection can be measured at the participant's scalp in an interval around 300-500ms after stimulus onset. A subelement of this late positive ERP component, P300, is considered sensitive to the attentional and working memory demands of the task: in situations when attention is exclusively focused on one issue, P300 amplitudes emerged larger than usual, whereas the reverse is true (i.e. decreased amplitudes) whenever attention was compromised by other mental activities, or when information storage in the working memory occurred competitively (Gevins *et al.*, 1996; McEvoy *et al.*, 1998).

The influence of *SLC2A3* copy number on P300 amplitudes during the n-back was particularly prominent during target trials in our experiments, i.e. when participants were actually supposed to react, as well as under 1-back conditions, i.e. when participants required memory for stimuli occurring exactly 1 trial previously. The first result suggests that the late positive ERP to non-matching stimuli was higher than that of matching ones as also reported within other studies, and ascribed to the higher amount of resources required for updating the working memory in terms of non-matching stimuli (McEvoy *et al.*, 1998). The second result underscores the relevance of nominal task difficulty and required memory load, although both were comparatively low in this case (1-back condition). A possible interpretation of this discovery is that reduced P300 amplitudes of *SLC2A3* duplication carriers with ADHD may ameliorate when the complexity of the challenge, and thus the cognitive effort, drive the participant's attention to the task.

Interestingly and similar to our findings in the aforementioned CPT, the genotype effect was restricted to the ADHD group, i.e. n-back test-related P300 amplitudes did not significantly differ between healthy carriers of two or three *SLC2A3* copies. It remains to be elucidated if these results are owing to a lack of statistical power, or whether they are indicative of an interaction effect between *SLC2A3* genotype and ADHD. Unlike respective CPT results, the lack of a significant association of the duplication status with working memory in healthy controls ($p>0.25$) rather speaks in favour of the assumed interaction effect.

While rs12842 genotype status had no significant influence on n-back test-related P300 amplitudes, the ERP component ‘N200’ was overall affected by trend ($p<0.1$). N200 is known as a negative-directed EEG wave that is evoked ~200 to 350ms after the onset of a specific visual or auditory stimulus, and is suggested to be associated with conflict processing and executive cognitive control functions (Folstein and van Petten, 2008). Notably, the latency of N200 was reported to be changeable as a function of discrimination difficulty, which implies increased N200 latencies in situations when decision-making is rather tough (Towey *et al.*, 1980).

In our case, a closer observation of the genotype effect revealed that rs12842 C-allele carriers displayed significantly increased N200 latencies in non-target trials compared to target trials, across diagnostic groups and n-back test conditions. Interestingly, such an effect did not occur within the group of T-allele carriers exhibiting quite steady N200 latencies, independent of trial type, n-back test condition or ADHD diagnosis. The aforementioned observation of Towey and colleagues, suggesting a positive correlation between N200 latencies and discrimination difficulty, and thus higher latencies in 2-back than in 1-back conditions, could not be generally confirmed; rather, the ADHD subgroup of C-allele carriers only showed this effect in terms of non-target conditions, whereas all healthy subgroups appeared relatively modulation-resistant.

Overall, our findings indicate a rather negative influence of the rs12842 C-allele compared to the T-allele, given that increased (i.e. delayed) N200 latencies following non-target stimuli have been discussed as markers for slowed automatic cognitive processing and weakened cognitive inhibition (Wang *et al.*, 1999; Williams *et al.*, 2000). In this respect, our n-back data is consistent with the aforementioned CPT results, pointing towards higher (i.e. ameliorated) NGA values in ADHD patients with T-allele than those with C-allele. Moreover, similar to all aforementioned EEG results, genotype effects on N200 latencies were considerably more pronounced in the ADHD than the healthy control group, strongly supporting the assumed interaction effect between *SLC2A3* gene variants and this neurodevelopmental disorder.

4.2 *Lphn3*

4.2.1 Confirmation of homologous recombination in murine ES cells

Following electroporation and antibiotic selection of ES cells, a multitude of techniques were used to check whether the *Lphn3* targeting vector was actually taken up by the cells as well as if the *Lphn3*.flx/frt construct within the vector was entirely and correctly integrated into the ES cell genome by replacing the respective wildtype allele.

According to the International Knockout Mouse Consortium (IKMC; www.knockoutmouse.org), several quality checks for ES cells are generally recommended before commencing with the generation of chimeric mice, not least PCR-based assays. Such experiments are intended to not only confirm the presence of highly important vector-specific DNA sequences (via short-range PCR) but also the proper, i.e. site-directed, integration of the vector construct into the respective genomic locus (via long-range PCR).

In terms of our ES cell clones, three different short-range PCR and one long-range-PCR assays were designed. Starting with the short-range PCRs, we were able to sort out all clones that repeatedly did not give rise to amplicons of the correct size in all three PCRs, indicating the absence of one or multiple essential vector construct-specific DNA sequences (5’ FRT, 3’ FRT and 3’ loxP site). Using a positive (*Lphn3* targeting vector DNA) and negative control sample (wildtype ES cell clone DNA) in parallel to the transfected ES cell samples, the short-range PCR experiments proved reliable.

To verify whether the vector construct was not only present within the ES cells but also correctly integrated into their genome, a long-range PCR spanning the whole 5’ homology arm was performed. Owing to the nature of this integrative PCR (involving a forward primer that does not bind within the targeting vector), we were unable to apply a positive control sample, thus hindering the establishment of this assay. Nevertheless, the long-range PCR proved useful in selecting a fistful of ES cell clones that unambiguously exhibited the expected amplicon of 4.8kb.

The aforementioned web page of the IKMC also mentions a supplementary method that helps reliably verifying site-directed homologous recombination in ES cells, namely Southern blotting. According to the IKMC, around 18% of ES cell clones that emerge positive in two or more different PCR-based quality checks still do not pass a subsequent Southern blotting assay, which is probably due to irregular recombination events or mixed clones.

Therefore, we decided to confirm the correct integration of the *Lphn3*.flx/frt construct at the 3' homology arm via a Southern blotting analysis. By testing those ES cells that passed all preceding PCR assays, we found that 8 of 10 clones clearly gave rise to the anticipated 7.9kb fragment, representing the correctly recombined allele, whereas the remaining two clones only exhibited the 9.5kb wildtype fragment. Accordingly, our Southern blotting-related rejection rate resembled that determined by the IKMC. However, owing to the slightly distorted band front-line and particularly the high overall background (which unfortunately could not be improved without losing the target band signals), the assessment of our Southern blotting membrane was rather difficult. Consequently, some samples had to be repeated and were rejected in case of ongoing doubt. Though unlikely, it may thus be the case that the 2 discarded ES cell clones were false-negatives – a possibility that remained acceptable given the number of clearly positive samples.

4.2.2 Additional quality checks for recombined ES cells

Despite not being included in the IKMC list of quality checks, we further decided to check the correctness of some crucial sequences (FRT and loxP sites) within the *Lphn3*.flx/frt allele via DNA sequencing. Importantly, the results showed that all amplicons fully complied with the predicted sequences, indicating functional integrity of respective sites. Admittedly, we did not check the correctness of all three loxP sites within the construct: the single loxP site in between the lacZ cassette and the neomycin resistance cassette (see Figure 7), enabling separately removing the latter, was considered rather negligible and thus not included in the sequencing assay.

As recommended by the IKMC, further quality checks for ES cells comprised a Mycoplasma test and chromosome counting (karyotyping). Fortunately, the PCR-based Mycoplasma test revealed only the negative control amplicon when using DNA

extracts of ES cell clones, suggesting that they were all free of Mycoplasma bacteria, which are known to constitute a detrimental factor for several cell parameters and postnatal development of the resulting chimeric mice (Markoullis *et al.*, 2009).
Furthermore, karyotyping revealed that our ES cell clones were euploid and exhibited macrostructurally normal chromosomes in all but one case. Given that aneuploidy and other chromosomal anomalies in ES cells were shown to interfere with their capability to contribute to the germline in mice (Liu *et al.*, 1997), this finding was very vital for our subsequent experiments.

An elementary yet very essential quality check was naturally also the surveillance of ES cell morphology. Despite our ES cells being constantly grown on SNL feeder cells and in fresh medium that contained Leukemia Inhibitory Factor (LIF), i.e. in an environment that suppressed differentiation processes (Williams *et al.*, 1988), they were nonetheless inspected frequently and by different persons. Fortunately, the aforementioned ES cell clones appeared morphologically normal and undifferentiated throughout the whole cultivation phase.

With an overall quantity of 7 ES cell clones being positive for all quality checks, we eventually had an even higher number than recommended by the European Mouse Mutant Cell Repository (EuMMCR), suggesting the use of at least 3 ES cell clones per gene to ensure germline transmission in mice.

4.2.3 Generation of chimeric mice

A comparably advanced method was applied for the generation of mice embryos, relying on (laser-assisted) injection of ES cells into murine eight cell-stage embryos (morulae). In contrast to classical blastula injection techniques, this procedure allows the efficient production of mice whose body cells almost entirely derive from injected cells, considerably enhancing germline transmission rates without interfering with their viability or health (Poueymirou *et al.*, 2007).

Indeed, we were able to generate highly chimeric, phenotypically unremarkable and (with some exceptions) fertile mice by using 4 of the aforementioned 7 ES cell clones. Unfortunately, evidence has yet to be found indicating that the *Lphn3*.flx/frt

allele was inherited to the offspring of the chimeras. All tested animals only gave rise to the *Lphn3* wildtype amplicon in an allele-specific PCR assay, which was double-checked and appeared reliable in terms of the negative and positive controls. Moreover, all offspring produced so far (>100 animals) were of black coat colour, strongly arguing against germline transmission of injected ES cells (which in our case derive from mice heterozygously carrying the dominant agouti coat colour gene).

However, the project is still in progress. Indeed, as the 4 ES clones were not injected simultaneously but rather with a large time-delay, our chimeric mice are of different ages. Therefore, more than 50% of the chimeras still are too young to be mated, and their expected offspring has yet to be genotyped. Given that our ES cell clones were thoroughly tested before morula injection and derive from the cell line ‘JM8A3’, which is reported to have a germline transmission rate around 82% (Pettitt *et al.*, 2009), there currently is no reason to seriously doubt the quality of our cell clones and hence the success of the entire project.

5 Conclusion and outlook

5.1 *SLC2A3*

Overall, our results indicate that *SLC2A3* polymorphisms associated with ADHD are accompanied by transcriptional and functional changes in humans. In peripheral blood cell models, *SLC2A3* duplication carriers displayed dramatically increased *SLC2A3* mRNA levels, whereas corresponding GLUT3 protein amounts and overall glucose uptake appeared unaltered under basal conditions. ADHD patients with *SLC2A3* duplication exhibited significantly diminished NGA values when observing ERP recordings during a test of cognitive response control, possibly involving altered prefrontal brain activity. By contrast, this effect appeared reversed in ADHD patients carrying the T-allele of the ADHD-associated SNP rs12842 when compared to respective C-allele carriers. Moreover, during a neuropsychological test of working memory, EEG measurements of *SLC2A3* duplication carriers within the ADHD group revealed drastically reduced P300 amplitudes, suggestive of altered attention and working memory processes, whereas no such influence was observed for the SNP rs12842. However, T-allele carriers in both diagnostic groups showed lower N200 latencies in response to non-target stimuli than participants with C-allele, possibly reflecting faster cognitive processing in the former. Overall, our EEG findings suggest that the *SLC2A3* CNV (duplication) and SNP (rs12842 T-allele) exert dissimilar or even opposed effects on various EEG parameters, indicative of opposed molecular mechanisms; moreover these genotype effects generally were much more pronounced in the ADHD group, implying a considerable interaction.

A large debate has recently emerged concerning the complex genetic topography of ADHD, with some studies showing the impact of common variants such as SNPs and others emphasising the effect of rare variants such as CNVs. In this regard, our *SLC2A3* study somewhat constitutes an amalgamation that combines these competing models and underlines the broad continuum between both extremes, i.e. common variants with small effect size and arising from very distant ancestors on the one hand and extremely rare *de novo* variants with very large effect size on the other (Lupski *et al.*, 2011). Given the comparably little research conducted in terms of ADHD-associated CNVs to date, our findings may contribute to shed some light on

the murk of ADHD genetics, including the question of ‘missing heritability’, namely the considerable percentage of heritability for many complex traits and diseases that is presently unaccounted for (Manolio *et al.*, 2009).

Future research of *SLC2A3* polymorphisms will possibly comprise a variety of techniques and models. For human carriers of *SLC2A3* variants, additional functional methods could be used such as fMRI imaging during food-related tasks or PET imaging of central glucose metabolism. As indicated in the discussion (chapter 4.1.1), this may also include participants showing a deletion of *SLC2A3,* which has not yet been associated with a particular phenotype in human. To obtain a suitable animal model for the *SLC2A3* CNV, it is conceivable to develop and characterise a mouse line overexpressing the orthologous gene *Slc2a3*. Additionally, other cellular models might be established, for example *SLC2A3*-overexpressing primary neurons or neuronal cell cultures deriving from reprogrammed fibroblasts (Vierbuchen *et al.*, 2010). Overall, these and other models may particularly help to elucidate the molecular networks that somewhat compose the ‘black box’ in between genes and behaviour, i.e. in our case the ‘black box’ between polymorphisms of a certain glucose transporter gene and the complex traits representing the neurobehavioural disorder ADHD.

5.2 *Lphn3*

Given that this project involves the principal goal of developing a *Lphn3* mouse model with conditional knockout potential, intermediate results are available at this point. Indeed, we were able to successfully transfect murine ES cells with a *Lphn3* targeting vector and confirm correct homologous recombination between the vector and the genomic *Lphn3* locus via several PCR- and Southern blotting-based assays. Moreover, we performed various quality checks for these cells, such as DNA sequencing, Mycoplasma testing and karyotyping. Overall, our tests led to more than half a dozen positive ES cell clones, some of which were used for subsequent microinjection of murine morulae. Numerous highly chimeric and phenotypically unremarkable mice were generated by this means and crossed with wildtype animals, albeit without yet giving rise to germline transmission of the *Lphn3*.flx/frt allele. Fortunately, there is a distinct chance of achieving the goal in the near future,

as the majority of our chimeras are currently too young to produce offspring and thus are yet to be tested for germline transmission.

Given the large number of recent publications underscoring the implication of the gene *LPHN3* in several physiological processes and psychiatric disorders such as ADHD, the establishment of an appropriate mammalian model of latrophilin-3 deficiency certainly constitutes an important prerequisite for future research of this gene. Generating a mouse line that exhibits the *Lphn3*.flx/frt allele involves several considerable advantages. For instance, owing to the lacZ trapping cassette within the gene construct, it is possible to simultaneously disrupt and report *Lphn3* gene function *in vivo.* Consequently, mice homozygously carrying this allele are expected to resemble constitutive *Lphn3* knockout animals (knockout-first principle), enabling an early phenotypical characterisation. Moreover, the lacZ reporter gene provides the opportunity to reliably analyse the expression pattern of *Lphn3* in mice via beta-galactosidase staining of (brain) tissue (Kaelin *et al.*, 2004). Importantly, the *Lphn3*.flx/frt allele can also be modified *in vivo* when crossing respective mice with transgenic animals expressing Flp recombinase. By this means, it is possible to remove both the lacZ and neo cassette, resulting in a ‘clean’ floxed allele, which is a prerequisite for the conditional knockout of murine *Lphn3* in a time- or tissue-specific manner (e.g. only in dopaminergic cells). The subsequent phenotypical analysis of such a mouse line may involve a multitude of aspects and methods, such as morphology, immunohistochemistry and neuroimaging, and also electrophysiology, pharmacology and not least behaviour, thus likely providing a comprehensive view. As mentioned in chapter 1.1.7 describing the evaluation of animal models, this multifaceted analysis will also serve to check whether or not conditional *Lphn3* knockout mice meet all required validity criteria and thus can be considered an appropriate mammalian model of ADHD.

6 Appendix

6.1 References

Antshel, K.M., Hargrave, T.M., Simonescu, M., Kaul, P., Hendricks, K., Faraone, S.V., 2011. Advances in understanding and treating ADHD. BMC Med 9, 72.

Arcos-Burgos, M., Jain, M., Acosta, M.T., Shively, S., Stanescu, H., Wallis, D., Domene, S., Velez, J.I., Karkera, J.D., Balog, J., Berg, K., Kleta, R., Gahl, W.A., Roessler, E., Long, R., Lie, J., Pineda, D., Londono, A.C., Palacio, J.D., Arbelaez, A., Lopera, F., Elia, J., Hakonarson, H., Johansson, S., Knappskog, P.M., Haavik, J., Ribases, M., Cormand, B., Bayes, M., Casas, M., Ramos-Quiroga, J.A., Hervas, A., Maher, B.S., Faraone, S.V., Seitz, C., Freitag, C.M., Palmason, H., Meyer, J., Romanos, M., Walitza, S., Hemminger, U., Warnke, A., Romanos, J., Renner, T., Jacob, C., Lesch, K.-P., Swanson, J., Vortmeyer, A., Bailey-Wilson, J.E., Castellanos, F.X., Muenke, M., 2010. A common variant of the latrophilin 3 gene, LPHN3, confers susceptibility to ADHD and predicts effectiveness of stimulant medication. Mol Psychiatry 15, 1053–1066.

Arime, Y., Kubo, Y., Sora, I., 2011. Animal models of attention-deficit/hyperactivity disorder. Biol Pharm Bull 34, 1373–1376.

Augustin, R., 2010. The protein family of glucose transport facilitators: It's not only about glucose after all. IUBMB Life 62, 315–333.

Baddeley, A., 1992. Working memory. Science 255, 556–559.

Baehne, C.G., Ehlis, A.-C., Plichta, M.M., Conzelmann, A., Pauli, P., Jacob, C., Gutknecht, L., Lesch, K.-P., Fallgatter, A.J., 2009. Tph2 gene variants modulate response control processes in adult ADHD patients and healthy individuals. Mol. Psychiatry 14, 1032–1039.

Banaschewski, T., Becker, K., Scherag, S., Franke, B., Coghill, D., 2010. Molecular genetics of attention-deficit/hyperactivity disorder: an overview. Eur Child Adolesc Psychiatry 19, 237–257.

Banerjee, T.D., Middleton, F., Faraone, S.V., 2007. Environmental risk factors for attention-deficit hyperactivity disorder. Acta Paediatr 96, 1269–1274.

Barkley, R.A., Fischer, M., Smallish, L., Fletcher, K., 2004. Young adult follow-up of hyperactive children: antisocial activities and drug use. J Child Psychol Psychiatry 45, 195–211.

Biederman, J., 2005. Attention-deficit/hyperactivity disorder: a selective overview. Biol. Psychiatry 57, 1215–1220.

Bin Sun, H., Ruan, Y., Xu, Z.C., Yokota, H., 2002. Involvement of the calcium-independent receptor for alpha-latrotoxin in brain ischemia. Brain Res Mol Brain Res 104, 246–249.

Boucard, A.A., Ko, J., Sudhof, T.C., 2012. High affinity neurexin binding to cell adhesion G-protein-coupled receptor CIRL1/latrophilin-1 produces an intercellular adhesion complex. J Biol Chem 287, 9399–9413.

Bourey, R.E., Koranyi, L., James, D.E., Mueckler, M., Permutt, M.A., 1990. Effects of altered glucose homeostasis on glucose transporter expression in skeletal muscle of the rat. J. Clin. Invest. 86, 542–547.

Bryant, N.J., Govers, R., James, D.E., 2002. Regulated transport of the glucose transporter GLUT4. Nat Rev Mol Cell Biol 3, 267–277.

Bush, G., Valera, E.M., Seidman, L.J., 2005. Functional neuroimaging of attention-deficit/hyperactivity disorder: a review and suggested future directions. Biol Psychiatry 57, 1273–1284.

Castellanos, F.X., Lee, P.P., Sharp, W., Jeffries, N.O., Greenstein, D.K., Clasen, L.S., Blumenthal, J.D., James, R.S., Ebens, C.L., Walter, J.M., Zijdenbos, A., Evans, A.C., Giedd, J.N., Rapoport, J.L., 2002. Developmental trajectories of brain volume abnormalities in children and adolescents with attention-deficit/hyperactivity disorder. JAMA 288, 1740–1748.

Cohen, J.D., Perlstein, W.M., Braver, T.S., Nystrom, L.E., Noll, D.C., Jonides, J., Smith, E.E., 1997. Temporal dynamics of brain activation during a working memory task. Nature 386, 604–608.

Copeland, N.G., Jenkins, N.A., Court, D.L., 2001. Recombineering: a powerful new tool for mouse functional genomics. Nat. Rev. Genet. 2, 769–779.

Davletov, B.A., Shamotienko, O.G., Lelianova, V.G., Grishin, E.V., Ushkaryov, Y.A., 1996. Isolation and biochemical characterization of a Ca2+-independent alpha-latrotoxin-binding protein. J Biol Chem 271, 23239–23245.

Domene, S., Stanescu, H., Wallis, D., Tinloy, B., Pineda, D.E., Kleta, R., Arcos-Burgos, M., Roessler, E., Muenke, M., 2011. Screening of human LPHN3 for variants with a potential impact on ADHD susceptibility. Am J Med Genet B Neuropsychiatr Genet 156, 11–18.

Elia, J., Glessner, J.T., Wang, K., Takahashi, N., Shtir, C.J., Hadley, D., Sleiman, P.M.A., Zhang, H., Kim, C.E., Robison, R., Lyon, G.J., Flory, J.H., Bradfield, J.P., Imielinski, M., Hou, C., Frackelton, E.C., Chiavacci, R.M., Sakurai, T., Rabin, C., Middleton, F.A., Thomas, K.A., Garris, M., Mentch, F., Freitag, C.M., Steinhausen, H.-C., Todorov, A.A., Reif, A., Rothenberger, A., Franke, B., Mick, E.O., Roeyers, H., Buitelaar, J., Lesch, K.-P., Banaschewski, T., Ebstein, R.P., Mulas, F., Oades, R.D., Sergeant, J., Sonuga-Barke, E., Renner, T.J., Romanos, M., Romanos, J., Warnke, A., Walitza, S., Meyer, J., Palmason, H., Seitz, C., Loo, S.K., Smalley, S.L., Biederman, J., Kent, L., Asherson, P., Anney, R.J.L., Gaynor, J.W., Shaw, P., Devoto, M., White, P.S., Grant, S.F.A., Buxbaum, J.D., Rapoport, J.L., Williams, N.M., Nelson, S.F., Faraone, S.V., Hakonarson, H., 2012. Genome-wide copy number variation study associates metabotropic glutamate receptor gene networks with attention deficit hyperactivity disorder. Nat Genet 44, 78–84.

Estrada, D.E., Elliott, E., Zinman, B., Poon, I., Liu, Z., Klip, A., Daneman, D., 1994. Regulation of glucose transport and expression of GLUT3 transporters in human circulating mononuclear cells: studies in cells from insulin-dependent diabetic and nondiabetic individuals. Metab. Clin. Exp. 43, 591–598.

Fallgatter, A.J., Bartsch, A.J., Herrmann, M.J., 2002. Electrophysiological measurements of anterior cingulate function. J Neural Transm 109, 977–988.

Fallgatter, A.J., Ehlis, A.-C., Rösler, M., Strik, W.K., Blocher, D., Herrmann, M.J., 2005. Diminished prefrontal brain function in adults with psychopathology in childhood related to attention deficit hyperactivity disorder. Psychiatry Res 138, 157–169.

Fallgatter, A.J., Ehlis, A.-C., Dresler, T., Reif, A., Jacob, C.P., Arcos-Burgos, M., Muenke, M., Lesch, K.-P., 2012. Influence of a Latrophilin 3 (LPHN3) risk haplotype on event-related potential measures of cognitive response control in attention-deficit hyperactivity disorder (ADHD). Eur Neuropsychopharmacol.

Faraone, S.V., Biederman, J., Mick, E., 2006. The age-dependent decline of attention deficit hyperactivity disorder: a meta-analysis of follow-up studies. Psychol Med 36, 159–165.

Faraone, S.V., Mick, E., 2010. Molecular genetics of attention deficit hyperactivity disorder. Psychiatr Clin North Am 33, 159–180.

Faraone, S.V., Perlis, R.H., Doyle, A.E., Smoller, J.W., Goralnick, J.J., Holmgren, M.A., Sklar, P., 2005. Molecular genetics of attention-deficit/hyperactivity disorder. Biol Psychiatry 57, 1313–1323.

Fayyad, J., Graaf, R. de, Kessler, R., Alonso, J., Angermeyer, M., Demyttenaere, K., Girolamo, G. de, Haro, J.M., Karam, E.G., Lara, C., Lépine, J.-P., Ormel, J., Posada-Villa, J., Zaslavsky, A.M., Jin, R., 2007. Cross-national prevalence and correlates of adult attention-deficit hyperactivity disorder. Br J Psychiatry 190, 402–409.

Field, L.L., Shumansky, K., Ryan, J., Truong, D., Swiergala, E., Kaplan, B.J., 2013. Dense-map genome scan for dyslexia supports loci at 4q13, 16p12, 17q22; suggests novel locus at 7q36. Genes Brain Behav 12, 56–69.

Folstein, J.R., van Petten, C., 2008. Influence of cognitive control and mismatch on the N2 component of the ERP: a review. Psychophysiology 45, 152–170.

Fredriksson, R., Lagerstrom, M.C., Lundin, L.-G., Schioth, H.B., 2003. The G-protein-coupled receptors in the human genome form five main families. Phylogenetic analysis, paralogon groups, and fingerprints. Mol Pharmacol 63, 1256–1272.

Frodl, T., Skokauskas, N., 2012. Meta-analysis of structural MRI studies in children and adults with attention deficit hyperactivity disorder indicates treatment effects. Acta Psychiatr Scand 125, 114–126.

Fu, C.H., Reed, L.J., Meyer, J.H., Kennedy, S., Houle, S., Eisfeld, B.S., Brown, G.M., 2001. Noradrenergic dysfunction in the prefrontal cortex in depression: an 15O H2O PET study of the neuromodulatory effects of clonidine. Biol Psychiatry 49, 317–325.

Gau, S.S.-F., Liao, H.-M., Hong, C.-C., Chien, W.-H., Chen, C.-H., 2012. Identification of two inherited copy number variants in a male with autism supports two-hit and compound heterozygosity models of autism. Am J Med Genet B Neuropsychiatr Genet 159, 710–717.

Gazzara, R.A., Altman, J., 1981. Early postnatal x-irradiation of the hippocampus and discrimination learning in adult rats. J Comp Physiol Psychol 95, 484–495.

Gevins, A., Smith, M.E., Le, J., Leong, H., Bennett, J., Martin, N., McEvoy, L., Du, R., Whitfield, S., 1996. High resolution evoked potential imaging of the cortical dynamics of human working memory. Electroencephalogr Clin Neurophysiol 98, 327–348.

Gould, G.W., Thomas, H.M., Jess, T.J., Bell, G.I., 1991. Expression of human glucose transporters in Xenopus oocytes: kinetic characterization and substrate specificities of the erythrocyte, liver, and brain isoforms. Biochemistry 30, 5139–5145.

Gramatte, T., Schmidt, J., 1986. The effect of early postnatal hypoxia on the development of locomotor activity in rats. Biomed Biochim Acta 45, 523–529.

Grishin, E.V., 1998. Black widow spider toxins: the present and the future. Toxicon 36, 1693–1701.

Haber, R.S., Weinstein, S.P., O'Boyle, E., Morgello, S., 1993. Tissue distribution of the human GLUT3 glucose transporter. Endocrinology 132, 2538–2543.

Halmøy, A., Fasmer, O.B., Gillberg, C., Haavik, J., 2009. Occupational outcome in adult ADHD: impact of symptom profile, comorbid psychiatric problems, and treatment: a cross-sectional study of 414 clinically diagnosed adult ADHD patients. J Atten Disord 13, 175–187.

Hannestad, J., Gallezot, J.-D., Planeta-Wilson, B., Lin, S.-F., Williams, W.A., van Dyck, C.H., Malison, R.T., Carson, R.E., Ding, Y.-S., 2010. Clinically relevant doses of methylphenidate significantly occupy norepinephrine transporters in humans in vivo. Biol. Psychiatry 68, 854–860.

Heather West Greenlee, M., Uemura, E., Carpenter, S.L., Doyle, R.T., Buss, J.E., 2003. Glucose uptake in PC12 cells: GLUT3 vesicle trafficking and fusion as revealed with a novel GLUT3-GFP fusion protein. J. Neurosci. Res. 73, 518–525.

Heijnen, H.F., Oorschot, V., Sixma, J.J., Slot, J.W., James, D.E., 1997. Thrombin stimulates glucose transport in human platelets via the translocation of the glucose transporter GLUT-3 from alpha-granules to the cell surface. J Cell Biol 138, 323–330.

Hervey, A.S., Epstein, J.N., Curry, J.F., 2004. Neuropsychology of adults with attention-deficit/hyperactivity disorder: a meta-analytic review. Neuropsychology 18, 485–503.

Hinney, A., Scherag, A., Jarick, I., Albayrak, O., Putter, C., Pechlivanis, S., Dauvermann, M.R., Beck, S., Weber, H., Scherag, S., Nguyen, T.T., Volckmar, A.-L., Knoll, N., Faraone, S.V., Neale, B.M., Franke, B., Cichon, S., Hoffmann, P., Nothen, M.M., Schreiber, S., Jockel, K.-H., Wichmann, H.-E., Freitag, C., Lempp, T., Meyer, J., Gilsbach, S., Herpertz-Dahlmann, B., Sinzig, J., Lehmkuhl, G., Renner, T.J., Warnke, A., Romanos, M., Lesch, K.-P., Reif, A., Schimmelmann, B.G., Hebebrand, J., 2011. Genome-wide association study in German patients with attention deficit/hyperactivity disorder. Am J Med Genet B Neuropsychiatr Genet 156, 888–897.

Ichtchenko, K., Bittner, M.A., Krasnoperov, V., Little, A.R., Chepurny, O., Holz, R.W., Petrenko, A.G., 1999. A novel ubiquitously expressed alpha-latrotoxin receptor is a member of the CIRL family of G-protein-coupled receptors. J Biol Chem 274, 5491–5498.

Izumi, K., Conlin, L.K., Berrodin, D., Fincher, C., Wilkens, A., Haldeman-Englert, C., Saitta, S.C., Zackai, E.H., Spinner, N.B., Krantz, I.D., 2012. Duplication 12p and Pallister-Killian syndrome: a case report and review of the literature toward defining a Pallister-Killian syndrome minimal critical region. Am. J. Med. Genet. A 158, 3033–3045.

Kaelin, C.B., Xu, A.W., Lu, X.-Y., Barsh, G.S., 2004. Transcriptional regulation of agouti-related protein (Agrp) in transgenic mice. Endocrinology 145, 5798–5806.

Kahn, R.S., Khoury, J., Nichols, W.C., Lanphear, B.P., 2003. Role of dopamine transporter genotype and maternal prenatal smoking in childhood hyperactive-impulsive, inattentive, and oppositional behaviors. J Pediatr 143, 104–110.

Kan, Z., Jaiswal, B.S., Stinson, J., Janakiraman, V., Bhatt, D., Stern, H.M., Yue, P., Haverty, P.M., Bourgon, R., Zheng, J., Moorhead, M., Chaudhuri, S., Tomsho, L.P., Peters, B.A., Pujara, K., Cordes, S., Davis, D.P., Carlton, V.E.H., Yuan, W., Li, L., Wang, W., Eigenbrot, C., Kaminker, J.S., Eberhard, D.A., Waring, P., Schuster, S.C., Modrusan, Z., Zhang, Z., Stokoe, D., Sauvage, F.J. de, Faham, M., Seshagiri, S., 2010. Diverse somatic mutation patterns and pathway alterations in human cancers. Nature 466, 869–873.

Kasper, L.J., Alderson, R.M., Hudec, K.L., 2012. Moderators of working memory deficits in children with attention-deficit/hyperactivity disorder (ADHD): a meta-analytic review. Clin Psychol Rev 32, 605–617.

Katritch, V., Cherezov, V., Stevens, R.C., 2012. Diversity and modularity of G protein-coupled receptor structures. Trends Pharmacol Sci 33, 17–27.

Kayano, T., Fukumoto, H., Eddy, R.L., Fan, Y.S., Byers, M.G., Shows, T.B., Bell, G.I., 1988. Evidence for a family of human glucose transporter-like proteins. Sequence and gene localization of a protein expressed in fetal skeletal muscle and other tissues. J Biol Chem 263, 15245–15248.

Khayat, Z.A., McCall, A.L., Klip, A., 1998. Unique mechanism of GLUT3 glucose transporter regulation by prolonged energy demand: increased protein half-life. Biochem. J. 333 (Pt 3), 713–718.

Kostrzewa, R.M., Kostrzewa, J.P., Kostrzewa, R.A., Nowak, P., Brus, R., 2008. Pharmacological models of ADHD. J Neural Transm 115, 287–298.

Krain, A.L., Castellanos, F.X., 2006. Brain development and ADHD. Clin Psychol Rev 26, 433–444.

Krasnoperov, V.G., Bittner, M.A., Beavis, R., Kuang, Y., Salnikow, K.V., Chepurny, O.G., Little, A.R., Plotnikov, A.N., Wu, D., Holz, R.W., Petrenko, A.G., 1997. alpha-Latrotoxin stimulates exocytosis by the interaction with a neuronal G-protein-coupled receptor. Neuron 18, 925–937.

Krasnoperov, V., Bittner, M.A., Mo, W., Buryanovsky, L., Neubert, T.A., Holz, R.W., Ichtchenko, K., Petrenko, A.G., 2002. Protein-tyrosine phosphatase-sigma is a novel member of the functional family of alpha-latrotoxin receptors. J. Biol. Chem. 277, 35887–35895.

Krasnoperov, V., Deyev, I.E., Serova, O.V., Xu, C., Lu, Y., Buryanovsky, L., Gabibov, A.G., Neubert, T.A., Petrenko, A.G., 2009. Dissociation of the subunits of the calcium-independent receptor of alpha-latrotoxin as a result of two-step proteolysis. Biochemistry 48, 3230–3238.

Kuzman, M.R., Medved, V., Terzic, J., Krainc, D., 2009. Genome-wide expression analysis of peripheral blood identifies candidate biomarkers for schizophrenia. J Psychiatr Res 43, 1073–1077.

Lange, M., Norton, W., Coolen, M., Chaminade, M., Merker, S., Proft, F., Schmitt, A., Vernier, P., Lesch, K.-P., Bally-Cuif, L., 2012. The ADHD-susceptibility gene lphn3.1 modulates dopaminergic neuron formation and locomotor activity during zebrafish development. Mol Psychiatry 17, 946–954.

Langenhan, T., Promel, S., Mestek, L., Esmaeili, B., Waller-Evans, H., Hennig, C., Kohara, Y., Avery, L., Vakonakis, I., Schnabel, R., Russ, A.P., 2009. Latrophilin signaling links anterior-posterior tissue polarity and oriented cell divisions in the C. elegans embryo. Dev Cell 17, 494–504.

Lelianova, V.G., Davletov, B.A., Sterling, A., Rahman, M.A., Grishin, E.V., Totty, N.F., Ushkaryov, Y.A., 1997. Alpha-latrotoxin receptor, latrophilin, is a novel member of the secretin family of G protein-coupled receptors. J Biol Chem 272, 21504–21508.

Lesch, K.-P., Selch, S., Renner, T.J., Jacob, C., Nguyen, T.T., Hahn, T., Romanos, M., Walitza, S., Shoichet, S., Dempfle, A., Heine, M., Boreatti-Hummer, A., Romanos, J., Gross-Lesch, S., Zerlaut, H., Wultsch, T., Heinzel, S., Fassnacht, M., Fallgatter, A., Allolio, B., Schafer, H., Warnke, A., Reif, A., Ropers, H.-H., Ullmann, R., 2011. Genome-wide copy number variation analysis in attention-deficit/hyperactivity disorder: association with neuropeptide Y gene dosage in an extended pedigree. Mol Psychiatry 16, 491–503.

Liu, P., Jenkins, N.A., Copeland, N.G., 2003. A highly efficient recombineering-based method for generating conditional knockout mutations. Genome Res 13, 476–484.

Liu, Q.-R., Drgon, T., Johnson, C., Walther, D., Hess, J., Uhl, G.R., 2006. Addiction molecular genetics: 639,401 SNP whole genome association identifies many "cell adhesion" genes. Am J Med Genet B Neuropsychiatr Genet 141, 918–925.

Liu, X., Wu, H., Loring, J., Hormuzdi, S., Disteche, C.M., Bornstein, P., Jaenisch, R., 1997. Trisomy eight in ES cells is a common potential problem in gene targeting and interferes with germ line transmission. Dev Dyn 209, 85–91.

Liu, Y., Liu, F., Iqbal, K., Grundke-Iqbal, I., Gong, C.-X., 2008. Decreased glucose transporters correlate to abnormal hyperphosphorylation of tau in Alzheimer disease. FEBS Lett. 582, 359–364.

Lupski, J.R., Belmont, J.W., Boerwinkle, E., Gibbs, R.A., 2011. Clan genomics and the complex architecture of human disease. Cell 147, 32–43.

Malide, D., Davies-Hill, T.M., Levine, M., Simpson, I.A., 1998. Distinct localization of GLUT-1, -3, and -5 in human monocyte-derived macrophages: effects of cell activation. Am J Physiol 274, E516-26.

Manolio, T.A., Collins, F.S., Cox, N.J., Goldstein, D.B., Hindorff, L.A., Hunter, D.J., McCarthy, M.I., Ramos, E.M., Cardon, L.R., Chakravarti, A., Cho, J.H., Guttmacher, A.E., Kong, A., Kruglyak, L., Mardis, E., Rotimi, C.N., Slatkin, M., Valle, D., Whittemore, A.S., Boehnke, M., Clark, A.G., Eichler, E.E., Gibson, G., Haines, J.L., Mackay, T.F.C., McCarroll, S.A., Visscher, P.M., 2009. Finding the missing heritability of complex diseases. Nature 461, 747–753.

Mantych, G.J., James, D.E., Chung, H.D., Devaskar, S.U., 1992. Cellular localization and characterization of Glut 3 glucose transporter isoform in human brain. Endocrinology 131, 1270–1278.

Markoullis, K., Bulian, D., Hölzlwimmer, G., Quintanilla-Martinez, L., Heiliger, K.-J., Zitzelsberger, H., Scherb, H., Mysliwietz, J., Uphoff, C.C., Drexler, H.G., Adler, T., Busch, D.H., Schmidt, J., Mahabir, E., 2009. Mycoplasma contamination of murine embryonic stem cells affects cell parameters, germline transmission and chimeric progeny. Transgenic Res. 18, 71–87.

Martinez, A.F., Muenke, M., Arcos-Burgos, M., 2011. From the black widow spider to human behavior: Latrophilins, a relatively unknown class of G protein-coupled receptors, are implicated in psychiatric disorders. Am J Med Genet B Neuropsychiatr Genet 156, 1–10.

Matsushita, H., Lelianova, V.G., Ushkaryov, Y.A., 1999. The latrophilin family: multiply spliced G protein-coupled receptors with differential tissue distribution. FEBS Lett 443, 348–352.

Mazumder, B., Seshadri, V., Fox, P.L., 2003. Translational control by the 3'-UTR: the ends specify the means. Trends Biochem. Sci. 28, 91–98.

McEvoy, L.K., Smith, M.E., Gevins, A., 1998. Dynamic cortical networks of verbal and spatial working memory: effects of memory load and task practice. Cereb Cortex 8, 563–574.

Muth, E.A., Haskins, J.T., Moyer, J.A., Husbands, G.E., Nielsen, S.T., Sigg, E.B., 1986. Antidepressant biochemical profile of the novel bicyclic compound Wy-45,030, an ethyl cyclohexanol derivative. Biochem Pharmacol 35, 4493–4497.

Nagamatsu, S., Kornhauser, J.M., Burant, C.F., Seino, S., Mayo, K.E., Bell, G.I., 1992. Glucose transporter expression in brain. cDNA sequence of mouse GLUT3, the brain facilitative glucose transporter isoform, and identification of sites of expression by in situ hybridization. J Biol Chem 267, 467–472.

Nehlig, A., Rudolf, G., Leroy, C., Rigoulot, M.-A., Simpson, I.A., Vannucci, S.J., 2006. Pentylenetetrazol-induced status epilepticus up-regulates the expression of glucose transporter mRNAs but not proteins in the immature rat brain. Brain Res. 1082, 32–42.

O'Sullivan, M.L., Wit, J. de, Savas, J.N., Comoletti, D., Otto-Hitt, S., Yates, J.R.3., Ghosh, A., 2012. FLRT proteins are endogenous latrophilin ligands and regulate excitatory synapse development. Neuron 73, 903–910.

Ozeki, Y., Matsui, T., Suzuki, M., Titani, K., 1991. Amino acid sequence and molecular characterization of a D-galactoside-specific lectin purified from sea urchin (Anthocidaris crassispina) eggs. Biochemistry 30, 2391–2394.

Pao, S.S., Paulsen, I.T., Saier, M.H., JR, 1998. Major facilitator superfamily. Microbiol Mol Biol Rev 62, 1–34.

Perrin, M.H., Sutton, S., Bain, D.L., Berggren, W.T., Vale, W.W., 1998. The first extracellular domain of corticotropin releasing factor-R1 contains major binding determinants for urocortin and astressin. Endocrinology 139, 566–570.

Pettitt, S.J., Liang, Q., Rairdan, X.Y., Moran, J.L., Prosser, H.M., Beier, D.R., Lloyd, K.C., Bradley, A., Skarnes, W.C., 2009. Agouti C57BL/6N embryonic stem cells for mouse genetic resources. Nat Methods 6, 493–495.

Piatkiewicz, P., Czech, A., Tatoń, J., 2007. Glucose transport in human peripheral blood lymphocytes influenced by type 2 diabetes mellitus. Arch. Immunol. Ther. Exp. (Warsz.) 55, 119–126.

Polich, J., 2007. Updating P300: an integrative theory of P3a and P3b. Clin Neurophysiol 118, 2128–2148.

Poueymirou, W.T., Auerbach, W., Frendewey, D., Hickey, J.F., Escaravage, J.M., Esau, L., Dore, A.T., Stevens, S., Adams, N.C., Dominguez, M.G., Gale, N.W., Yancopoulos, G.D., DeChiara, T.M., Valenzuela, D.M., 2007. F0 generation mice fully derived from gene-targeted embryonic stem cells allowing immediate phenotypic analyses. Nat Biotechnol 25, 91–99.

Rahman, M.A., Ashton, A.C., Meunier, F.A., Davletov, B.A., Dolly, J.O., Ushkaryov, Y.A., 1999. Norepinephrine exocytosis stimulated by alpha-latrotoxin requires both external and stored Ca2+ and is mediated by latrophilin, G proteins and phospholipase C. Philos Trans R Soc Lond B Biol Sci 354, 379–386.

Reekie, K.E., 2011. Technological and biological studies of human structural variation. University of Leicester.

Riccio, C.A., Reynolds, C.R., Lowe, P., Moore, J.J., 2002. The continuous performance test: a window on the neural substrates for attention? Arch Clin Neuropsychol 17, 235–272.

Roeske, D., Ludwig, K.U., Neuhoff, N., Becker, J., Bartling, J., Bruder, J., Brockschmidt, F.F., Warnke, A., Remschmidt, H., Hoffmann, P., Muller-Myhsok, B., Nothen, M.M., Schulte-Korne, G., 2011. First genome-wide association scan on neurophysiological endophenotypes points to trans-regulation effects on SLC2A3 in dyslexic children. Mol Psychiatry 16, 97–107.

Rommelse, N.N.J., 2008. Endophenotypes in the genetic research of ADHD over the last decade: have they lived up to their expectations? Expert Rev Neurother 8, 1425–1429.

Rowland-Jones, S., McMichael, A., 1999. Lymphocytes. A Practical Approach: A Practical Approach. OUP Oxford.

Rumsey, S.C., Kwon, O., Xu, G.W., Burant, C.F., Simpson, I., Levine, M., 1997. Glucose transporter isoforms GLUT1 and GLUT3 transport dehydroascorbic acid. J Biol Chem 272, 18982–18989.

Sagvolden, T., 2000. Behavioral validation of the spontaneously hypertensive rat (SHR) as an animal model of attention-deficit/hyperactivity disorder (AD/HD). Neurosci Biobehav Rev 24, 31–39.

Shiratsuchi, T., Nishimori, H., Ichise, H., Nakamura, Y., Tokino, T., 1997. Cloning and characterization of BAI2 and BAI3, novel genes homologous to brain-specific angiogenesis inhibitor 1 (BAI1). Cytogenet Cell Genet 79, 103–108.

Sie, L., Loong, S., Tan, E.K., 2009. Utility of lymphoblastoid cell lines. J. Neurosci. Res. 87, 1953–1959.

Towey, J., Rist, F., Hakerem, G., Ruchkin, D.S., Sutton, S., 1980. N250 latency and decision time. Bulletin of the Psychonomic Society, Vol 15(6), 365–368.

Silva, J.-P., Lelianova, V.G., Ermolyuk, Y.S., Vysokov, N., Hitchen, P.G., Berninghausen, O., Rahman, M.A., Zangrandi, A., Fidalgo, S., Tonevitsky, A.G., Dell, A., Volynski, K.E., Ushkaryov, Y.A., 2011. Latrophilin 1 and its endogenous ligand Lasso/teneurin-2 form a high-affinity transsynaptic receptor pair with signaling capabilities. Proc Natl Acad Sci U S A 108, 12113–12118.

Silva, J.-P., Lelianova, V., Hopkins, C., Volynski, K.E., Ushkaryov, Y., 2009. Functional cross-interaction of the fragments produced by the cleavage of distinct adhesion G-protein-coupled receptors. J Biol Chem 284, 6495–6506.

Simpson, I.A., Dwyer, D., Malide, D., Moley, K.H., Travis, A., Vannucci, S.J., 2008. The facilitative glucose transporter GLUT3: 20 years of distinction. Am J Physiol Endocrinol Metab 295, E242-53.

Snyder, D.A., Rivers, A.M., Yokoe, H., Menco, B.P., Anholt, R.R., 1991. Olfactomedin: purification, characterization, and localization of a novel olfactory glycoprotein. Biochemistry 30, 9143–9153.

Stuart, C.A., Wen, G., Jiang, J., 1999. GLUT3 protein and mRNA in autopsy muscle specimens. Metabolism 48, 876–880.

Sugita, S., Ichtchenko, K., Khvotchev, M., Sudhof, T.C., 1998. alpha-Latrotoxin receptor CIRL/latrophilin 1 (CL1) defines an unusual family of ubiquitous G-protein-linked receptors. G-protein coupling not required for triggering exocytosis. J Biol Chem 273, 32715–32724.

Thoidis, G., Kupriyanova, T., Cunningham, J.M., Chen, P., Cadel, S., Foulon, T., Cohen, P., Fine, R.E., Kandror, K.V., 1999. Glucose transporter Glut3 is targeted to secretory vesicles in neurons and PC12 cells. J Biol Chem 274, 14062–14066.

Ushkaryov, Y.A., Petrenko, A.G., Geppert, M., Sudhof, T.C., 1992. Neurexins: synaptic cell surface proteins related to the alpha-latrotoxin receptor and laminin. Science 257, 50–56.

Ushkaryov, Y.A., Rohou, A., Sugita, S., 2008. alpha-Latrotoxin and its receptors. Handb Exp Pharmacol, 171–206.

Vannucci, S.J., Maher, F., Simpson, I.A., 1997. Glucose transporter proteins in brain: delivery of glucose to neurons and glia. Glia 21, 2–21.

Vierbuchen, T., Ostermeier, A., Pang, Z.P., Kokubu, Y., Sudhof, T.C., Wernig, M., 2010. Direct conversion of fibroblasts to functional neurons by defined factors. Nature 463, 1035–1041.

Wallis, D., Hill, D.S., Mendez, I.A., Abbott, L.C., Finnell, R.H., Wellman, P.J., Setlow, B., 2012. Initial characterization of mice null for Lphn3, a gene implicated in ADHD and addiction. Brain Res 1463, 85–92.

Wang, L., Kuroiwa, Y., Kamitani, T., Takahashi, T., Suzuki, Y., Hasegawa, O., 1999. Effect of interstimulus interval on visual P300 in Parkinson's disease. J Neurol Neurosurg Psychiatry 67, 497–503.

Williams, L.M., Gordon, E., Wright, J., Bahramali, H., 2000. Late component ERPs are associated with three syndromes in schizophrenia. Int J Neurosci 105, 37–52.

Williams, N.M., Franke, B., Mick, E., Anney, R.J.L., Freitag, C.M., Gill, M., Thapar, A., O'Donovan, M.C., Owen, M.J., Holmans, P., Kent, L., Middleton, F., Zhang-James, Y., Liu, L., Meyer, J., Nguyen, T.T., Romanos, J., Romanos, M., Seitz, C., Renner, T.J., Walitza, S., Warnke, A., Palmason, H., Buitelaar, J., Rommelse, N., Vasquez, A.A., Hawi, Z., Langley, K., Sergeant, J., Steinhausen, H.-C., Roeyers, H., Biederman, J., Zaharieva, I., Hakonarson, H., Elia, J., Lionel, A.C., Crosbie, J., Marshall, C.R., Schachar, R., Scherer, S.W., Todorov, A., Smalley, S.L., Loo, S., Nelson, S., Shtir, C., Asherson, P., Reif, A., Lesch, K.-P., Faraone, S.V., 2012. Genome-wide analysis of copy number variants in attention deficit hyperactivity disorder: the role of rare variants and duplications at 15q13.3. Am J Psychiatry 169, 195–204.

Williams, R.L., Hilton, D.J., Pease, S., Willson, T.A., Stewart, C.L., Gearing, D.P., Wagner, E.F., Metcalf, D., Nicola, N.A., Gough, N.M., 1988. Myeloid leukaemia inhibitory factor maintains the developmental potential of embryonic stem cells. Nature 336, 684–687.

Willner, P., 1986. Validation criteria for animal models of human mental disorders: learned helplessness as a paradigm case. Prog Neuropsychopharmacol Biol Psychiatry 10, 677–690.

Wilson, C.M., Mitsumoto, Y., Maher, F., Klip, A., 1995. Regulation of cell surface GLUT1, GLUT3, and GLUT4 by insulin and IGF-I in L6 myotubes. FEBS Lett 368, 19–22.

Yang, S., Wang, K., Gregory, B., Berrettini, W., Wang, L.-S., Hakonarson, H., Bucan, M., 2009. Genomic landscape of a three-generation pedigree segregating affective disorder. PLoS ONE 4, e4474.

Zhao, Y., Fung, C., Shin, D., Shin, B.-C., Thamotharan, S., Sankar, R., Ehninger, D., Silva, A., Devaskar, S.U., 2010. Neuronal glucose transporter isoform 3 deficient mice demonstrate features of autism spectrum disorders. Mol Psychiatry 15, 286–299.

Zhou, K., Dempfle, A., Arcos-Burgos, M., Bakker, S.C., Banaschewski, T., Biederman, J., Buitelaar, J., Castellanos, F.X., Doyle, A., Ebstein, R.P., Ekholm, J., Forabosco, P., Franke, B., Freitag, C., Friedel, S., Gill, M., Hebebrand, J., Hinney, A., Jacob, C., Lesch, K.P., Loo, S.K., Lopera, F., McCracken, J.T., McGough, J.J., Meyer, J., Mick, E., Miranda, A., Muenke, M., Mulas, F., Nelson, S.F., Nguyen, T.T., Oades, R.D., Ogdie, M.N., Palacio, J.D., Pineda, D., Reif, A., Renner, T.J., Roeyers, H., Romanos, M., Rothenberger, A., Schafer, H., Sergeant, J., Sinke, R.J., Smalley, S.L., Sonuga-Barke, E., Steinhausen, H.-C., van der Meulen, E., Walitza, S., Warnke, A., Lewis, C.M., Faraone, S.V., Asherson, P., 2008. Meta-analysis of genome-wide linkage scans of attention deficit hyperactivity disorder. Am J Med Genet B Neuropsychiatr Genet 147, 1392–1398.

6.2 List of figures

6.3 List of abbreviations

5-HTT	Serotonin transporter
A	
ADHD	Attention-deficit/hyperactivity disorder
ALAS1	Delta-aminolevulinate synthase 1
α-LTX	Alpha-latrotoxin
ANOVA	Analysis of variance
au	Arbitrary unit
B	
B2M	Beta-2 microglobulin
BAC	Bacterial artificial chromosome
BDNF	Brain-derived neurotrophic factor
bp	Base pair
C	
CA1	Cornu ammonis region 1
cAMP	Cyclic adenosine monophosphate
cDNA	Complementary DNA
CB	Cerebellum
CGH	Comparative genomic hybridisation
CIRL	Ca^{2+}-independent receptors of alpha-latrotoxin
CNV	Copy number variation
CPM	Counts per minute
CPT	Continuous performance test
Ct	Cycle threshold
CTX	Cortex
D	
DAPI	4',6-diamidino-2-phenylindole
DAT	Dopamine transporter
DBH	Dopamine beta-hydroxylase
dCTP	Deoxcytidine triphosphate
DG	Dentate gyrus
DNA	Deoxyribonucleic acid
DNP	2,4-dinitrophenol
dNTP	Deoxynucleoside triphosphate
DRD	Dopamine receptor gene
DTA	Diphteria toxin A
dUTP	Deoxyuridine triphosphate

E

EBV	Epstein-Barr virus
EDTA	Ethylenediaminetetraacetic acid
EEG	Electroencephalography
e.g.	For example
ERP	Event-related potential
ES cell	Embryonic stem cell
EuMMCR	European Mouse Mutant Cell Repository

F

FISH	Fluorescence *in situ* hybridisation
FLP	FLP recombinase (Flippase)
Flx	Floxed, i.e. flanked by loxP sites
FLRT	Fibronectin leucine-rich repeat transmembrane protein
fMRI	Functional magnetic resonance imaging
FRT	Flippase recognition target

G

G418	Geneticin
GAPDH	Glyceraldehyde 3-phosphate dehydrogenase
GLUT	Facilitative glucose transporter
GPRC	G protein-coupled receptor
GPS	G protein-coupled receptor proteolysis site
GRM5	Metabotropic glutamate
GWAS	Genome-wide association study

H

hg19	Human genome assembly, version 19
HIP	Hippocampus
HMIT	Proton-dependent myoinositol transporter
HR	Homology region
HTR	Serotonin receptor gene

I

i.e.	That is
IKMC	International Knockout Mouse Consortium
IP_3	Inositol trisphosphate

K

kb	Kilobase pair
kDa	Kilodalton

L

lacZ	Beta-galactosidase gene
LCL	Lymphoblastoid cell line
LIF	Leukemia Inhibitory Factor
loxP	Cre recombinase recognition target
LPHN	Latrophilin gene family

M

MFS	Major facilitator superfamily
MPH	Methylphenidate
mRNA	Messenger ribonucleic acid
MWU	Mann-Whitney-U test
ms	Millisecond

N

NAHR	Non-allelic homologous recombination
NaOH	Sodium hydroxide
Neo	Neomycin resistance cassette
NGA	NoGo-Anteriorisation
NPY	Neuropeptide Y
n.s.	Not significant

O

OB	Olfactory bulb

P

PBMC	Peripheral blood mononuclear cell
PBS	Phosphate-buffered saline
PCB	Polychlorinated bisphenyl
PCR	Polymerase chain reaction
PEST	Sequences rich in proline, glutamic acid, serine & threonine
PET	Positron emission tomography
PGK1	Phosphoglycerate kinase 1

Q

qPCR	Quantitative polymerase chain reaction
qRT-PCR	Quantitative reverse transcription polymerase chain reaction

R

RIPA	Radioimmunoprecipitation assay buffer
RNase	Ribonuclease

S

SEM	Standard error of the mean
SGLT	Sodium glucose-linked transporter
SHR	Spontaneously hypertensive rat
SLC2A	Facilitative glucose transporter gene family
SLC5A	Sodium-glucose linked transporter gene family
SLC6A3	Dopamine transporter gene
SLC6A4	Serotonin transporter gene
SNAP25	Synaptosomal associated protein of 25kDa
SNL	Murine fibroblast STO cell line transformed with neomycin resistance and murine leukemia inhibitory factor (LIF) genes
SNP	Single-nucleotide polymorphism
SpecR	Spectinomycin resistance cassette
SUEL	Sea urchin egg lectin

T

TAE	Tris acetic acid EDTA buffer
TBS	Tris-buffered saline
TBS-T	Tris-buffered saline incl. Tween-20
TE	Tris EDTA buffer
TM	Transmembrane domain

U

UTR	Untranslated region
UV	Ultraviolet

V

v.s	Versus

W

WKY	Wistar-Kyoto

6.4 Academic education of the author

January 2010 until present	Dissertation in the Division of Molecular Psychiatry at the Department of Psychiatry, Psychosomatics and Psychotherapy, University of Würzburg
October 2007 until February 2008	Internship at the Institute of Pharmacology and Structural Biology (IPBS), Toulouse, France Topic: 'Characterization of a neuroblastoma cell line (SY-SY5Y) expressing the receptor NPFF2 tagged with YFP'
October 2005 until October 2009	Studies in Biology at the University of Würzburg (main study period) Area of concentration: neurobiology, biochemistry and pharmaceutical biology Diploma thesis in the Division of Molecular Psychiatry at the Department of Psychiatry, Psychosomatics and Psychotherapy, University of Würzburg Topic: 'The constitutive *Tph2* knockout mouse – impact of serotonin deficiency on histological, neurochemical and develop-mental phenotype'
October 2003 until September 2005	Studies in Biology at the University of Göttingen (basic study period) Graduation: Intermediate diploma

Würzburg…….

Date Signature

6.5 Publications of the author

Gutknecht, L., Araragi, N., **Merker, S.**, Waider, J., Sommerlandt, F.M.J., Mlinar, B., Baccini, G., Mayer, U., Proft, F., Hamon, M., Schmitt, A.G., Corradetti, R., Lanfumey, L., Lesch, K.-P., 2012. Impacts of brain serotonin deficiency following Tph2 inactivation on development and raphe neuron serotonergic specification. PLoS ONE 7, e43157.

Lange, M., Norton, W., Coolen, M., Chaminade, M., **Merker, S.**, Proft, F., Schmitt, A., Vernier, P., Lesch, K.-P., Bally-Cuif, L., 2012. The ADHD-susceptibility gene lphn3.1 modulates dopaminergic neuron formation and locomotor activity during zebrafish development. Mol. Psychiatry 17, 946–954.

Lesch, K.P., **Merker, S.**, Reif, A., Novak, M., 2012. Dances with black widow spiders: Dysregulation of glutamate signalling enters centre stage in ADHD. Eur Neuropsychopharmacol.

Moulédous, L., **Merker, S.**, Neasta, J., Roux, B., Zajac, J.-M., Mollereau, C., 2008. Neuropeptide FF-sensitive confinement of mu opioid receptor does not involve lipid rafts in SH-SY5Y cells. Biochem. Biophys. Res. Commun. 373, 80–84.

6.6 Acknowledgements

Ich möchte mich an dieser Stelle bei allen Personen bedanken, die mich in meiner Zeit als Doktorand begleitet und unterstützt haben.

Zuallererst bei Prof. Dr. Klaus-Peter Lesch dafür, dass er mir die Möglichkeit gegeben hat, meine Doktorarbeit in seiner Arbeitsgruppe zu schreiben und mir durch die Auswahl von zwei verschiedenen, sehr interessanten Projekten ermöglicht hat, eine Vielzahl an molekularbiologischen Methoden zu erlernen.

Prof. Dr. Erhard Wischmeyer und Prof. Dr. Esther Asan möchte ich dafür danken, dass sie mir als Mitglieder meines Promotionskomitees bei den regelmäßigen Treffen vielerlei Anregungen und konstruktive Kritik gegeben haben.

Besonderer Dank geht auch an PD Dr. Angelika Schmitt für die zusätzliche Betreuung meiner Projekte, die gute Zusammenarbeit in Strahlenschutz-Angelegenheiten und dafür, dass du immer ein offenes Ohr für Fragen aller Art hast.

Bei Prof. Dr. Paul Pauli und dem Graduiertenkolleg RTG 1253 (Emotions) bedanke ich mich für die mehrjährige Finanzierung, den interdisziplinären Austausch und die vielen tollen Veranstaltungen, die ich durch die Mitgliedschaft im GK erleben durfte.

Georg Ziegler danke ich für die langjährige gute Zusammenarbeit beim GLUT-Projekt, für deine große Sorgfalt im Labor sowie das Korrekturlesen meiner Thesis.

Ute Mayer danke ich für die viele Arbeit und Geduld, die du beim Blotten an den Tag gelegt hast, und bei Vera Dino & Florian Keles für die Unterstützung bei immunhistologischen Färbungen und Glukose-Aufnahme-Assays.

Großen Dank schulde ich auch Dr. Lise Gutknecht und Dr. Tobias Langenhan für die viele Hilfe beim Latrophilin-Projekt, sei es bei theoretischen Fragestellungen oder ganz konkret bei praktischen Versuchen.

Am Würzburger Biozentrum gibt es eine ganze Reihe von Personen, denen ich ganz herzlich danken möchte: Bei Dr. Cornelia Wiese, Prof. Dr. Manfred Gessler und allen Kollegen in der Entwicklungsbiochemie bedanke ich mich dafür, dass ich mehrere Monate lang in eurer Zellkultur arbeiten sowie euer Material benutzen durfte und in

dieser Zeit hervorragend von euch betreut wurde. Zudem bin ich Dr. Indrajit Nanda zu großem Dank verpflichtet für die enorme Hilfe, sowohl was das Karyotypisieren von Maus-Zellen als auch was die In-Situ-Färbungen an menschlichen Chromosomen angeht. Mein Dank geht auch an Prof. Dr. Clemens Müller-Reible für die Zurverfügungstellung zahlreicher Lymphoblasten-Proben.

Dr. Ann-Christine Ehlis danke ich für die vielen EEG-Messungen, die du organisiert und durchgeführt hast, sowie für die Unterstützung beim Schreiben des GLUT3-Papers.

Dr. Reinhard Ullmann samt Kollegen danke ich für die Hilfe bei der array CGH, und Ronald Naumann sowie seinem Team vom MPI für die Morula-Injektionen.

Dem Muttersprachler Richard Forsythe danke ich herzlich für das geduldige Gegenlesen vieler Passagen meiner Thesis.

Bei Antonia, Sandy, Olga und Jonas möchte ich mich für die viele Unterstützung und die guten Tipps bedanken (vor allem was Maus-spezifische Fragen angeht).

Lena und Joachim danke ich für die gute Zusammenarbeit in Sachen Latrophilin und Western Blotting sowie für das Gegenlesen meiner Thesis.

Allen TAs und der gesamten Labor-Crew bin ich sehr dankbar für die viele viele Unterstützung bei allen technischen & nicht-technischen Problemen und für die spitzenmäßige generelle Arbeitsatmosphäre.

Maggie und Manish möchte ich für die musikalischen und kulinarischen Exkursionen danken und Stephan & Judith für ein ganzes bzw halbes Jahrzehnt an Freundschaft. Ihr seid die Besten!

Nicht zuletzt danke ich meinen Eltern, Hartmut und Irma, sowie meiner Schwester Sinja dafür, dass ihr mich seit nunmehr 30 Jahren bei allem begleitet und fördert, was ich tue, und in mir überhaupt erst das Interesse für die weite Welt der Biologie geweckt habt.

6.7 Affidavit

I hereby declare that my thesis entitled *Genome-wide screenings in attention-deficit/hyperactivity disorder (ADHD): investigation of novel candidate genes SLC2A3 and LPHN3* is the result of my own work. I did not receive any help or support from commercial consultants. All sources and / or materials applied are listed and specified in the thesis.

Furthermore, I verify that this thesis has not yet been submitted as part of another examination process neither in identical nor in similar form.

Würzburg……

Date Signature

6.8 Eidesstattliche Erklärung

Hiermit erkläre ich an Eides statt, die Dissertation *Genomweite Untersuchungen des Aufmerksamkeitsdefizit/Hyperaktivitätssyndroms (ADHS): Analyse der neuen Kandidatengene SLC2A3 und LPHN3* eigenständig, d.h. insbesondere selbstständig und ohne Hilfe eines kommerziellen Promotionsberaters, angefertigt und keine anderen als die von mir angegebenen Quellen und Hilfsmittel verwendet zu haben.

Ich erkläre außerdem, dass die Dissertation weder in gleicher noch in ähnlicher Form bereits in einem anderen Prüfungsverfahren vorgelegen hat.

Würzburg……

Datum Unterschrift